

Dissertation zur Erlangung des Doktorgrades
der Fakultät für Chemie und Pharmazie
der Ludwig-Maximilians-Universität München

**Development of novel antibodies blocking
the CD47-SIRP α myeloid-specific immune
checkpoint as an improved strategy for
Acute Myeloid Leukemia immunotherapy**

Laia Pascual Ponce

aus

Vilanova i la Geltrú, Spain

2018

Erklärung

Diese Dissertation wurde im Sinne von § 7 der Promotionsordnung vom 28. November 2011 von Herrn Prof. Karl-Peter Hopfner betreut.

Eidesstattliche Versicherung

Diese Dissertation wurde eigenständig und ohne unerlaubte Hilfe erarbeitet.

München, am 16.02.2018

.....

Laia Pascual Ponce

Dissertation eingereicht am 20.02.2018

1. Gutachter: Herr Prof. Dr. Karl-Peter Hopfner

2. Gutachter: Herr Prof. Dr. Veit Hornung

Mündliche Prüfung am 19.04.2018

This thesis has been prepared from September 2014 to February 2018 in the laboratory of Prof. Dr. Karl-Peter Hopfner at the Gene Center of the Ludwig-Maximilians-University of Munich (LMU).

Parts of this thesis have been published or submitted for publication:

Ponce, L.P., Fenn, N.C., Moritz, N., Krupka, C., Kozik, J.H., Lauber, K., Subklewe, M., and Hopfner, K.P. SIRP α -antibody fusion proteins stimulate phagocytosis and promote elimination of acute myeloid leukemia cells. *Oncotarget*. 2017;8(7):11284-11301.

Ponce, L.P.*, Kozik, J.H.*, Schmitt, S., Kaufmann, A., Magauer, N., Schele, A., Fenn, N.C.[†], Subklewe, M.[†], and Hopfner, K.P.[†] SIRP α - α CD33 licMABs enhance phagocytosis and stimulate clearance of high CD47-expressing primary, patient-derived acute myeloid leukemia cells. *In preparation*.

*These authors contributed equally to this work

[†]These authors are co-corresponding authors

Parts of this thesis have been presented at international conferences:

Poster presentation at the Third CRI-EATI-AACR International Cancer Immunotherapy conference, September 6-9, 2017, Mainz, Germany

Parts of this thesis have been included in the following patent application:

LMU Munich, Hopfner K.P., Moritz N., Fenn N., and Subklewe M. Trispecific molecule combining specific tumor targeting and local immune checkpoint inhibition. EP 3165536 A1

TABLE OF CONTENTS

TABLE OF CONTENTS

1. SUMMARY	1
2. INTRODUCTION.....	3
2.1. Cancer immunotherapy.....	3
2.1.1. Monoclonal antibodies.....	4
2.1.2. Engineering of antibodies	7
2.2. Immune checkpoint-blocking antibodies	10
2.2.1. The “don’t eat me” immune checkpoint	11
2.2.2. Strategies targeting the CD47-SIRP α innate immune checkpoint.....	13
2.3. Acute Myeloid Leukemia.....	17
2.3.1. Current treatments for AML patients.....	18
2.3.2. Immunotherapy in AML	19
3. AIM OF THE THESIS	23
4. RESULTS	25
4.1. Cloning and expression of local inhibitory checkpoint molecules.....	25
4.1.1. Local inhibitory checkpoint monoclonal antibodies (licMABs)	25
4.1.2. Single-arm local inhibitory checkpoint monoclonal antibodies (licMABs ^{single})	27
4.1.3. Local inhibitory checkpoint antibody derivatives (liCADs).....	28
4.2. Biochemical characterization of local inhibitory checkpoint molecules	30
4.2.1. Thermal stability	30
4.2.2. Binding of local inhibitory checkpoint molecules to tumor cells	31
4.2.3. Local inhibition of the CD47-SIRP α innate immune checkpoint.....	35
4.2.4. CD33-dependent internalization of local inhibitory checkpoint molecules	38
4.2.5. Binding of local inhibitory checkpoint molecules to effector cells	40
4.3. Functional characterization of local inhibitory checkpoint molecules	42
4.3.1. Antibody-dependent cellular cytotoxicity in AML cell lines	42

TABLE OF CONTENTS

4.3.2. Antibody-dependent cellular cytotoxicity in AML patient samples	44
4.3.3. Antibody-dependent cellular phagocytosis in AML cell lines	45
4.3.4. Antibody-dependent cellular phagocytosis in AML patient samples	49
5. DISCUSSION	53
5.1. Local blockade of the CD47-SIRPα innate immune checkpoint.....	53
5.2. Advantages and limitations of liCADs	55
5.3. LicMABs and licMABs^{single} enhance phagocytosis of AML cells	55
5.4. Other determinants of macrophage-mediated phagocytosis.....	57
5.5. CD33-dependent internalization	59
5.6. Comparative analysis of licMABs, licMABs^{single} and liCADs	60
6. MATERIALS AND METHODS	63
6.1. Materials	63
6.1.1. <i>E. coli</i> strain, cell lines and media	63
6.1.2. Healthy donors' and AML patients' material	63
6.2. Molecular biology methods	65
6.2.1. Molecular cloning	65
6.2.2. Transformation of <i>E. coli</i>	66
6.3. Protein biochemistry methods.....	67
6.3.1. Expression and purification of licMABs and licMABs ^{single}	67
6.3.2. Expression and purification of liCADs	68
6.3.3. Fluorescence thermal shift assay	68
6.4. Binding and interaction studies	69
6.4.1. Binding studies by flow cytometry	69
6.4.2. Quantitative determination of cell surface antigens.....	69
6.4.3. CD47-blocking assay	69
6.4.4. K _D determination	70

TABLE OF CONTENTS

6.4.5. Internalization assay by flow cytometry	70
6.4.6. Internalization assay by confocal microscopy	70
6.4.7. Size exclusion chromatography analysis	71
6.5. Functional assays	71
6.5.1. Red blood cells competition assay	71
6.5.2. Antibody-dependent cellular cytotoxicity (ADCC).....	71
6.5.3. Antibody-dependent cellular cytotoxicity of primary AML cells	72
6.5.4. Antibody-dependent cellular phagocytosis (ADCP)	73
6.5.5. Antibody-dependent cellular phagocytosis of primary AML cells.....	74
6.6. Plotting and statistical analysis	74
7. REFERENCES.....	75
8. LIST OF ABBREVIATIONS	93
9. ACKNOWLEDGEMENTS	97
10. CURRICULUM VITAE	99

SUMMARY

1. SUMMARY

Recent developments in antibody-based immunotherapy, especially targeting immune checkpoints, have revolutionized cancer treatment. Immune checkpoints are inhibitory pathways responsible for dampening the immune response in order to ensure self-tolerance under physiological conditions. In cancer cells, however, immune checkpoints are often utilized as a mechanism to escape the immune system. Numerous studies have demonstrated that blocking immune checkpoints restores potent anti-tumor immune responses and ultimately leads to the elimination of cancer cells. Accordingly, several monoclonal antibodies (mAbs) targeting immune checkpoint receptors are currently in the market.

The CD47-SIRP α myeloid-specific immune checkpoint controls the immune response by negatively regulating phagocytosis. SIRP α , expressed on phagocytic cells, triggers a negative signal upon binding to CD47, ubiquitously expressed on healthy cells and overexpressed on several cancer types. Hence, the blockade of the CD47-SIRP α signaling pathway constitutes a promising approach to mediate phagocytosis of tumor cells. This blockade, however, may also induce unwanted toxicity to healthy cells, which also express CD47. In order to reduce systemic toxicity while promoting the elimination of tumor cells, the blockade of the CD47-SIRP α immune checkpoint should be restricted to cancer cells.

Acute myeloid leukemia (AML) is a severe hematological cancer with a five year survival rate of 25%. Furthermore, while immunotherapies are already in clinical use for other hematological diseases, chemotherapy remains the first-line treatment for AML. This indicates an urgent need for the development of new and effective approaches that offer a better prognosis to AML patients. In order to provide a novel therapeutic strategy, we generated local inhibitory checkpoint molecules, which are antibody derivatives that deliver the benefits of blocking the CD47-SIRP α immune checkpoint to AML cells. The disruption of the myeloid-specific immune checkpoint is achieved by the endogenous SIRP α domain, which is genetically fused to an antibody fragment targeting the AML antigen CD33. Since the physiologically low affinity of SIRP α to CD47 prevents it from targeting CD47 by itself, the binding of the local inhibitory checkpoint molecules is dictated by the high affinity CD33-binding domain. Consequently, the anti-tumor effects of these molecules are confined to CD33-expressing AML cells.

SUMMARY

In order to investigate the best strategy to block the CD47-SIRP α immune checkpoint on AML cells, three different local inhibitory checkpoint molecules were created: local inhibitory checkpoint mAbs (licMABs), single-arm licMABs (licMABs^{single}) and local inhibitory checkpoint antibody derivatives (liCADs). All three formats bind CD33 with high affinity, disrupt the CD47-SIRP α axis by the endogenous SIRP α domain and activate immune effector cells. They diverge, however, in the binding valency to CD33 and the immune effector cell-activating domain. LicMABs target CD33 with both antibody arms, while licMABs^{single} and liCADs target CD33 monovalently. Moreover, licMABs and licMABs^{single} activate effector cells by an IgG1 Fc domain and liCADs contain a single chain variable fragment (scFv) activating uniquely CD16. The *in vitro* evaluation of these molecules confirmed the preferential binding to CD33-expressing cells even in the presence of a large antigen sink created by CD47 expressed on healthy cells. In addition, all local inhibitory checkpoint molecules induced Natural Killer (NK) cell-mediated lysis of AML cells and licMABs and licMABs^{single}, but not liCADs, enhanced phagocytosis of AML cell lines and primary, patient-derived AML cells. Importantly, we determined that the expression levels of CD47 on primary AML cells influence the outcome of licMAB-mediated phagocytosis.

In summary, this work establishes licMABs as a promising strategy to block the CD47-SIRP α immune checkpoint on high CD47-expressing AML cells. Furthermore, the marginal binding of these molecules to CD47 on healthy cells ensures a highly specific immune response and lowers the risk of unwanted side effects.

2. INTRODUCTION

2.1. Cancer immunotherapy

Cancer immunotherapy harnesses certain components of the host's immune system to fight tumors. By inducing or potentiating anti-tumor immune effector functions, its main goal is to overcome the immunosuppressive environment created by cancer cells, thus leading to tumor cell clearance and long-term disease-free survival of cancer patients. Together with surgery, chemotherapy, radiation and targeted therapy, the rapidly advancing field of cancer immunotherapy can currently be considered as the fifth pillar of cancer treatment.¹

The first evidence of cancer immunotherapy was the Coley's toxin, which dates to the 19th century.² William Coley, a surgeon at the Hospital for the Ruptured and Crippled in New York, realized that patients suffering from metastatic sarcoma and with a concomitant infection of *Streptococcus pyogenes* achieved tumor remission. Based on that observation, Coley injected heat-inactivated bacteria and bacterial lysates into patients with inoperable cancers.^{2, 3} Coley's toxin achieved a remarkable clinical success, but its use was abandoned due to severe side effects and lack of suitable explanations. Little happened in the field until some decades later, when the era of modern immunology began with the discovery of the interferon, the first cancer vaccine and the initial characterization of the innate and the adaptive branches of the immune system.⁴⁻¹⁰ In addition to this, the development of the serum therapy by Emil von Behring, the posterior work of Paul Ehrlich and ultimately the establishment of the hybridoma technology by César Milstein and Georges J. F. Köhler lead to the discovery of monoclonal antibodies (mAbs), which are one of the main players of cancer immunotherapy.¹¹⁻¹⁵ Lastly, at the end of the 20th century, evidences supporting anti-tumor immune responses, tumor-specific immune surveillance and tumor immune escape shaped the actual understanding of cancer immunology.^{16, 17}

It is currently accepted that tumors result from a combination of genetic and epigenetic changes that facilitate an abnormal proliferation of any cell in the body, thus becoming immortal and outgrowing healthy cells.¹⁸ Throughout this process, new antigens denominated neo-antigens arise, which allows the immune system to selectively detect and eliminate tumor cells.¹⁹ Nevertheless, cancer cells develop mechanisms to evade immune recognition and gain immune tolerance. The upregulation of immune

INTRODUCTION

checkpoints, for instance, is one of these mechanisms commonly used by cancer cells.²⁰ Therefore, present efforts in cancer immunotherapy are focused on eliminating cancer cells by restoring anti-tumor immune responses.

2.1.1. Monoclonal antibodies

The function of antibodies was envisioned by Paul Ehrlich, who proposed the concept of the magic bullet in 1900.²¹ With this idea, Ehrlich described the ability of a compound to precisely bind and destroy its intended target without harming healthy tissues, just like a bullet fired from a gun to hit a specific object. Further studies confirmed the presence of such compounds in the blood and their importance in protection from bacterial and viral infections. Their origin, however, was unclear until plasma cells, responsible of producing antibodies, were identified by Astrig Fagraeus in 1947.²²

The following milestone in the history of antibodies was the determination of their structure, revealed by enzymatic digestion and crystallographic analyses (Figure 1).²³⁻²⁶ Antibodies, also called immunoglobulins, are 150 kDa molecules composed by two identical light chains (LC, 25 kDa) and two identical heavy chains (HC, 50 kDa) connected by disulfide bonds. There are five classes of HC (IgG, IgM, IgA, IgD and IgE), which define the isotype of the antibody and its biological functions.²⁷ All of them contain one variable domain (V_H), one constant domain (C_{H1}), a hinge region and two other constant domains (C_{H2} and C_{H3}). In addition, a C_{H4} domain is present for IgM and IgE. Subclasses are defined for IgG (IgG1, IgG2a/b, IgG3 and IgG4) and IgA (IgA1 and IgA2), being IgG1 the isotype most commonly used for cancer immunotherapy. Regarding the LC, two types are described: kappa (κ) and lambda (λ), both composed by one variable (V_L) and one constant (C_L) domain. Each antibody domain folds into a distinctive 3D structure termed the immunoglobulin-fold (Ig-fold). It consists of two β -sheets packed together and linked by a disulfide bond, resembling a barrel-shaped structure. The two β -sheets of the variable domains are composed of four and five strands. In the constant domains, the β -sheets are formed by three and four strands.

Functionally, an antibody can be divided into the antigen-binding fragment (Fab) and the fragment crystallizable (Fc). The Fab region is composed by the V_L - C_L and the V_H - C_{H1} domains and confers the specificity to the target antigen. The V_L and the V_H domains contain the complementary-determining regions (CDRs), which are stretches of high variability embodied between frameworks (FRs) and define the antigen-binding site.²⁸

INTRODUCTION

According to the Kabat numbering scheme, the amino acids 24-34, 50-56 and 89-97 constitute the three CDRs of the V_L and the amino acids 31-35, 50-65 and 95-102 determine the three CDRs of the V_H . The Fc region, consisting of the C_H2 and C_H3 domains, binds to Fc receptors (FcRs) expressed on immune cells and triggers immune activation. There are four types of FcRs, classified according to the antibody isotype that they recognize. Fc-gamma receptors (Fc γ R) and the neonatal Fc receptor (Fc n R) bind to IgG antibodies, Fc-alpha receptors (Fc α R) to IgA and Fc-epsilon receptors (Fc ϵ R) to IgE.²⁹

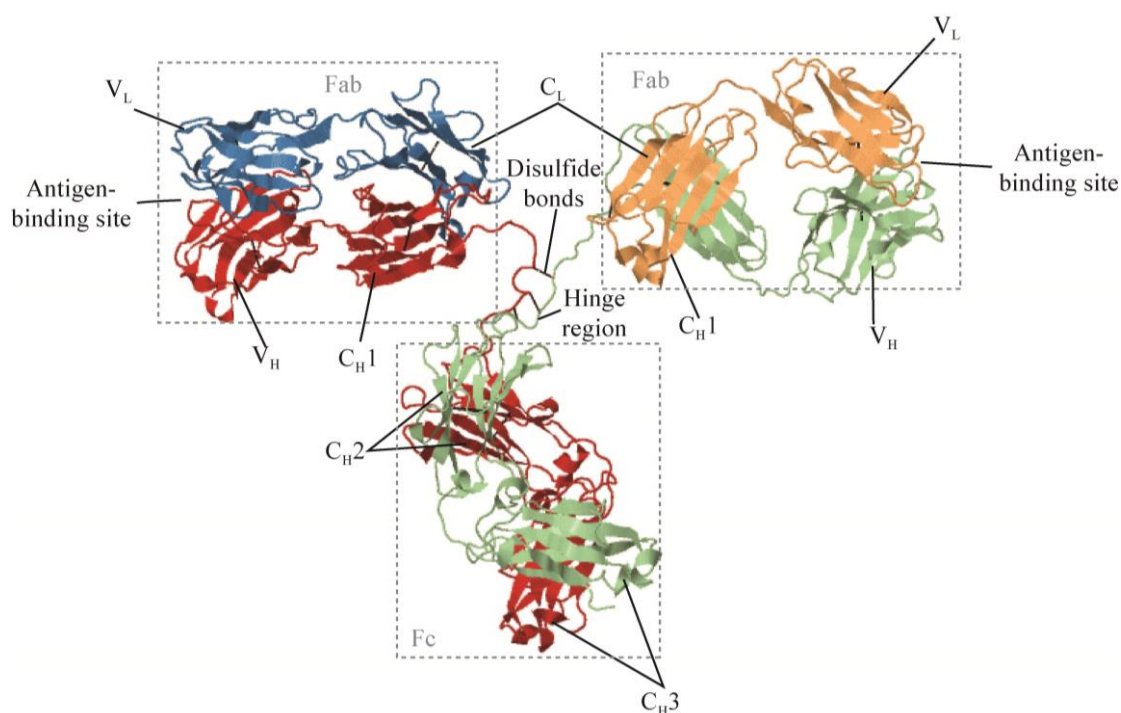


Figure 1. Crystal structure of a human IgG antibody

Human IgG antibodies consist of two heavy chains (red and green) and two light chains (blue and orange) stabilized by disulfide bonds (black lines). It can be divided into antigen-binding fragment (Fab), responsible for targeting specific antigens and fragment crystallizable (Fc), responsible for interacting with Fc-gamma receptors and mediate immune responses. Single domains are indicated. Figure adapted from PDB ID 1IGT.³⁰

Despite antibodies were already considered as very promising tools, difficulties in obtaining single antibodies of known specificity largely restricted the progression in the field. The development of the hybridoma technology, a method used for the production of antibodies with homogeneous antigen-binding (so-called monoclonal Abs, mAbs), solved this limitation.¹³⁻¹⁵ Hybridomas were initially obtained by fusing antibody-expressing B cells from an immunized mouse to immortal myeloma cells, thus generating a cell line producing murine mAbs. These murine antibodies, however, were typically immunogenic

INTRODUCTION

to humans and created graft-versus-host responses. Immunogenicity was overcome by the advent of advanced molecular cloning techniques, which facilitated the development of humanized antibodies by the engraftment of murine CDRs onto a human antibody framework.³¹ The establishment of these two tools advanced the biomedical research and rapidly led to an arsenal of mAbs for many diseases. Muronomab, a murine mAb targeting CD3, was the first mAb to achieve market approval by the US Food and Drug Administration (FDA) and CAMPATH-1H, targeting CD52, was the first clinical antibody to be fully humanized.^{32, 33}

Upon binding to the target tumor antigen, mAbs trigger potent tumor-specific immune responses. The type of immune response that IgG1 mAbs induce depends on binding to either the complement system or FcγRs (Figure 2). The complement component 1q (C1q) binds with high affinity to the Fc domain of two or more IgG1 mAbs opsonizing a tumor cell. This triggers the complement cascade, which ultimately leads to the formation of the membrane attack complex (MAC) on the target cell membrane, resulting in tumor cell lysis (Figure 2A). On the other hand, by binding to FcγRs, IgG1 mAbs trigger mechanisms mediated by innate immune cells. There are several types of FcγRs: CD16A/B (FcγRIIIA/B), CD32A/B (FcγRII) and CD64 (FcγRI). Except for CD32B, which transduces inhibitory signals through immunoreceptor tyrosine-based inhibitory motifs (ITIMs), all others contain immunoreceptor tyrosine-based activation motifs (ITAMs) and transduce activating signals to immune cells. CD16A, primary expressed on Natural Killer (NK) cells, is required for antibody-dependent cellular cytotoxicity (ADCC), and CD32A and CD64, expressed on macrophages, dendritic cells (DCs) and neutrophils, mediate antibody-dependent cellular phagocytosis (ADCP). During ADCC, NK cells degranulate and secrete perforin and granzymes that induce tumor cell lysis (Figure 2B); and if ADCP is mediated, tumor cells are engulfed and degraded in lysosomal compartments (Figure 2C). In addition, peptides derived from lysosomal degradation or lysis of tumor cells can be presented by DCs on either major histocompatibility complex (MHC) class II molecules and activate CD4⁺ T cells or on MHC class I molecules and prime CD8⁺ cytotoxic T cells, both leading to an induction of adaptive immune responses (Figure 2D).³⁴ Importantly, the relevance of the explained anti-tumor effects mediated by IgG1 mAbs has been clinically validated.^{35, 36}

INTRODUCTION

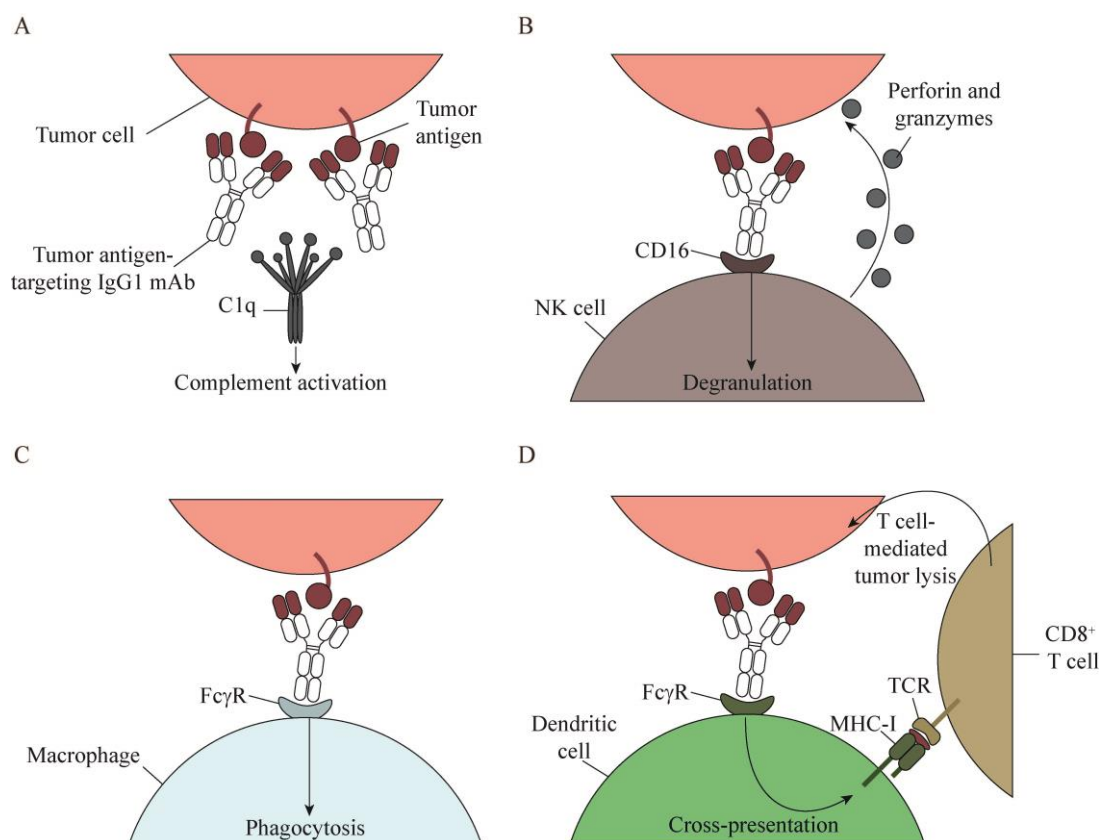


Figure 2. Effector functions of IgG1 antibodies

Binding of IgG1 antibodies to antigens expressed on tumor cells can induce four effector mechanisms that ultimately lead to the destruction of the tumor cell: (A) complement activation, (B) antibody-dependent cellular cytotoxicity, (C) antibody-dependent cellular phagocytosis and (D) tumor antigen cross-presentation and T cell activation.

2.1.2. Engineering of antibodies

Currently, more than 70 mAbs are approved by the FDA and the European Medicines Agency (EMA) for the treatment of cancer and other diseases. The clinical and commercial success of these drugs encouraged the development of the next generation of antibody-based therapeutics including antibody-drug conjugates (ADCs), bispecific antibodies (bsAbs) and antibody-derivatives (Figure 3).

ADCs combine the beneficial effects of mAbs and the potency of chemotherapy. By attaching a toxin to an antibody, ADCs become highly selective and cytotoxic drugs for cancer therapy (Figure 3B).³⁷ Two main types of cytotoxic payloads are used in ADCs: microtubule inhibitors and deoxyribonucleic acid (DNA)-damaging components. For tumor-specific delivery and to reduce off-tumor effects, the mAb is designed to target an antigen predominantly expressed on tumor cells, with minimal shedding and with receptor-mediated endocytosis. Regarding the isotype, most ADCs are either IgG1 and

INTRODUCTION

retain the ability to induce immune effector functions or IgG4, which does not significantly activate immune cells and therefore rely on the delivery of the drug to the tumor cell. The type of linker connecting the toxin to the mAb greatly influences the efficacy of the ADC. It should be stable until reaching the targeted tumor cell and, once internalized, capable of releasing the cytotoxic payload. The first ADC that received fast-track FDA approval in 2000 was gemtuzumab ozogamicin (GO, Mylotarg, Pfizer), an ADC targeting CD33. However, it was voluntarily withdrawn from the market in 2010 due to safety-related concerns and lack of clinical benefit. Despite this, the approval of two new toxin-coupled mAbs in 2013 and the re-approval of GO in 2017 re-validated the potential of ADCs as immunotherapeutic agents.³⁸

BsAbs retain the specificities of two different antibodies in one molecule and therefore are able to simultaneously bind to two target antigens (Figure 3C). Several approaches to force HC heterodimerization are now available, but the knobs-into-holes technology was the first one to be established.³⁹ In this technology, a bulky amino acid in the C_H3 domain of one HC is replaced by smaller one (Y407T), and the opposite exchange is performed in the other HC (T366Y) to enable the correct HC pairing. Other options to achieve HC heterodimerization include IgG/IgA hybrid C_H3 domains and electrostatic steering effects.^{40, 41} These approaches, however, are limited by the random pairing of the LCs. Some strategies to circumvent this problem are the use of a common light chain that allows binding to both antigens and the CrossMab technology, which exchanges the C_H1 and the C_L domain of one HC-LC complex to constrain the correct pairing.⁴² One advantage of bsAbs over mAbs is the increased binding specificity, achieved by interacting with two antigens on one cell. Moreover, bsAbs can also be used to bring targets to close proximity in order to support protein complex formation on one cell, or to trigger contacts between two different cells. For example, bsAbs targeting a tumor antigen and an immune cell, such as T cells via CD3, induce T cell-mediated killing of cancer cells. Similarly to ADCs, the Fc domain of the bsAbs can be functional and induce NK cell- and macrophage-mediated anti-tumor responses or silenced if such effects are not desired. Catumaxomab, targeting EpCAM and CD3, was the first bsAb to receive FDA approval in 2014 and several more are currently being investigated in clinical trials.

Antibody-derivatives are usually based on single domains of conventional mAbs. The main element is the single-chain fragment variable (scFv), which consist on the V_L and the V_H domains of a mAb connected by a flexible linker (Figure 3D). Similarly to bsAbs,

INTRODUCTION

the specificity can be increased by fusing two or more scFv domains, obtaining tandem scFvs (two scFvs) and single chain triplebodies (sctbs, three scFvs), among others.^{43, 44} The most known approach is the bispecific T cell engager (BiTE) molecule. BiTEs are composed of two scFvs, one activating T cells by targeting CD3 and the other recognizing a tumor antigen. Blinatumomab, a BiTE targeting CD19 fast-track approved in 2014, obtained the upgrade to full FDA approval in 2017 due to successful clinical results.⁴⁵ Motivated by the promising activity of BiTEs, this strategy was transferred to NK cells by exchanging the CD3-targeting scFv by a CD16-targeting scFv, and the new molecule was termed BiKE (bispecific NK cell engager).⁴⁶ The major advantage of antibody-derivatives and specifically tandem scFvs, with respect to conventional mAbs, is their smaller size (around 50 to 70 kDa), which may facilitate the formation of tighter cytolytic synapses and the penetration into solid tumors, thus achieving better anti-tumor effects. Their smaller size, however, is also a disadvantage since these molecules are susceptible to renal clearance and therefore have very short serum half-life.

In addition to the formats described above, more sophisticated technologies have been developed during the last years, giving rise to a huge array of antibody-based therapeutics. Obtained by exploiting the modular architecture of antibodies, each novel format harvests different properties regarding binding valency and specificity, effector function and half-life. Mostly being pre-clinically evaluated, it seems likely that new antibody-based drugs will emerge in clinical studies over the coming years, which will broaden the actual view of cancer immunotherapy.

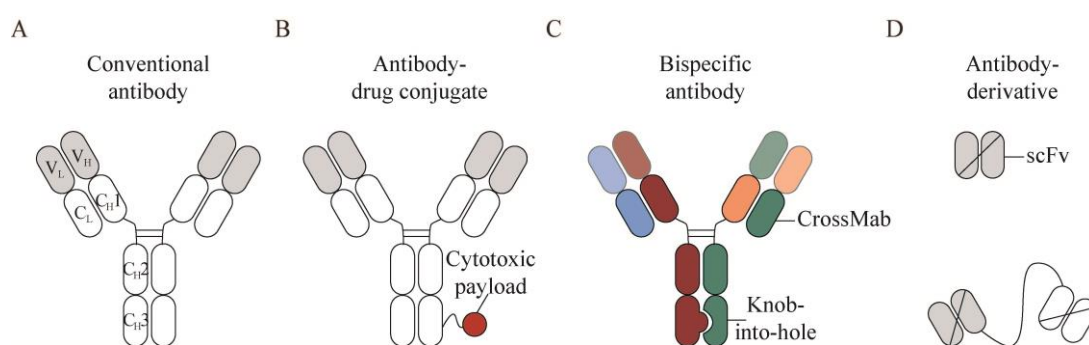


Figure 3. Second generation of antibody-based cancer therapeutics

(A) Conventional antibodies have been engineered to develop several antibody-based therapies. (B) Antibody-drug conjugates deliver a toxin into the tumor cell by binding to an internalizing tumor antigen. (C) Bispecific antibodies, obtained by technologies ensuring the correct pairing of all antibody chains, are able to simultaneously bind to two antigens. (D) Antibody-derivatives, of smaller molecular weight, are based on single chain fragment variable (scFv) domains and target two or more antigens simultaneously.

INTRODUCTION

2.2. Immune checkpoint-blocking antibodies

An adequate and specific immune response is ensured by a balance of stimulatory and inhibitory signals into the immune cells. Stimulatory signals induce immune responses against bacteria, viruses and foreign and harmful substances. In contrast, inhibitory signals, also known as immune checkpoints, maintain self-tolerance and modulate the immune attack to reduce collateral tissue damage.⁴⁷ These inhibitory pathways, however, are exploited by tumor cells to evade the immune system. More specifically, by upregulating immune checkpoint receptors, cancer cells are able to dampen the immune response. Thus, antagonists of immune checkpoints, such as immune checkpoint-blocking antibodies, are able to neutralize inhibitory signals and therefore restore and potentiate anti-tumor immune responses.

Over the past decade, the use of immune checkpoint inhibitors led to very promising pre-clinical and clinical results and has revolutionized the field of cancer immunotherapy. Since T cells were the first immune cell type described to play a major role in tumor clearance and immune surveillance, initial studies were focused on restoring adaptive immune responses.^{48, 49} Cytotoxic T-lymphocyte-associated antigen 4 (CTLA-4), an inhibitory receptor regulating T cell responses during the priming phase, was the first immune checkpoint to be described and utilized as a therapeutic target. CTLA-4 is the counterbalance receptor of CD28, a stimulatory receptor also expressed on T cells. Both trigger opposite signals to T cells by binding to B7, expressed on antigen-presenting cells.⁵⁰ Furthermore, CTLA-4 is required for regulatory T cells in order to maintain their immunosuppressive function.⁵¹ Consequently, blocking CTLA-4 with mAbs not only promotes the binding of B7 to CD28 leading to T cell activation, but also inactivates the pro-tumorigenic functions of regulatory T cells. Ipilimumab, an IgG1 mAb targeting CTLA-4, was the first immune checkpoint inhibitor to be approved by the FDA in 2011 for the treatment of advanced melanoma. Its administration, alone or in combination with other anti-tumor drugs, significantly improved the overall survival of patients.⁵² However, immune-related adverse events due to non-specific T cell activation occurred in 10-15% of the patients, which outlines the need for more specific therapies.

Another well-studied immune checkpoint receptor negatively regulating T cell activation is programmed cell death 1 (PD-1). PD-1, expressed on T cells, interacts with programmed cell death ligand 1 (PD-L1), which is upregulated in tumor cells as an

INTRODUCTION

immune escape mechanism.⁵³⁻⁵⁵ Upon binding to PD-L1, PD-1 triggers a negative signal into T cells inducing T cell exhaustion and dysfunction. Accordingly, the blockade of the interaction between PD-1 and PD-L1 reverses the dysfunctional state of T cells and reestablishes anti-tumor T cell responses. There are two blocking mAbs targeting PD-1 (pembrolizumab and nivolumab) and three PD-L1 inhibitors (atezolizumab, avelumab and durvalumab) currently approved by the FDA, and several more candidates under clinical development. These agents extended the overall and disease-free survival of a significant minority of patients, but as for CTLA-4 inhibitors, adverse events were observed due to off-tumor toxicities.⁵⁶

Despite the unquestionable clinical efficacy of immune checkpoint-blocking mAbs, new strategies are being explored in order to improve clinical outcomes by reducing immune-related adverse events and broadening the responsive patient subset. On one hand, studies based on predictive biomarkers, load of neo-antigens and inflammatory gene signatures are being performed in order to clarify patient responses.⁵⁷⁻⁵⁹ On the other, immune checkpoint-blocking antibodies are being evaluated in combination with other anti-tumor therapeutics to induce more specific and efficient anti-tumor responses. For instance, combining the blockade of the PD-1 axis and a BiTE molecule targeting CD33 significantly increased the lysis of AML cells with respect to the single agents *in vitro*.⁶⁰ Furthermore, another approach approved by the FDA in 2015 was the combination of two immune checkpoint-blocking mAbs, one targeting PD-1 and the other CTLA-4, which improved the overall survival of advanced melanoma patients with respect to monotherapies.⁶¹

All in all, the blockade of the CTLA-4 and the PD-1 signaling pathways was the cornerstone for the field of immune checkpoint-based cancer therapies, which is expected to expand with the development of new and more powerful strategies including novel immune checkpoint inhibitors and optimal combinations.

2.2.1. The “don’t eat me” immune checkpoint

The encouraging results obtained with CTLA-4 and PD-1 inhibitors promoted the investigation of additional immune checkpoints that could potentially be targeted in cancer immunotherapy. One of the recently described immune checkpoints is the CD47-SIRPα myeloid-specific immune checkpoint, which negatively regulates phagocytosis in macrophages and other myeloid cells. Also known as the “don’t eat me” immune

INTRODUCTION

checkpoint, the CD47-SIRP α axis was initially described as the pathway responsible for maintaining homeostasis of red blood cells (RBCs).⁶² More specifically, CD47 was recognized as a marker of self by experiments in which CD47-negative RBCs were cleared much faster than CD47-expressing RBCs by macrophages of immunocompetent mice. This was followed by the identification of SIRP α as the receptor of CD47 and a negative regulator of macrophage-mediated phagocytosis of RBCs.⁶³⁻⁶⁵

The cluster of differentiation 47 (CD47), also known as integrin-associated protein (IAP), is a surface glycoprotein that contains a single extracellular Ig-like domain resembling the antibody variable domain (so-called V-set domain), five transmembrane domains and a short cytoplasmic tail, which is subject to alternative splicing.^{66, 67} CD47 is ubiquitously expressed on all cells in the body and its expression varies depending on the immune status or disease. Since expressing CD47 protects the cell from clearance by phagocytosis, long-lived memory T cells and circulating hematopoietic stem cells (HSC), among others, present high levels of CD47.^{68, 69} Similarly, CD47 has been described to be upregulated in cancer cells, including several types of leukemia and solid malignancies, as an escape mechanism.⁷⁰⁻⁷⁴

Signal regulatory protein alpha (SIRP α), expressed on all myeloid cells, is one of the five members of the SIRP family of immunoreceptors, which also includes SIRP β 1, SIRP β 2, SIRP γ and SIRP δ .^{75, 76} SIRP α , also known as CD172a and SHSP-1, is the most studied member and the best conserved among different species. It is composed of three extracellular Ig-like domains, a transmembrane domain and a cytoplasmic tail. Regarding the three extracellular domains, the domain located at the N-terminus is responsible of interacting with CD47 and presents a V-set structure, whereas the other two domains resemble the structure of antibody constant regions (C1-set domain).^{76, 77} SIRP β 1 and SIRP γ have a high degree of homology with the extracellular fragment of SIRP α , and SIRP γ , but not SIRP β 1, is able to interact with CD47.⁷⁸ Due to the lack of the cytoplasmic domain of SIRP γ , its binding to CD47 is proposed to trigger a unidirectional signaling via CD47 possibly involved in transendothelial migration of T cells.^{79, 80} On the contrary, engagement of SIRP α by CD47 triggers the phosphorylation of the tyrosine residues at the ITIM motifs in the cytoplasmic tail of SIRP α . This recruits and activates Src homology region 2-domain-containing phosphatases 1 and 2 (SHP-1 and SHP-2), which dephosphorylate a variety of proximal substrates, thus regulating downstream signaling pathways and ultimately inhibiting the phagocytic function. One of the

INTRODUCTION

substrates dephosphorylated, for instance, is the motor protein myosin IIA, which controls the rearrangement of the actin cytoskeleton required for phagocytosis (Figure 4A).^{67, 81-83}

It is important to note that CD47 interacts not only with SIRP α and SIRP γ , but also with other ligands, such as thrombospondin-1 (TSP-1), an extracellular matrix protein expressed on the stroma of various tumors.⁸⁴ The contact between CD47 and TSP-1 restricts tumor growth and therefore the blockade of this interaction enhances angiogenesis.^{85, 86} Thus, contrary to SIRP α , TSP-1 triggers anti-tumor mechanisms by binding to CD47. Importantly, it was described that CD47-TSP-1 interaction and CD47-SIRP α binding are mutually exclusive.⁸⁴ This, and the fact TSP-1 and SIRP α induce opposite tumor responses, raises some concerns on how to best tackle CD47 as a target for cancer immunotherapy.

2.2.2. Strategies targeting the CD47-SIRP α innate immune checkpoint

The anti-tumor effects resulted from the blockade of the CD47-SIRP α innate immune checkpoint were initially reported using the well-known CD47-targeting antibody B6H12, a mouse IgG1 mAb that blocks CD47 interactions with SIRP α .⁷⁰ Evaluated in many studies, B6H12 successfully induced macrophage-mediated elimination of hematopoietic and solid tumors *in vitro* as well as *in vivo* (Figure 4B, left).^{70, 71, 87, 88} Since the murine IgG1 isotype is considered to be equivalent to the human IgG4 isotype, which does not mediate significant effector functions, the anti-tumor effects of B6H12 were attributed to the disruption of the CD47-SIRP α axis.⁸⁹ However, subsequent studies with Fab fragments of B6H12 proved that the original murine IgG1 mAb was also triggering Fc-dependent effector functions.⁹⁰ These results indicated that, in addition to the blockade of the CD47-SIRP α axis, a pro-phagocytic stimulus mediated by the Fc domain of an antibody was required in order to obtain an effective tumor cell clearance. Further investigations with an engineered high affinity SIRP α variant (SIRP α CV1), not able to promote tumor cell lysis neither *in vitro* nor *in vivo*, supported this idea (Figure 4B, right).⁹¹ In addition to this, the observation that CD47-blocking agents successfully synergized with tumor antigen-targeting antibodies and lead to an increased anti-tumor activity than the single components, motivated the view of CD47-blocking molecules as an adjuvant therapy (Figure 4C, left).^{70, 71}

A major drawback of CD47-targeting agents is the ubiquitous expression of CD47, which may not only act as an antigen sink, but also cause on-target/off-tumor toxicities. Even if

INTRODUCTION

this potential risk will be clarified with the ongoing clinical evaluation of CD47-blocking candidates, pre-clinical studies of SIRP α CV1 and Hu5F9-G4, a CD47-targeting human IgG4 mAb, already reported different levels of hematotoxicities in non-human primates.^{91, 92} In order to tackle this problem, more sophisticated fusion proteins have been developed. These include bsAbs targeting CD47 and a tumor antigen, such as CD20 or CD19 for B cell lymphoma, and mesothelin for pancreatic cancer (Figure 4C, right).^{93, 94} Interestingly, the affinity of the CD47-binding arm of these molecules was reduced in order to guide the binding to the tumor antigen-expressing cells and, accordingly, all bsAbs contained a functional Fc domain. The combination of the blockade of the CD47-SIRP α axis, the ability to induce Fc-mediated immune responses and the tumor specificity provided by the tumor-antigen binding arm led to very promising results *in vitro* and in xenograft mouse models.

In vivo studies with CD47-targeting agents demonstrated remarkable efficacy with significant reductions of tumor growth and extensions of survival for an impressive diversity of cancers.^{70, 71, 87, 88, 95-98} However, most of these experiments were performed using NOD/SCID or NOD/SCID/GAMMA (NSG) mice engrafted with human tumor cells. While these mouse models have been widely utilized for pre-clinical evaluation of many anti-tumor agents, they present some characteristics that may influence the effect of CD47-targeting drugs. First, NOD/SCID and NSG mice are immunocompromised mouse models that lack the adaptive immune system and this might oversimplify the immune response. Furthermore, the SIRP α expressed on cells from NOD mice has an affinity of 0.08 μ M for human CD47, whereas human SIRP α has an affinity of 0.6 μ M.⁹⁹ This 7-fold stronger binding of NOD SIRP α to human CD47 possibly emphasizes the CD47-SIRP α axis in these models and therefore a disruption of it may result in stronger effects. Lastly, as most of the CD47-targeting agents are not cross-reactive to murine CD47, they bypass the antigen sink created by the ubiquitously expressed murine CD47 and potential side effects cannot be detected. In order to have a more accurate evaluation of CD47-targeting therapeutics, mouse strains that do not derive from the NOD brand, like the BALB/c strain, which expresses the wildtype murine SIRP α with a 5.2 μ M affinity to human CD47, should be used.⁹⁹ However, human engraftment in such a mouse strain is less efficient than in the NOD strain and it limits the evaluation of therapeutic drugs for human cancers. Interestingly, the low engraftment rate in BALB/c mice is mainly attributed to the affinity of wildtype murine SIRP α to human CD47, since a higher CD47-

INTRODUCTION

SIRP α affinity promotes xenogeneic engraftment.¹⁰⁰ A new mouse model, so-called MISTRG, was generated in order to improve the engraftment of human cells.^{101, 102} MISTRG is a BALB/c-derived humanized mouse model knocked-in with genes encoding for human cytokines and, most importantly, bearing a BAC-transgene encoding for human SIRP α . As these characteristics lead to a better human cell engraftment, MISTRG mice are currently the best candidates to investigate more precisely the effects of CD47-targeting agents for cancer immunotherapy.

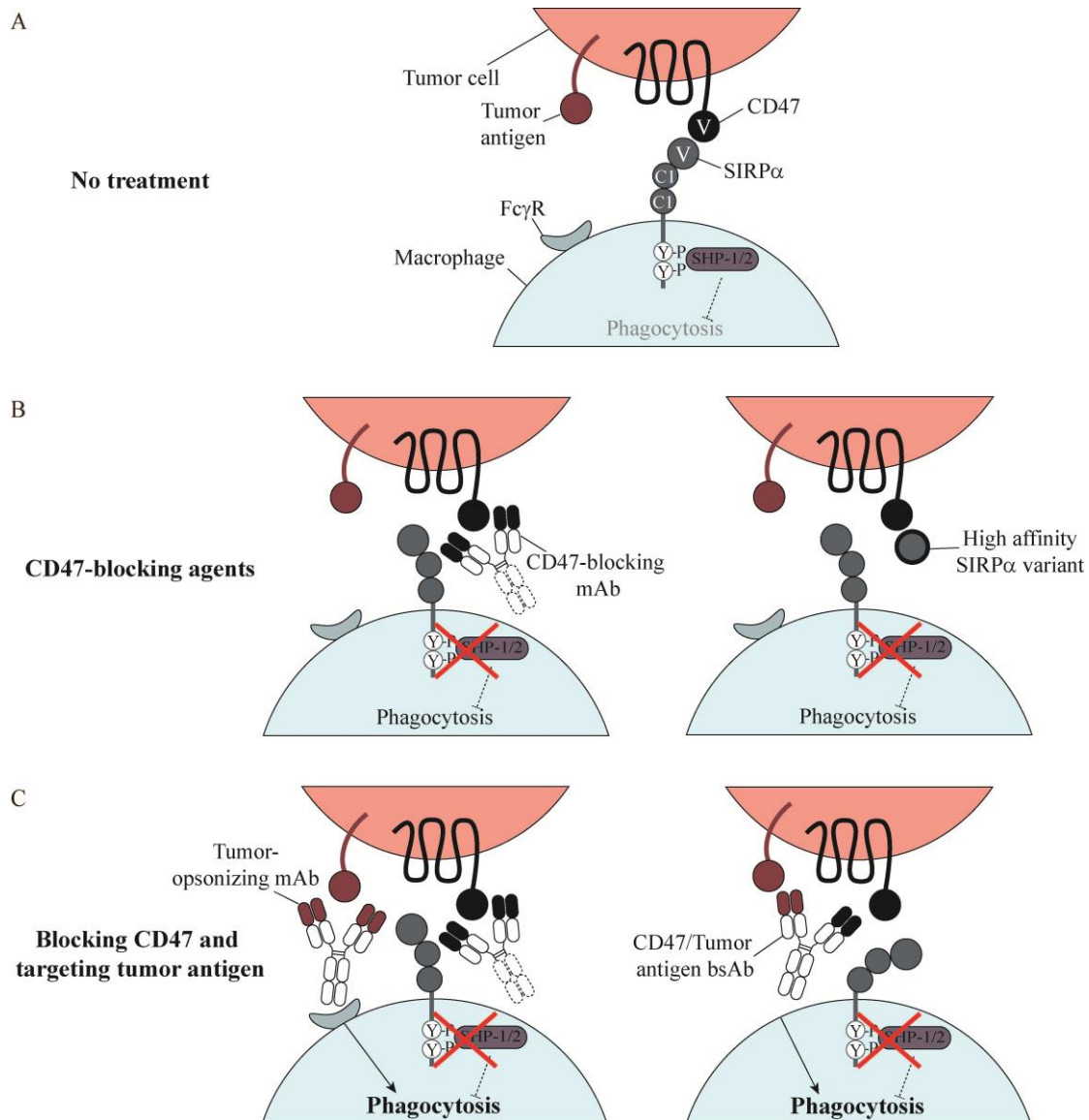
Approaches to target CD47 to disrupt the CD47-SIRP α interaction have been focus on describing macrophage-mediated effects. This is due to the direct involvement of the CD47-SIRP α axis in regulating phagocytosis and the lack of adaptive immune responses of the utilized mouse models. Notably, recent reports using immunocompetent mice have described that the blockade of CD47 not only potentiates phagocytosis of targeted tumor cells, but also triggers a T cell-mediated immune response. On one side, by inhibiting the CD47-SIRP α interaction, macrophages were shown to activate CD8⁺ T cells and decrease priming of CD4⁺ T cells, thus stimulating tumor-specific T cell responses.¹⁰³ On the other, the blockade of CD47 led to activation of primary DCs, but not macrophages, through stimulator of interferon genes (STING)-mediated DNA sensing followed by the cross-priming of CD8⁺ T cells against tumor antigens (Figure 4E).¹⁰⁴⁻¹⁰⁶ Despite the two described mechanisms by which a CD47-dependent T cell response is induced differ, these studies support the participation of the CD47-SIRP α innate immune checkpoint in the stimulation of adaptive immune responses.

Besides targeting CD47, another option to disrupt this immune checkpoint is to target SIRP α . Two different approaches have been so far investigated: mAbs against SIRP α and high affinity versions of the extracellular domain of CD47 (so-called velcro-CD47).¹⁰⁷⁻¹⁰⁹ Both strategies were evaluated in combination with tumor-opsonizing mAbs and efficiently enhanced ADCC and ADCP effects *in vitro* (Figure 4D). Furthermore, for hematological cancers, it has been described that engaging either CD47 or SIRP α with blocking mAbs eliminated tumor cells by promoting caspase-dependent or –independent apoptotic cell death.¹¹⁰⁻¹¹³

Accumulating evidences suggest the blockade of the CD47-SIRP α innate immune checkpoint as a promising strategy for cancer immunotherapy. Therapeutics targeting this axis, such as Hu5F9-G4 and SIRP α -Fc fusions, recently entered early phases of clinical

INTRODUCTION

trials for solid and hematological malignancies, being investigated either as a monotherapy or in combination with tumor-opsonizing mAbs or other immune checkpoints inhibitors.¹¹⁴ First clinical results are expected to provide a better understanding of the potential efficacy as well as toxicity of high affinity CD47-targeting agents. Nevertheless, novel strategies to confine the benefits of the blockade of the CD47-SIRP α immune checkpoint to tumor cells to avoid systemic side effects are being under pre-clinical evaluation.



INTRODUCTION

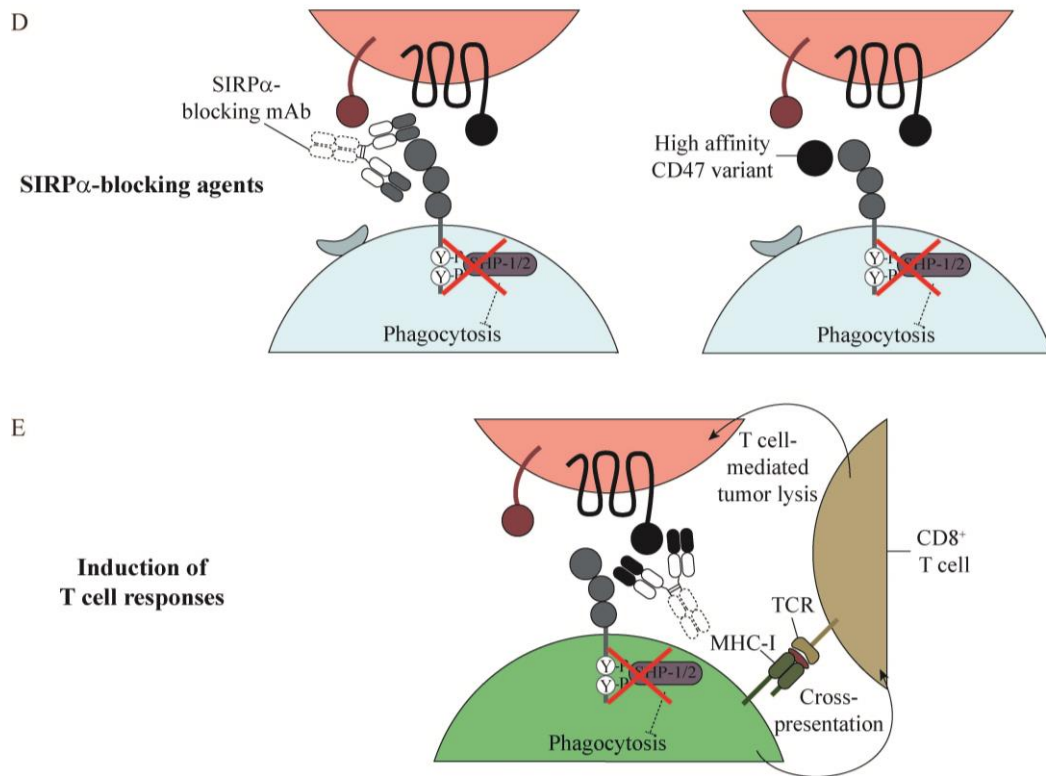


Figure 4. The CD47-SIRPα innate immune checkpoint as a target for cancer immunotherapy

(A) Tumor cells escape the immune attack by upregulating CD47, which binds to SIRPα expressed on myeloid cells. Upon binding, tyrosine residues of the ITIM motifs in the cytoplasmic tail of SIRPα are phosphorylated and SHP-1 and SHP-2 phosphatases (SHP-1/2) are recruited. SHP-1/2 dephosphorylate several substrates and ultimately lead to the inhibition of tumor cell-phagocytosis. V, V-set domain; C1, C1-set domain. (B) One of the mechanisms to disrupt the CD47-SIRPα immune checkpoint is to engage CD47 with either CD47-blocking mAb (left) or high affinity SIRPα variants, such as SIRPα CV1 (right), both not triggering active immune responses. (C) These CD47-blocking agents have been combined with tumor-opsonizing mAbs in order to induce an activating signal through FcγRs and obtain a more potent tumor-specific immune response. This has been achieved either by combination therapy (left) or by generating bsAbs targeting CD47 and a tumor antigen (right). (D) Targeting SIRPα by either blocking mAbs (left) or high affinity CD47 variants (velcro-CD47, right), is another approach to disrupt the CD47-SIRPα immune checkpoint. (E) In addition to the explained macrophage-mediated immune responses, disrupting the CD47-SIRPα axis in DCs triggers DC's activation and cytosolic DNA sensing through the STING pathway. This leads to tumor-antigen cross-presentation to CD8⁺ T cells and a T cell-mediated tumor lysis.

2.3. Acute Myeloid Leukemia

Acute myeloid leukemia (AML) is a hematological disorder that arises from an abnormal expansion of myeloid stem cell clones and subclones in the bone marrow and the peripheral blood.¹¹⁵ It is the most common type of acute leukemia, with approximately 18,000 individuals in Europe and 20,000 in the United States diagnosed every year.

INTRODUCTION

Additionally, AML is a very aggressive leukemia, presenting an overall five years survival rate of 25% and being fatal within months if untreated.¹¹⁶ The median age of AML patients at initial diagnosis is 67 years and one third of the patients are older than 75 years, but an age of 60 years or older is associated with poor outcomes.^{117, 118}

Etiologically, AML can be originated *de novo*, derived from previous myeloid proliferative disorders or caused by prior exposure to chemotherapy.¹¹⁹ The advent of next generation sequencing improved the understanding of AML and led to a better classification and risk stratification of the patients. Moreover, it shed some light on the clonal evolution during treatment, the development of resistance mechanisms and the causes of relapse.^{115, 120} It has become evident that AML is not a homogenous disease, but rather an assembly of many genetically unique subtypes in one patient. An average of thirteen mutations have been identified to occur in each AML patient, eight of them being random (or passenger) and five of them recurrent (or driver).¹²¹ Importantly, these mutations influence the prognosis and the treatment of the patients.¹²¹ For instance, NPM1 mutations with monocytic morphology and intact FLT3 predict favorable overall survival, while DNMT3A mutations are associated with a poor prognosis.^{116, 122} These factors are taken into account in the current classification system, which was described by the World Health Organization (WHO) and replaced the old French-American-British (FAB) classification. There are seven AML subtypes according to the WHO: (1) AML with recurrent genetic abnormalities and with NPM1 and CEBPA gene mutations, (2) AML with myelodysplasia-related changes, (3) AML with therapy-related myeloid neoplasms, (4) AML not otherwise specified, (5) myeloid sarcoma, (6) myeloid proliferation related to down syndrome and (7) blastic plasmacytoid dendritic cell neoplasm.¹²³

Nevertheless, despite recent developments in the understanding, the diagnosis and the classification of AML, the treatment of this disease did not improve over the last decades and the prognosis remains grim.

2.3.1. Current treatments for AML patients

Since 1970s, the first-line treatment for AML patients with a good performance status is induction chemotherapy.¹¹⁷ The goal of induction chemotherapy is that AML patients achieve complete remission (CR), which is defined as less than 5% blast in the bone marrow and less than 1,000 neutrophils and 100,000 platelets per µl of peripheral

INTRODUCTION

blood.¹²⁴ Patients that achieve CR after the first chemotherapy cycle, which are 65-73% of the patients younger than 60 years and 38-62% of the patients older than 60 years, proceed to consolidation therapy.¹¹⁶ Patients with a poor performance status, not eligible for induction therapy, receive lower doses of chemotherapy as a palliative measure or best supportive care.

Consolidation therapy is administered in order to eradicate the so-called minimal residual disease (MRD) and prevent relapse. MRD is caused by leukemic cells that resisted induction chemotherapy. These resistant leukemic cells, also known as AML leukemic stem cells (LSC), are believed to continue proliferating and cause the return of the disease or relapse. Depending on the individual risk of the patient, consolidation therapy consists of either chemotherapy, allogeneic hematopoietic stem cell transplantation (allo-SCT) or a combination of both.^{116, 125, 126} Allo-SCT is the most effective long-term treatment for AML and results in cure for 30-40% of the treated patients in first CR. However, comorbidities, failure to achieve CR and the lack of suitable donors reduce the number of patients suitable for allo-SCT to 25-35%.¹²⁷

Despite consolidation therapy, AML LSC may not be fully eliminated and patients may require a second cycle of induction chemotherapy to achieve a second CR. After the first relapse, the five year survival rate is only 11%, indicating that the second CR is accomplished by a minority of the patients.¹²⁸ Hence, there is an urgent need to develop novel immunotherapies in order to eliminate MRD and prevent relapse of AML patients.

2.3.2. Immunotherapy in AML

Most of the advances in immunotherapy to treat hematological malignancies have been made for B-cell lymphomas, such as acute lymphoblastic leukemia (ALL). In contrast to AML, conventional mAbs (e.g. rituximab) and BiTEs (e.g. blinatumomab) are already considered first-line treatment for ALL.^{129, 130} Hope is high that the clinical efficacy of these agents will be translated into AML, but most of the immunotherapeutic strategies for AML are still under development.¹³¹

One disadvantage of immunotherapy for AML is the broad expression pattern of its antigens. Whereas ALL antigens present a more restricted expression, AML antigens can also be expressed on healthy immature myeloid cells. Nonetheless, several AML antigens have been identified as potential targets for immunotherapeutic agents.¹³² Amongst them,

INTRODUCTION

CD33 and CD123 are the most commonly targeted antigens in AML.¹³³ CD33, a member of the sialic acid immunoglobulin like lectins (siglecs), is expressed on HSCs, particularly on early stages of myeloid differentiation. Importantly, expression levels are significantly increased in AML blasts and AML LSCs, identifying CD33 as a promising tumor antigen.¹³⁴ CD33 consists of two Ig-like extracellular domains with V-set and C2-set structures, a transmembrane region and a cytoplasmic tail.^{135, 136} The cytoplasmic tail contains two ITIM motifs, which upon extracellular engagement of CD33 are phosphorylated and recruit SHP-1 and SHP-2. These phosphatases dephosphorylate CD33 as negative feedback loop and may also negatively regulate nearby receptors.¹³⁷ Furthermore, suppressor of cytokine signaling 3 (SOCS3) binds to phosphorylated CD33, thus competing with SHP-1 and SHP-2 and recruiting the ECS E3 ubiquitin ligase complex. This induces the ubiquitination of several residues of the cytoplasmic tail and leads to CD33 internalization and proteasomal degradation.¹³⁸ The function of CD33 remains not fully understood, but it has been described to negatively regulate inflammatory and immune responses.^{139, 140}

Over the last three decades, several attempts have been made to use CD33 as a therapeutic target in AML. The most known CD33-targeting agent is GO, an IgG4 mAb conjugated to calicheamicin that utilizes the internalization capabilities of CD33 to deliver a drug inside the cell. As mentioned before, GO received accelerated FDA approval in 2000, but it was voluntarily withdrawn from the market in 2010 due to safety concerns and lack of clinical efficacy.^{141, 142} In 2017, however, the re-evaluation of GO in clinical trials re-gained the FDA approval with a new dosage and administration schedule.¹⁴³ Furthermore, a next generation CD33-targeting ADC, SGN-CD33A, was developed and entered clinical trials.¹⁴⁴ Besides ADCs, conventional mAbs targeting CD33 have also been clinically tested. Lintuzumab (SGN-33), a CD33-specific IgG1 mAb, showed a very promising anti-tumor activity in pre-clinical studies. However, clinical tests resulted in very little benefits for AML patients and this led to the termination of the clinical trials in 2010.^{145, 146} An Fc-engineered α CD33 mAb, BI 836858, with increased binding for Fc γ R2, was created as an improved strategy and is being evaluated in phase I clinical trials.^{147, 148} Other immunotherapeutic agents targeting CD33 in clinical development are bispecific constructs, such as BiTEs and BiKEs. AMG 330, a CD33-specific BiTE, entered clinical trials addressing safety and efficacy in 2015 after very promising pre-clinical results.^{134, 149} Similarly, a CD33-targeting BiKE

INTRODUCTION

induced potent NK cell-mediated cytotoxicity of AML cells *in vitro* and it is expected to enter clinical trials in the near future.^{46, 150} In addition, CD33-directed chimeric antigen receptor (CAR) T cells, which reduced the burden of human AML cells in *in vivo* studies with immunodeficient mice, are also being tested in a clinical setting.¹⁵¹

Besides targeting tumor antigens, immune checkpoint inhibitors are also under investigation for the treatment of AML. Previous studies described CD47 to be upregulated on AML cells and LSCs and to be associated with a poor prognosis, supporting the blockade of the CD47-SIRP α axis as a strategy for immunotherapy of AML.^{70, 152, 153} Moreover, the CD47-blocking mAb B6H12 mediated phagocytosis of AML cells *in vitro* and inhibited the engraftment of AML LSC *in vivo*.⁷⁰ In mice engrafted with AML LSCs, the administration of B6H12 resulted in the clearance of tumor cells through macrophage-mediated phagocytosis. These successful pre-clinical results led to the evaluation in clinical trials of two mAbs targeting CD47, Hu5F9-G4 and CC-90002. The ubiquitous expression of CD47 and the hematotoxicities caused by CD47-targeting agents in *in vivo* studies, however, raise some concerns on the potential toxicity of these checkpoint inhibitors. In order to achieve effective anti-tumor responses while minimizing the risk of side effects, the blockade of the CD47-SIRP α immune checkpoint should be restricted to AML cells. This confinement can be obtained, for example, with a high affinity tumor-specific mAb that guides the blockade of the immune checkpoints to tumor antigen-expressing cells. Accordingly, single molecules that combine AML antigen-targeting and the blockade of the CD47-SIRP α axis constitute a very promising and potentially safe approach to mediate the elimination of AML cells.

3. AIM OF THE THESIS

Despite recent advances in the understanding of AML, most of the patients still relapse and ultimately succumb to the disease. Hence, novel immunotherapies are required to lower relapse rates and offer a better prognosis to AML patients. The blockade of immune checkpoints has become one of the most promising approaches to induce anti-tumor responses. However, immune checkpoint inhibitors also revealed immune related adverse events due to on-target/off-leukemia toxicities.

As an improved strategy for the treatment of AML, this work aimed at exploiting the benefits of blocking the CD47-SIRPα myeloid-specific immune checkpoint to promote the clearance of AML cells, while lowering side effects. The specific blockade of the CD47-SIRPα axis on AML cells was achieved by engrafting the endogenous N-terminal domain of SIRPα, which has a physiologically low affinity for CD47, to a mAb or derivative thereof targeting the AML antigen CD33. In contrast to the high affinity CD47 inhibitors, the SIRPα domain is unable to effectively bind to CD47-expressing cells by itself. The binding to tumor cells is therefore facilitated by the high affinity binding to CD33. As a consequence, SIRPα-αCD33 molecules should only bind and disrupt the anti-phagocytic CD47-SIRPα immune checkpoint on CD33-expressing AML cells.

In order to find an optimized approach, three antibody formats were generated: local inhibitory checkpoint mAbs (licMABs), single-arm licMABs (licMABs^{single}) and local inhibitory checkpoint antibody derivatives (liCADs). All local inhibitory molecules bind to the AML antigen CD33 with high affinity, block the CD47-SIRPα immune checkpoint with the endogenous SIRPα domain and activate immune effector cells. Nevertheless, licMABs, licMABs^{single} and liCADs differ on the binding valency and the nature of the immune cell-activating domain, which has an impact on their efficacy. The most promising candidate was selected based on tumor-specificity and capability to enhance the elimination of AML cell lines and primary AML cells via ADCC and ADCP mechanisms *in vitro*.

RESULTS

4. RESULTS

4.1. Cloning and expression of local inhibitory checkpoint molecules

During this work, three types of molecules, local inhibitory checkpoint monoclonal antibodies (licMAB), single-arm licMABs (licMABs^{single}) and local inhibitory checkpoint antibody derivatives (liCADs) were designed, generated and characterized. All molecules target the AML antigen CD33, recruit immune effector cells via interactions with FcγRs and inhibit the CD47-SIRPα axis by blocking CD47 antigens expressed on tumor cells. However, the molecular architecture of these proteins differs, thus allowing the evaluation of various antibody formats in the same AML context.

4.1.1. Local inhibitory checkpoint monoclonal antibodies (licMABs)

LicMABs are IgG1 mAbs that bind to CD33 and contain either one or two SIRPα domains (here denominated as SIRPα-αCD33 or 2xSIRPα-αCD33, respectively). The SIRPα domain, located at the N-terminus of the light chain, is designed to interact with CD47 on CD33⁺ AML cells and therefore locally block the CD47-SIRPα myeloid-specific immune checkpoint. In order to investigate the benefits of the SIRPα domain of licMABs, a conventional αCD33 mAb was produced. The following DNA vectors were cloned for expression and purification of licMABs and αCD33 mAb (Figure 5). All vectors contain the IgKappa leader sequence, which facilitates the secretion of the protein in the cell culture media.

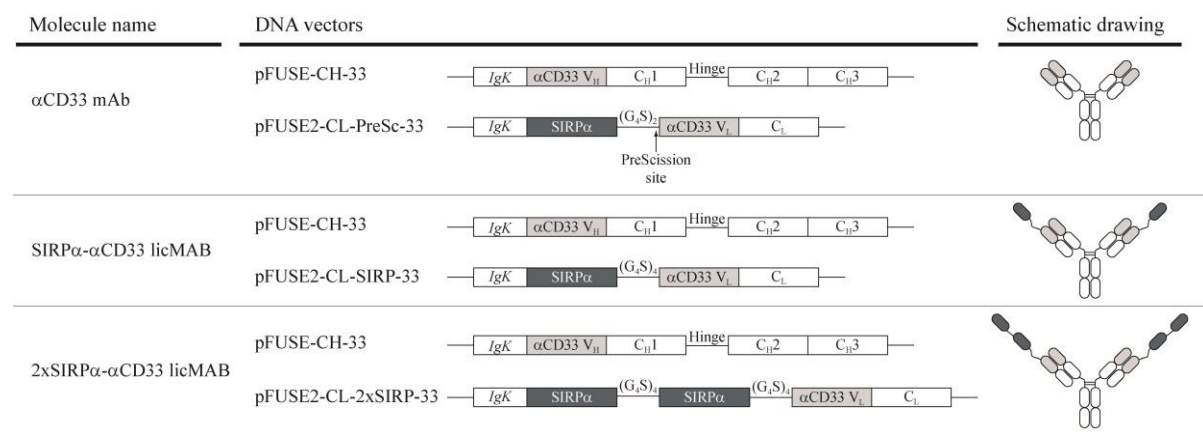


Figure 5. Schematic view of local inhibitory checkpoint monoclonal antibodies (licMABs) and encoding DNA vectors

RESULTS

LicMABs were purified from Expi293F cells by protein A chromatography. To obtain the α CD33 mAb, the SIRP α domain was cleaved by PreScission protease. Size exclusion chromatography (SEC) with a Superdex 200 GL column was performed as a second purification step (Figure 6A-C). The single SEC peak obtained for all the molecules demonstrated the absence of significant aggregations, degradations or contaminations. The purity of the purified molecules was further evaluated by sodium dodecyl sulfate polyacrylamide gel electrophoresis (SDS-PAGE) analysis (Figure 6D). As depicted on the SDS-PAGE, heavy and light chains of licMABs and mAb were expressed equimolarly and corresponded to the computed masses. Moreover, α CD33 mAb, SIRP α - α CD33 licMAB and 2xSIRP α - α CD33 licMAB were purified in high quantities, with yields of 31.0, 83.5 and 67.5 mg/L of culture medium, respectively.

Taken together, these results show that α CD33 mAb, SIRP α - α CD33 licMAB and 2xSIRP α - α CD33 licMAB can be produced in monomeric species and with high yields.

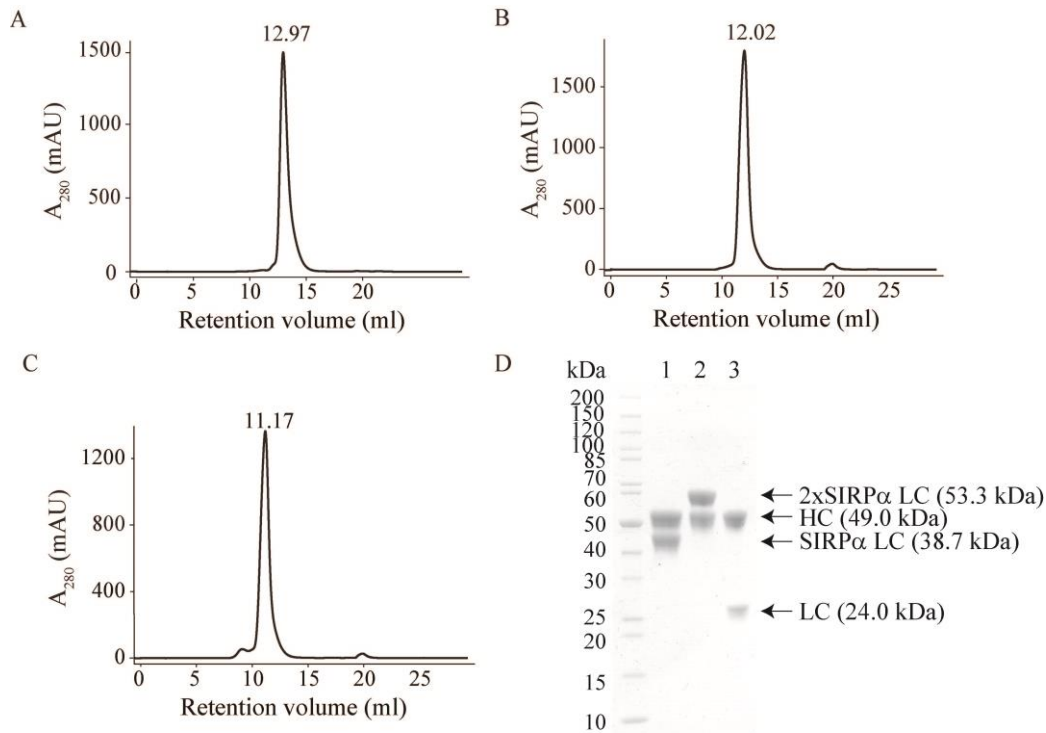


Figure 6. Purification of local inhibitory checkpoint monoclonal antibodies (licMABs)

Size exclusion chromatography of (A) α CD33 mAb, (B) SIRP α - α CD33 licMAB and (C) 2xSIRP α - α CD33 licMAB performed with a Superdex 200 increase 10/300 GL column after protein A purification. Retention volume at which the protein was eluted is indicated. (D) SDS-PAGE analysis of purified (1) α CD33 mAb, (2) SIRP α - α CD33 licMAB and (3) 2xSIRP α - α CD33 licMAB under reducing conditions. Computed masses of each antibody chain are indicated.

RESULTS

4.1.2. Single-arm local inhibitory checkpoint monoclonal antibodies (licMABs^{single})

LicMABs^{single} were derived from licMABs and kindly provided by Dr. Anna Kaufmann. The single-arm molecules target CD33 with one Fab fragment. The second Fab fragment was replaced by the endogenous SIRP α domain. MAb^{single}, a control molecule that does not contain the endogenous SIRP α domain, was as well generated. In order to assure the correct pairing of the two distinct heavy chains, charged mutations were inserted at the C_H3 domain, thus obtaining a positively and a negatively charged HC (HC^{K392D, K409D} and HC^{E356K, D399K}, respectively).⁴¹ Therefore, three vectors were transfected to Expi293F cells to obtain licMABs^{single} and mAb^{single} (Figure 7).

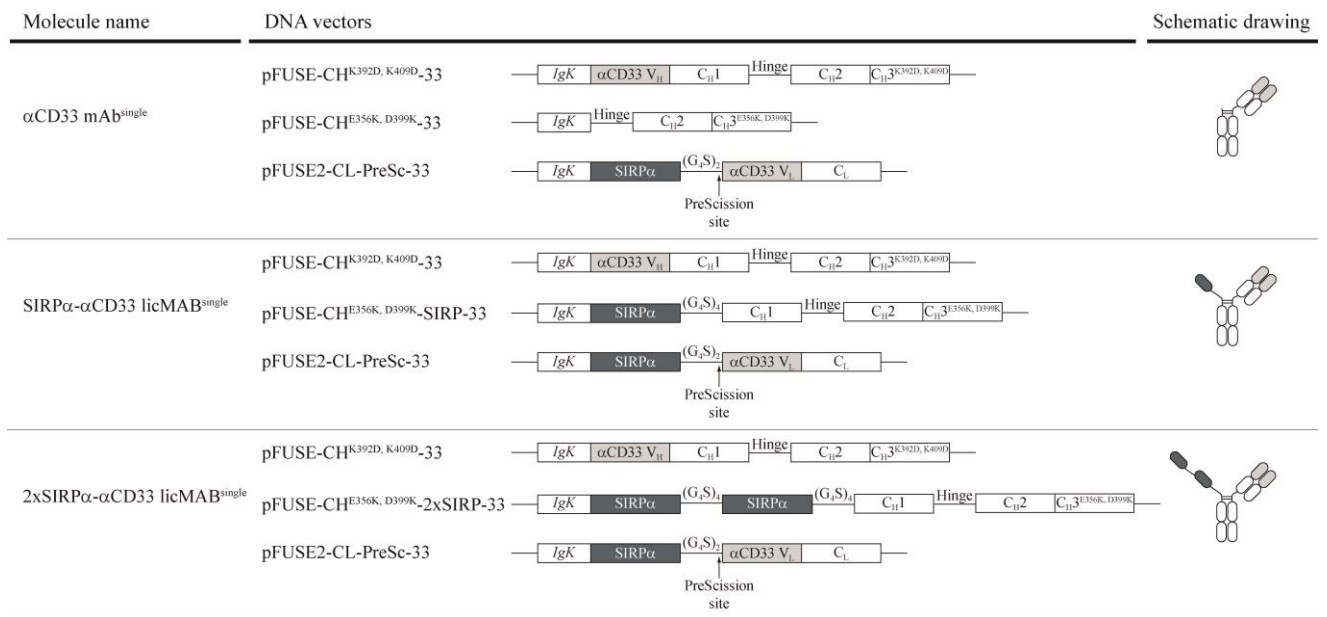


Figure 7. Schematic view of single-arm local inhibitory checkpoint monoclonal antibodies (licMABs^{single}) and encoding DNA vectors

Since the vector pFUSE2-CL-PreSc-33, encoding for the LC, was used to express mAb^{single} and licMABs^{single}, the purification of these molecules required protein A chromatography and PreScission protease treatment. A final SEC showed the presence of monomeric peaks corresponding to retention volumes of 13.85, 12.90 and 12.24 for α CD33 mAb^{single}, SIRP α - α CD33 and 2xSIRP α - α CD33 licMAB^{single}, respectively (Figure 8A-C). A second peak at retention volume 16.17 was obtained for mAb^{single}, which could be attributed to degradations or impurities. No degradations were observed on SEC of licMABs^{single}, but aggregation peaks were present, presumably due to the incorrect pairing of the distinct heavy chains. SDS-PAGE analysis confirmed the absence of contaminations and degradations on the collected samples (Figure 8D). Three different

RESULTS

bands were observed for all the purified molecules, corresponding to the HC^{E356K, D399K}, the HC^{K392D, K409D} and the LC, all in agreement with the computed masses.

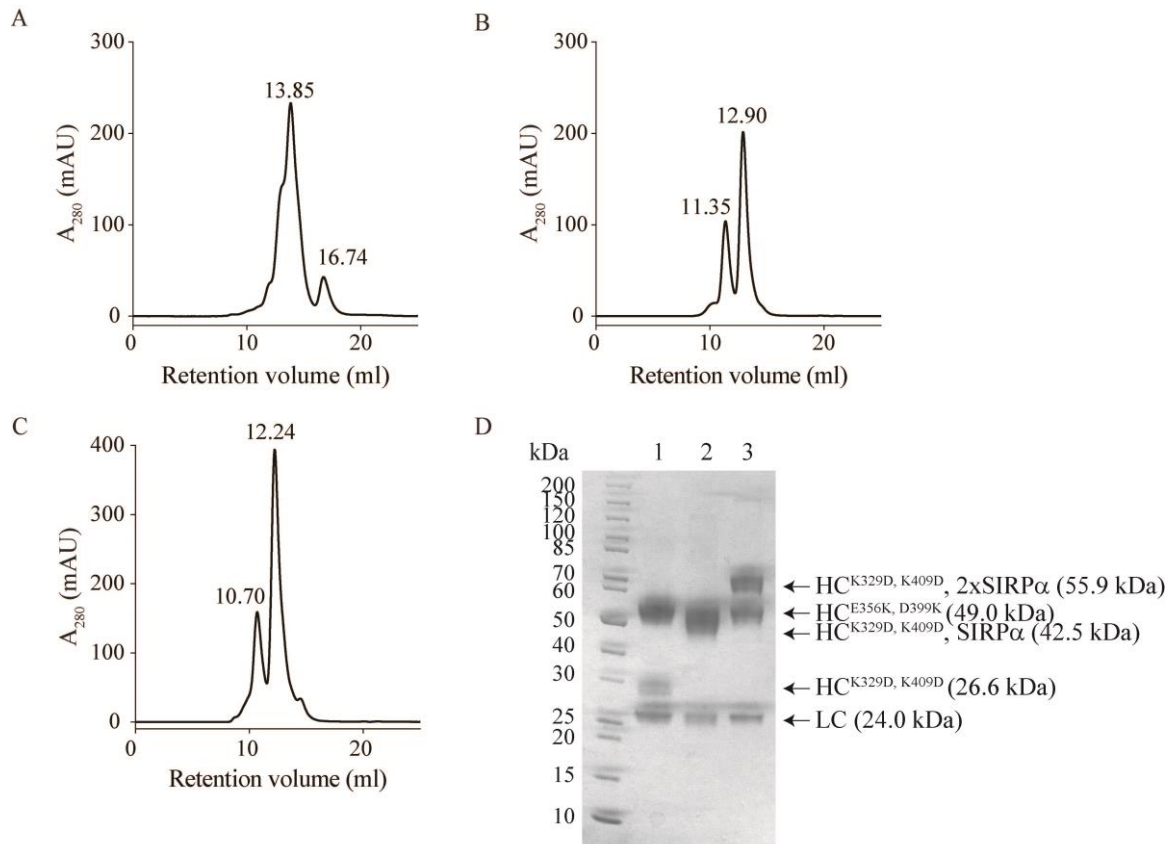


Figure 8. Purification of single-arm local inhibitory checkpoint monoclonal antibodies (licMABs^{single})
Size exclusion chromatography of (A) α CD33 mAb^{single}, (B) SIRP α - α CD33 licMAB^{single} and (C) 2xSIRP α - α CD33 licMAB^{single} performed with a Superdex 200 increase 10/300 GL column after protein A purification and PreScission protease treatment. Retention volumes of monomeric peaks, aggregations and degradations are indicated. (D) SDS-PAGE analysis of purified (1) α CD33 mAb^{single}, (2) SIRP α - α CD33 licMAB^{single} and (3) 2xSIRP α - α CD33 licMAB^{single} under reducing conditions. Computed masses of each antibody chain are displayed.

To sum up, the yield of mAb^{single} and licMABs^{single} was lower than mAb and licMABs due to the protein loss in aggregations and degradations. Nevertheless, monomeric species of mAb^{single} and licMABs^{single} could be obtained and were used for further experiments.

4.1.3. Local inhibitory checkpoint antibody derivatives (liCADs)

LiCADs are single polypeptide molecules based on the BiKE format (Figure 9).⁴⁶ These molecules, cloned into the pExpreS2-1 vector, consist of two scFvs against CD16 and CD33 connected by a (G₄S)₄ linker. The third domain of liCADs, located N-terminally and preceding a (G₄S)₄ linker, is the extracellular endogenous SIRP α domain. Similarly to

RESULTS

licMABs and licMABs^{single}, liCADs target the AML antigen CD33 and simultaneously inhibit the CD47-SIRP α axis. On the contrary, liCADs lack the Fc domain and therefore activate effector cells by a scFv targeting the Fc γ RIII (CD16). In addition, a His₆-tag was fused C-terminal of the construct for purification reasons.

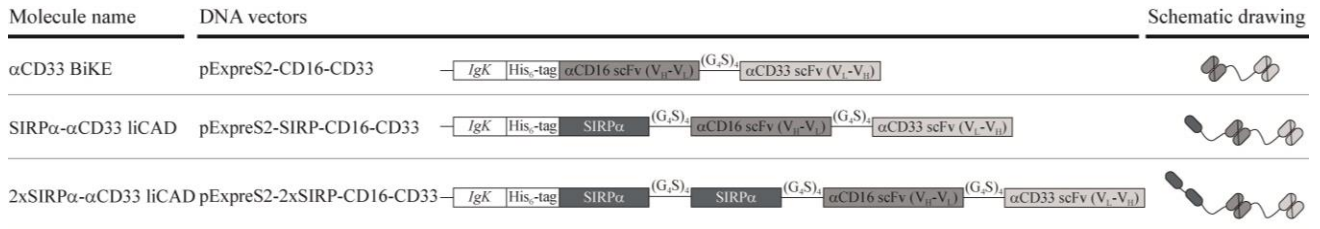


Figure 9. Schematic view of local inhibitory checkpoint antibody derivatives (liCADs) and encoding DNA vectors

LiCADs and the control molecule α CD33 BiKE were purified from Schneider S2 cells by nickel-nitrilotriacetic acid (Ni-NTA) affinity chromatography and anion exchange chromatography, kindly performed by Dr. Nadine Magauer and Saskia Schmitt. To ensure protein quality, an analytical SEC was executed (Figure 10A-C). SEC chromatograms showed very little aggregation peaks for α CD33 BiKE and liCADs, indicating that these proteins were mainly present in its monomeric form. Purity was further confirmed by SDS-PAGE analysis, where no aggregation or degradation was visible (Figure 10D). Furthermore, protein bands on the SDS-PAGE corresponded to the computed masses of BiKE and liCADs.

Overall, the integrity and purity of liCADs and α CD33 BiKE demonstrated by SEC and SDS-PAGE analysis qualified these molecules for further studies.

RESULTS

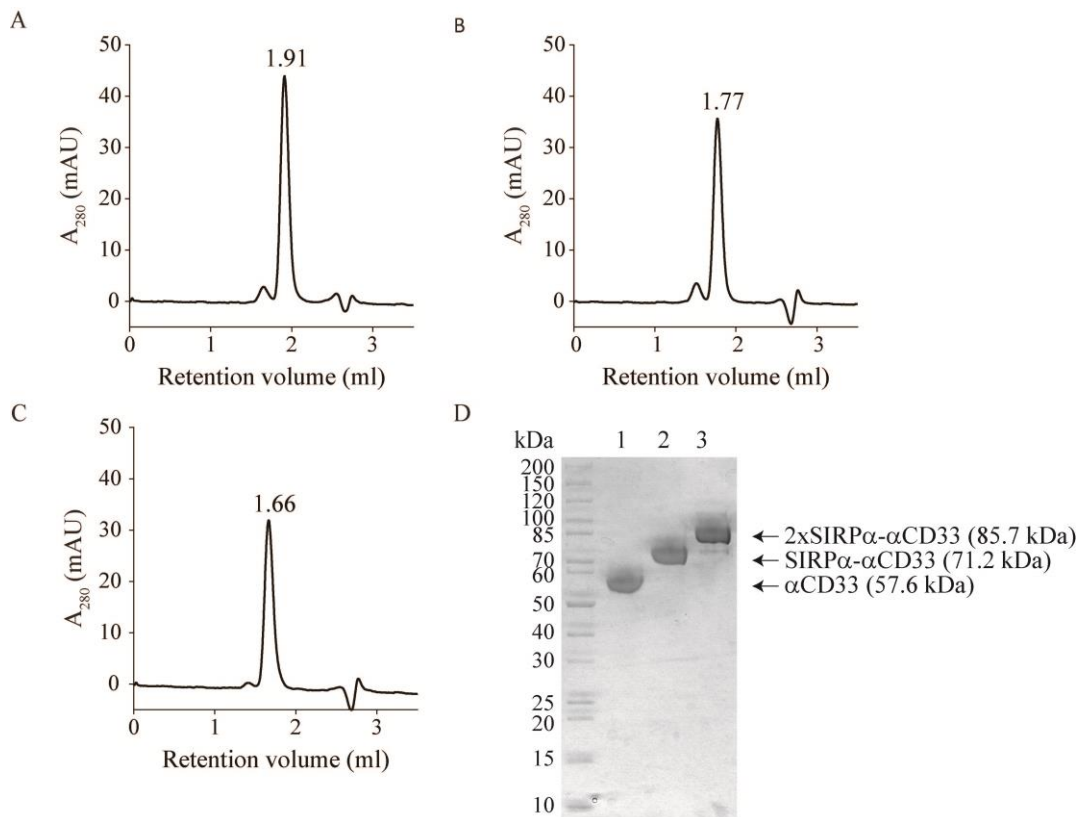


Figure 10. Purification of local inhibitory checkpoint antibody derivatives (liCADs)

Analytical size exclusion chromatography of (A) α CD33 BiKE, (B) SIRP α - α CD33 liCAD and (C) 2xSIRP α - α CD33 liCAD performed with a Superdex 200 increase 5/150 GL column. Retention volume of monomeric peaks is displayed. (D) SDS-PAGE analysis of purified (1) α CD33 BiKE, (2) SIRP α - α CD33 liCAD and (3) 2xSIRP α - α CD33 liCAD under reducing conditions. Computed masses of each antibody chain are indicated.

4.2. Biochemical characterization of local inhibitory checkpoint molecules

4.2.1. Thermal stability

In order to study the stability of the local inhibitory checkpoint molecules, fluorescence thermal shift assays were performed (Figure 11, data kindly provided by Saskia Schmitt). Of all antibody formats, liCMABs displayed the highest melting points (Figure 11A). The melting temperatures of liCMABs^{single} were similar than liCMABs, suggesting that the pairing of the positively and negatively charged HC does not significantly influence the thermal stability (Figure 11B). However, the SIRP α domains have a slight impact on the thermal stability of liCMABs and liCMABs^{single}.

In comparison to liCMABs and liCMABs^{single}, the recorded melting points of liCADs were lower (Figure 11C and D). This is explained by the fact that Fab fragments are the domains most sensitive to heat treatment within a full mAb.¹⁵⁴ Since liCADs consists of

RESULTS

scFvs, it is expected that the melting temperature of these is lower than licMABs and licMABs^{single}. Nevertheless, it is important to note that the melting points of all local inhibitory checkpoint molecules were higher than 37°C, demonstrating the stability of licMABs, licMABs^{single} and liCADs at body temperature.

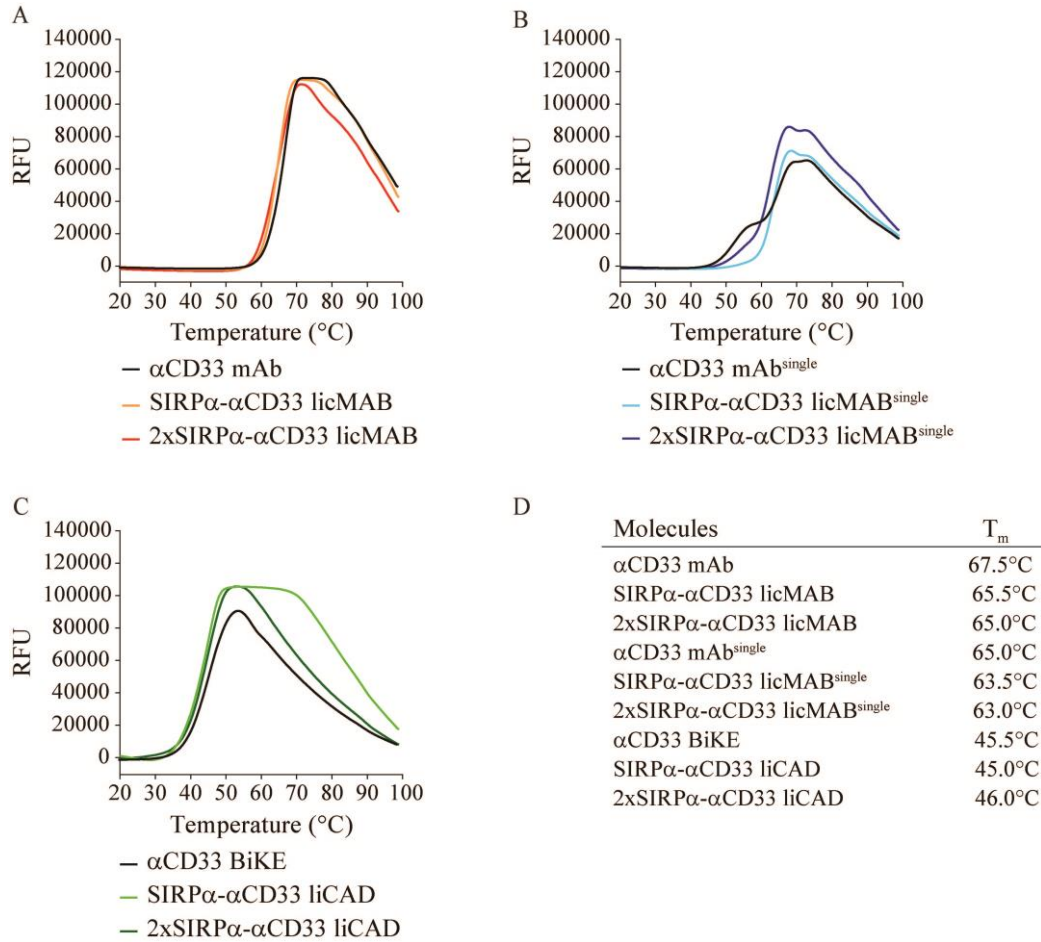


Figure 11. Thermal stability of local inhibitory checkpoint molecules

Melting curves of (A) licMABs, (B) licMABs^{single} and (C) liCADs were determined by fluorescence thermal shift assays. RFU, relative fluorescence units. (D) Measured melting temperatures of each molecule.

4.2.2. Binding of local inhibitory checkpoint molecules to tumor cells

Local inhibitory checkpoint molecules were designed to bind to the AML antigen CD33 and locally inhibit the CD47-SIRP α axis on tumor cells. In order to characterize the ability of local inhibitory checkpoint molecules to bind to CD33 and CD47 antigens, four different cell lines were used. MOLM-13, a CD33- and CD47-expressing AML cell line derived from the peripheral blood of a patient with AML at relapse, was the main cell line used throughout this thesis. The SEM cell line was established from the peripheral blood

RESULTS

of a patient with ALL at relapse. Since SEM cells express CD47 but not CD33, this cell line was used to study the interaction of licMABs, licMABs^{single} and liCADs to CD47 independent of CD33. Moreover, Flp-INTM-CHO cells were stably transfected with CD33 and CD47 to obtain single positive cell lines, here designated as CHO_CD33 and CHO_CD47.

Preceding the binding studies, CD33 and CD47 antigens expressed on the above mentioned cell lines were quantified by calibrated flow cytometry (Table 1). MOLM-13 cells express around 50 thousand CD33 surface molecules and around 9 thousand CD47, which is in agreement with previous studies.^{69, 149, 155} CD33 is expressed 4.4-fold higher on CHO_CD33 cells than on MOLM-13 cells and CD47 expression is 3.3-fold higher on SEM cells and 68.8-fold higher on CHO_CD47 cells than on MOLM-13 cells.

Table 1. Quantification of CD33 and CD47 surface antigens expression on cell lines (number of surface antigens per cell)

Cell line	CD33	CD47
MOLM-13	$53.1 \times 10^3 \pm 2.8 \times 10^3$	$8.6 \times 10^3 \pm 1.3 \times 10^3$
SEM	negative	$28.7 \times 10^3 \pm 5.3 \times 10^3$
CHO_CD33	$232.0 \times 10^3 \pm 31.6 \times 10^3$	negative
CHO_CD47	negative	$600.3 \times 10^3 \pm 73.9 \times 10^3$

Flow cytometry-based binding studies of local inhibitory checkpoint molecules revealed that all molecules comparably bind to MOLM-13 cells (Figure 12). Due to the elevated amount of CD33 and CD47 antigens expressed on CHO_CD33 and CHO_CD47 cells, these cell lines were used to assess the capability of the binding domains to interact with CD33 and CD47 (Figure 12A). The staining intensity of both licMABs to CHO_CD47 cells was comparable and extremely high due to the elevated surface expression of CD47 on these cells. Since SEM cells express CD47 to a similar level than human RBCs, binding studies with the SEM cell line were performed in order to characterize the SIRP α domain.¹⁵⁶ Notably, binding to SEM cells correlated with the quantity of SIRP α domains on the molecules and was detected for local inhibitory checkpoint molecules containing at least two SIRP α domains, such as SIRP α - α CD33 licMAB, 2xSIRP α - α CD33 licMAB and 2xSIRP α - α CD33 licMAB^{single} (Figure 12B). A less prominent binding was determined by

RESULTS

2xSIRP α - α CD33 liCAD and no binding was perceived for molecules with a single SIRP α domain (SIRP α - α CD33 licMAB^{single} and SIRP α - α CD33 liCAD).

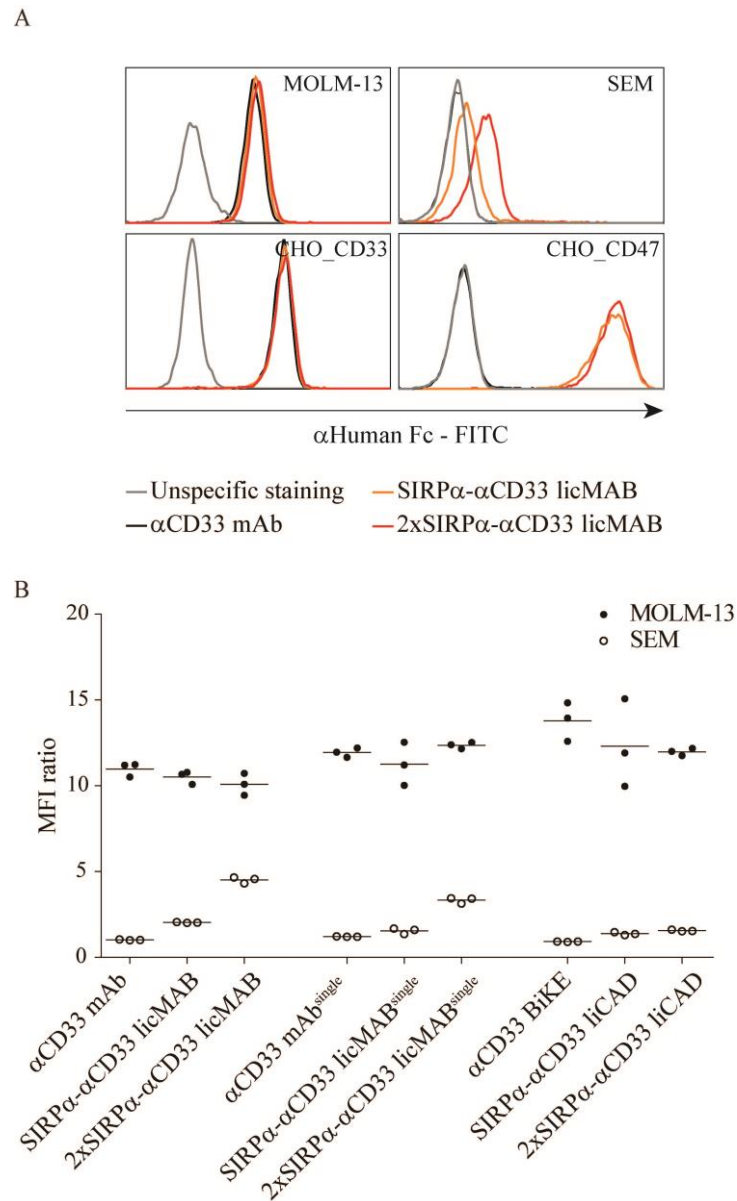


Figure 12. Binding analysis of local inhibitory checkpoint molecules to cell lines

(A) Exemplary histograms of mAb and licMABs binding to MOLM-13, SEM, CHO_CD33 and CHO_CD47 cells. Binding was detected by flow cytometry with a FITC-conjugated secondary antibody. Grey line shows unspecific staining of the secondary antibody to the corresponding cells. (B) Binding of all local inhibitory checkpoint molecules on MOLM-13 and SEM cells. Experiments with MOLM-13 and SEM were carried out separately. Median fluorescence intensity (MFI) ratio of specific antibody staining with respect to the unspecific staining is displayed.

After describing the ability of local inhibitory checkpoint molecules to bind to CD33⁺ MOLM-13 cells, a quantitative characterization of the binding strength of licMABs, licMABs^{single} and liCADs was performed. To this end, MOLM-13 cells were incubated

RESULTS

with increasing concentrations of local inhibitory checkpoint molecules and the binding avidity of the molecules was analyzed by calibrated flow cytometry (Figure 13).

All local inhibitory checkpoint molecules comparably bound to MOLM-13 cells, obtaining half maximum binding values in the low nM range, which is in agreement with other CD33-binding agents.^{144, 147, 149} The stronger binding to MOLM-13 cells was described for α CD33 mAb and α CD33 mAb^{single}, followed by single or double SIRP α licMABs and licMABs^{single} (Figure 13A and B). LiCADs, however, bound to MOLM-13 cells with a lower binding strength, obtaining half maximal binding values between 15 and 30 nM (Figure 13C). Interestingly, the avidity of licMABs for MOLM-13 cells slightly decreased with the addition of SIRP α domains. This effect, not observed for licMABs^{single} and liCADs, suggested that the location of the SIRP α domain at the N-terminus of the light chain may disturb the CD33-binding site.

In conclusion, all local inhibitory checkpoint molecules bound to MOLM-13 with high affinity and weakly interacted with CD47. Moreover, the binding strength was minimally influenced by the presence of SIRP α domains or its interaction with CD47.

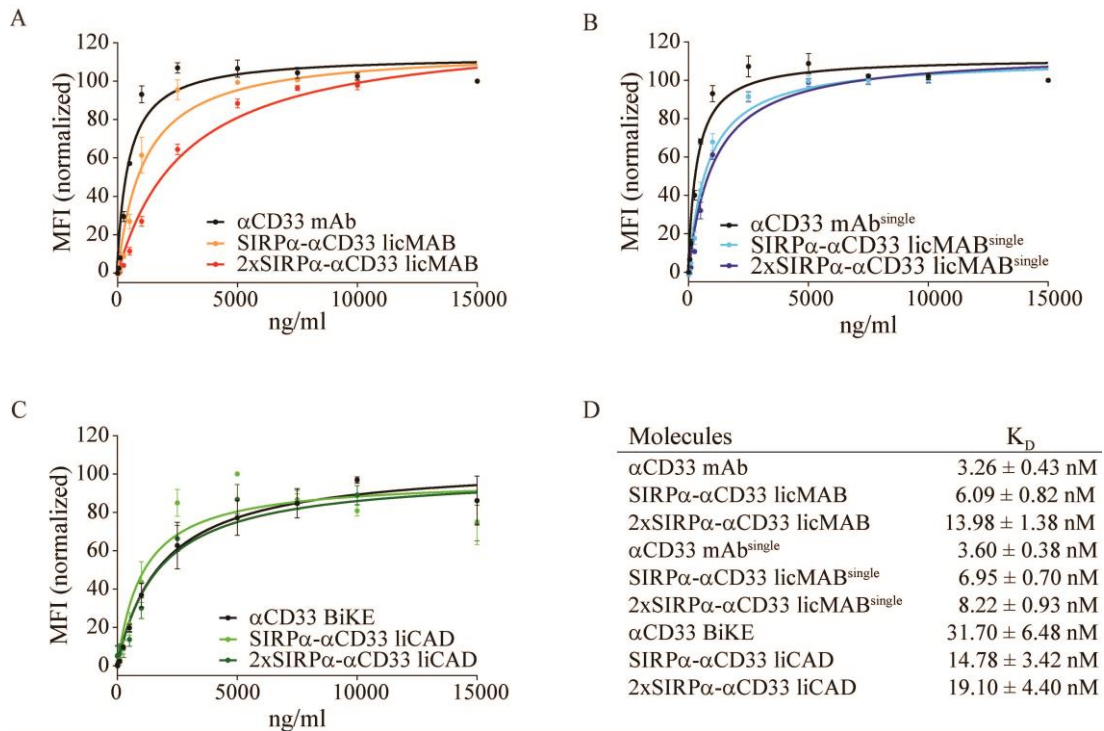


Figure 13. Binding curves of local inhibitory checkpoint molecules on MOLM-13 cells

Binding curves of (A) licMABs, (B) licMABs^{single} and (C) liCADs on MOLM-13 cells were analyzed by calibrated flow cytometry. Mean values of three to four independent experiments and standard error of the mean (SEM, error bars) are depicted. (D) K_D values, as an avidity measurement, were determined.

RESULTS

4.2.3. Local inhibition of the CD47-SIRP α innate immune checkpoint

The possible interaction of the SIRP α domain of local inhibitory checkpoint molecules to CD47 on healthy cells independently of binding to CD33 is a matter of concern. As a “don’t eat me” molecule, CD47 is expressed on most of the cells of our body and is responsible of maintaining self-tolerance. Therefore, if CD47 on healthy cells would be engaged by the SIRP α domain of local inhibitory checkpoint molecules, self-tolerance would be interrupted and unwanted adverse effects could occur. In particular RBCs, which express CD47 and are abundant and accessible in the bloodstream, constitute a potential site of on-target toxicity and antigen sink. Previous studies of high affinity CD47-targeting agents showed on-target toxicity in rodents and non-human primates.^{91, 92} Furthermore, a therapeutic molecule able to overcome the antigen sink by not binding to CD47 on healthy cells would require a lower dose and hence the production costs would be reduced.

Because of the naturally occurring low affinity of SIRP α to CD47, we hypothesized that the SIRP α domain of licMABs, licMABs^{singles} and liCADs interacts with CD47 on antigen-expressing tumor cells and not on healthy cells. Specifically, we reasoned that the distinction between healthy and tumor cells, and the binding to the latest, is conducted by the high affinity CD33-binding domain.

In order to characterize the preferential binding of local checkpoint inhibitory molecules to tumor cells, a competition assay with MOLM-13 cells and RBCs was performed. PKH26-labelled MOLM-13 cells were co-incubated with excess of RBCs and either α CD33 mAb, SIRP α - α CD33 licMAB, 2xSIRP α - α CD33 licMAB or a high affinity α CD47 mAb (B6H12). Local inhibitory checkpoint molecules were detected by secondary staining using flow cytometry and the percentage of MOLM-13 cells (PKH26⁺) and RBCs (PKH26⁻) from the antibody-bound compartment was determined (Figure 14).

Importantly, a favorable binding to MOLM-13 cells was observed for the α CD33 mAb and licMABs in the presence of 5-, 10- or 20-fold excess of RBCs, indicating that licMABs guide its binding through the high affinity CD33-binding site (Figure 14A). On the other hand, the high affinity α CD47 mAb, used as a control molecule, bound to RBCs in all conditions. We also evaluated the preferred binding of licMABs^{single} and liCADs in a mixture of MOLM-13 cells and 20-fold excess of RBCs. Similarly to licMABs,

RESULTS

licMAB^{single} and liCADs preferentially bound to MOLM-13 cells (Figure 14B). A minimal binding to RBCs, however, was detected uniquely by licMABs and correlated with the quantity of SIRP α domains.

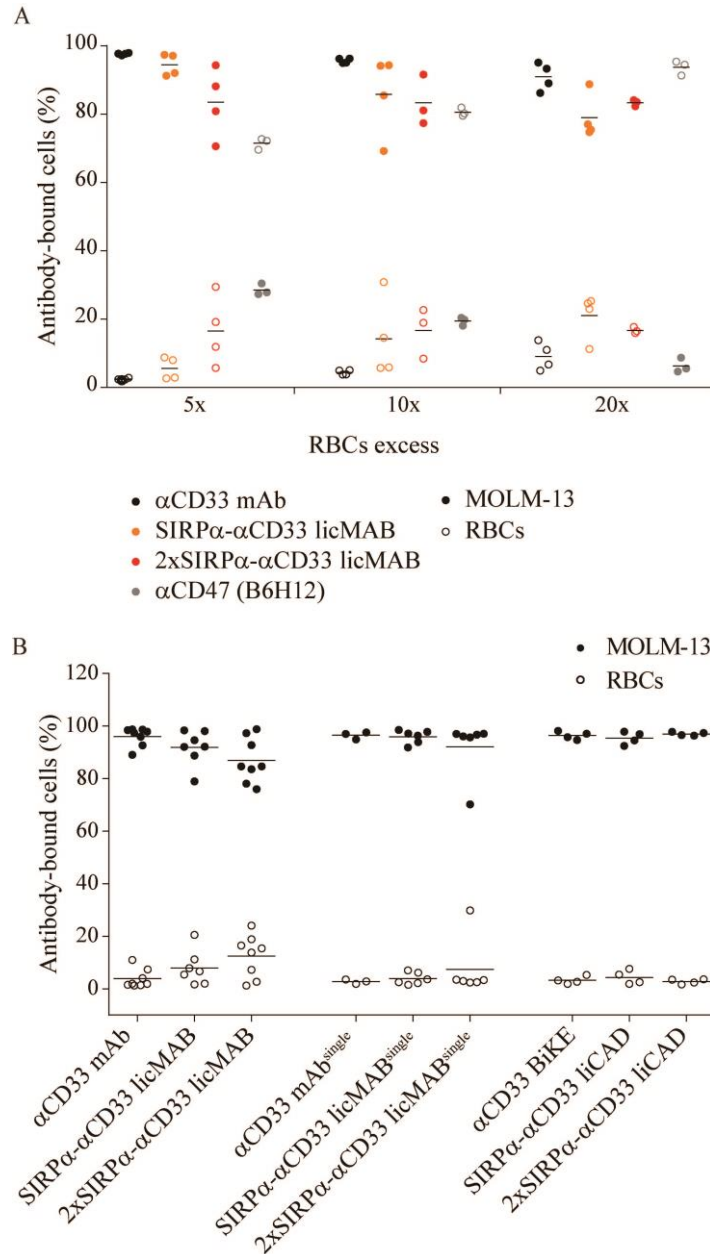


Figure 14. Preferential binding of local inhibitory checkpoint molecules

(A) Binding preferences of licMABs, α CD33 mAb and α CD47 mAb (clone B6H12) were evaluated in a mixture of MOLM-13 and 5-, 10- or 20-fold excess of RBCs. (B) LicMABs, licMAB^{single} and liCADs were co-incubated with MOLM-13 cells and 20-fold excess of RBCs and analyzed for binding by flow cytometry. On both graphs, percentage of MOLM-13 or RBCs within the antibody-bound compartment is plotted.

RESULTS

Next, the ability of the SIRP α domain of local inhibitory checkpoint molecules to block CD47 on cells co-expressing CD33 was investigated. To this end, MOLM-13 cells were initially incubated with licMABs, licMABs^{single}, liCADs, control molecules or PBS. The accessibility of CD47 was subsequently measured with a FITC-conjugated α CD47 mAb (clone B6H12) by flow cytometry and the median fluorescence intensity (MFI) ratio of the FITC mAb with respect to unstained cells was displayed (Figure 15). An MFI ratio lower than 1.5 indicated that CD47 was completely blocked by the investigated molecule and an MFI ratio higher than 1.5 showed certain accessibility of CD47. CD47's accessibility was reduced when incubated with the CD33-targeting licMABs, licMABs^{single} and liCADs, which demonstrates that the SIRP α domain occupied CD47. Moreover, the blockade of CD47 correlated with the quantity of SIRP α domains on the CD33-binding local inhibitory checkpoint molecules. Due to the lack of SIRP α domains, α CD33 mAb, mAb^{single} and BiKE did not block CD47, thus achieving a staining intensity comparable to the incubation with PBS. Importantly, CD47 was similarly accessible by either the endogenous low affinity SIRP α domain or other local inhibitory checkpoint molecules that target CD19, an antigen not expressed on MOLM-13 cells. This suggests that the blockade of CD47 on MOLM-13 cells by local inhibitory checkpoint molecules is dependent on the binding to CD33, which induces an avidity effect for the naturally weak interaction between SIRP α and CD47. Contrarily, the complete blockade of CD47 was observed for the high affinity binders SIRP α CV1 and α CD47 mAb (CC2C6), which displayed MFI ratios lower than 1.5.

Taken together, all local inhibitory checkpoint molecules preferentially bind to the CD33⁺ CD47⁺ AML cell line MOLM-13 even in the excess of CD33⁻ CD47⁺ RBCs. These results confirm that local inhibitory checkpoint molecules bind through the high affinity CD33-binding site while not interacting with CD47 on healthy cells. Moreover, we showed that CD47 is blocked on MOLM-13 only by the SIRP α domain of CD33-targeting local inhibitory checkpoint molecules. These results further support the idea that by combining a high affinity CD33-targeting domain and a low affinity SIRP α domain, the blockade of the CD47-SIRP α signaling pathway can be restricted to CD33⁺ AML cells. Based on that, local inhibitory checkpoint molecules not only present lower on-target toxicity than high affinity CD47-targeting agents, but also escape the antigen sink created by CD33⁻ CD47⁺ healthy cells.

RESULTS

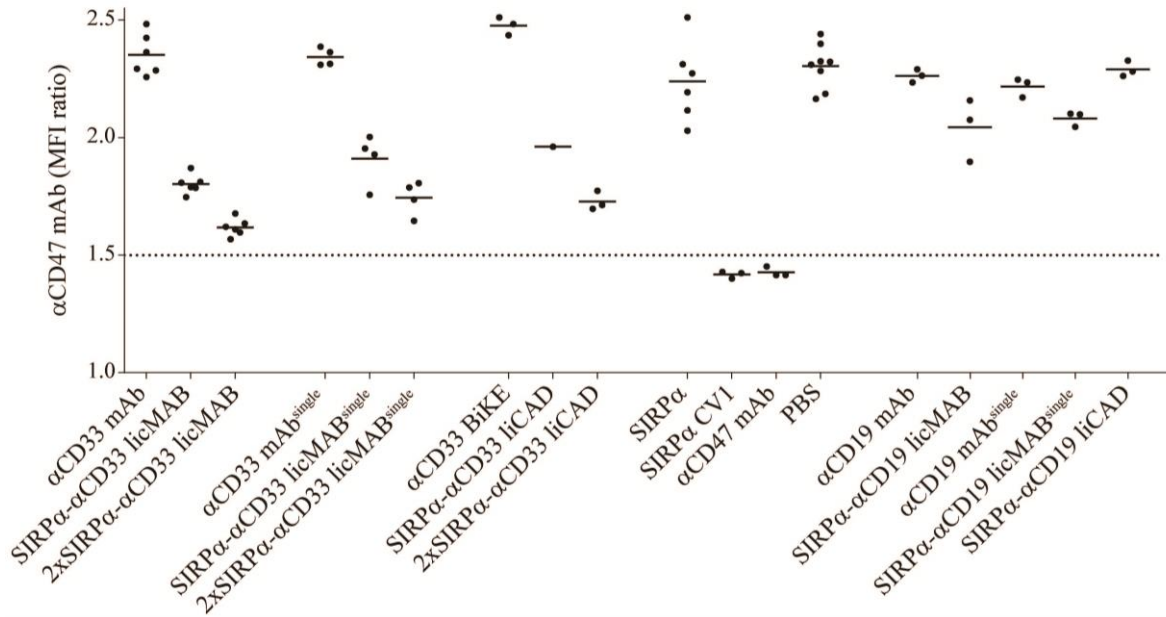


Figure 15. Blockade of CD47 on MOLM-13 cells by the SIRP α domain of local inhibitory checkpoint molecules

CD33- and CD19-targeting local inhibitory checkpoint molecules and control molecules were incubated with MOLM-13 and accessible CD47 molecules were detected by FITC- α CD47 mAb staining by flow cytometry. MFI ratio of FITC- α CD47 staining with respect to the unstained condition is displayed.

4.2.4. CD33-dependent internalization of local inhibitory checkpoint molecules

It has been reported that CD33 internalizes upon bivalent binding of mAbs.¹⁵⁷ As internalization of licMABs, which also target CD33 bivalently, would lessen the recruitment and activation of immune effector cells, the uptake of these molecules was evaluated. To this end, MOLM-13 cells were incubated with local inhibitory checkpoint molecules at 37°C and internalization was studied by flow cytometry and confocal microscopy (Figure 16).

First, time-dependent internalization of α CD33 mAb and licMABs was assessed (Figure 16A). All three molecules displayed a similar internalization rate, increasing over time and reaching an internalization of around 60% after 120 min. These results were further confirmed by confocal microscopy using directly labeled licMABs or mAb (Figure 16B). For samples incubated at 4°C, a clear membrane-bound staining was visible. Incubation at 37°C, however, showed a re-localization of the molecules to intracellular sites increasing over time until intracellular signal was not detectable presumably due to degradation of the molecules or bleaching of the coupled dye in low pH lysosomal compartments.

RESULTS

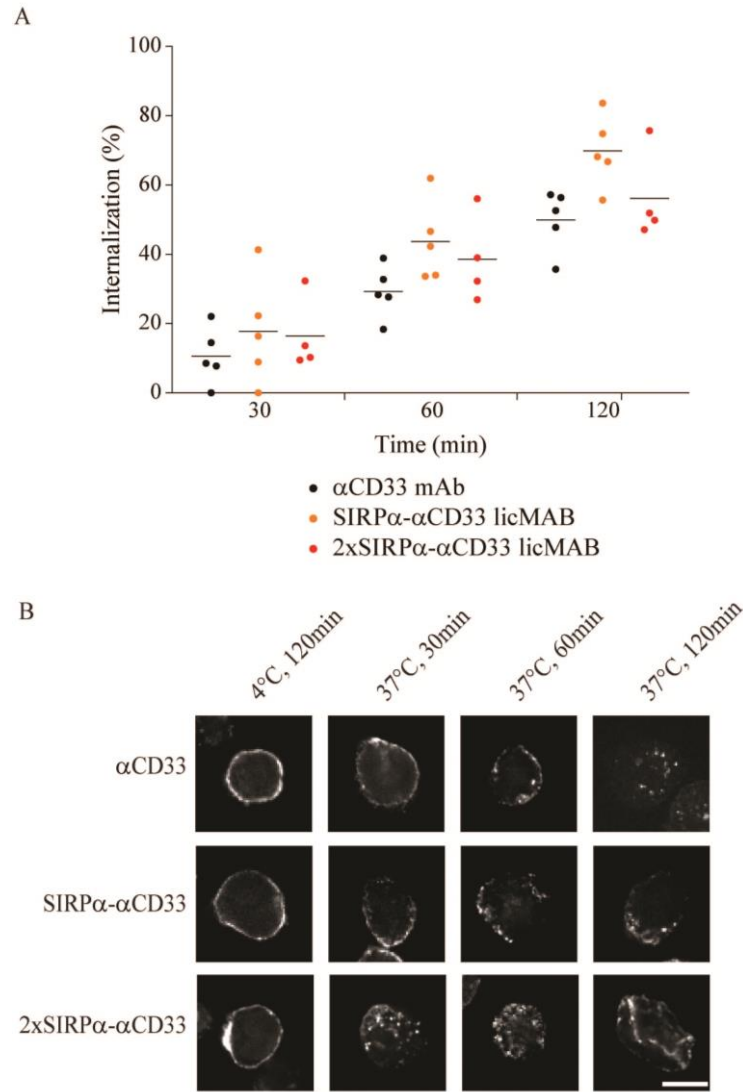


Figure 16. Time-dependent internalization of CD33 upon incubation with licMABs

(A) Time-dependent internalization of mAb and licMABs on MOLM-13 cells assessed by flow cytometry. (B) Representative confocal microscopy images of MOLM-13 cells incubated with directly labeled licMABs or mAb for 30, 60 or 120 min at 37°C or for 120 min at 4°C. Scale bar = 10 μ m.

Since whether monovalent targeting of CD33 reduces its internalization is a discussed topic in the field, the internalization of licMABs after 120 min was compared to licMABs^{single} and liCADs (Figure 17).^{158, 159} In our hands, monovalent targeting of CD33 by licMABs^{single} did not diminish CD33-dependent endocytosis. Interestingly, internalization was reduced by liCADs, particularly 2xSIRP α - α CD33 liCAD and α CD33 BiKE. The reason for the lower uptake rate of these molecules, however, remains unclear and further assays would need to be performed in order to understand the biology of CD33-dependent internalization.

RESULTS

In summary, CD33-dependent internalization was minimized by 2xSIRP α - α CD33 liCAD but licMABs and licMABs^{single} mediated CD33 endocytosis. This indicates that other mechanisms, in addition to the mono- or bivalent targeting of CD33, can be involved in this process.

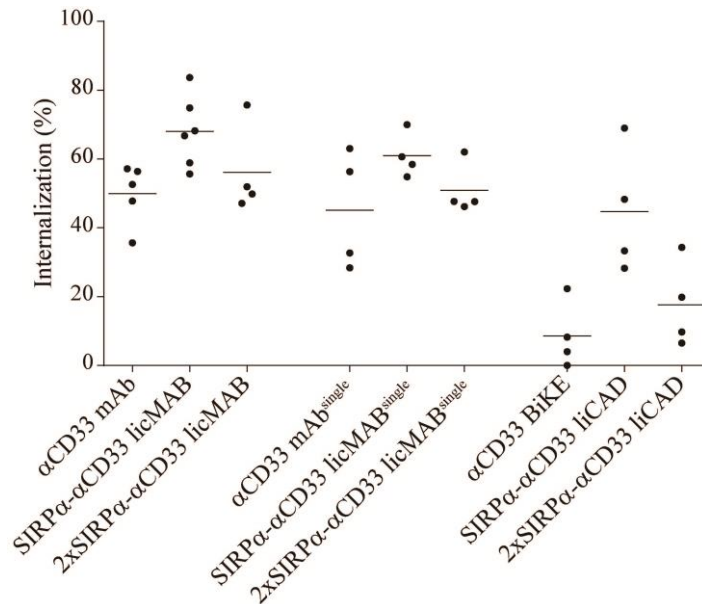


Figure 17. CD33-dependent internalization of local inhibitory checkpoint molecules

Internalization of licMABs, licMABs^{single} and liCADs after incubation with MOLM-13 cells for 120 min and detected by flow cytometry.

4.2.5. Binding of local inhibitory checkpoint molecules to effector cells

Despite the different binding valency of licMABs, licMABs^{single} and liCADs to CD33, these molecules also diverge on the effector cell-activating domain. LicMABs and licMABs^{single} contain an IgG1 Fc domain, which is recognized by all Fc γ Rs, whereas liCADs uniquely bind to CD16 through a scFv. Moreover, the IgG1 Fc region was shown to have a low affinity for CD16 and the α CD16 scFv was described to bind to CD16 with high affinity.¹⁶⁰⁻¹⁶² SEC was kindly performed by Saskia Schmitt in order to further characterize the interaction between CD16 and either the Fc domain or the α CD16 scFv (Figure 18).

Initially, single SEC chromatograms of SIRP α - α CD33 licMAB, SIRP α - α CD33 liCAD and the extracellular domain of CD16, which was recombinantly expressed by Alexandra Schele, were obtained. Next, interactions were studied by loading the mixed samples. An interaction between the licMAB and CD16 was not detectable, presumably due to the low affinity of the Fc domain for CD16 (Figure 18A). Nonetheless, the high binding affinity

RESULTS

of liCADs to CD16 was confirmed by the SEC peak corresponding to the formation of a complex of higher molecular weight (Figure 18B). The complex formation between the extracellular domain of CD16 and the liCAD, but not with the liMAB, was further visualized by SDS-PAGE analysis (Figure 18C). Taken together, our results are in agreement with the aforementioned previous studies, which demonstrate a low affinity of the Fc domain to CD16 and a high affinity of α CD16 scFv to CD16.

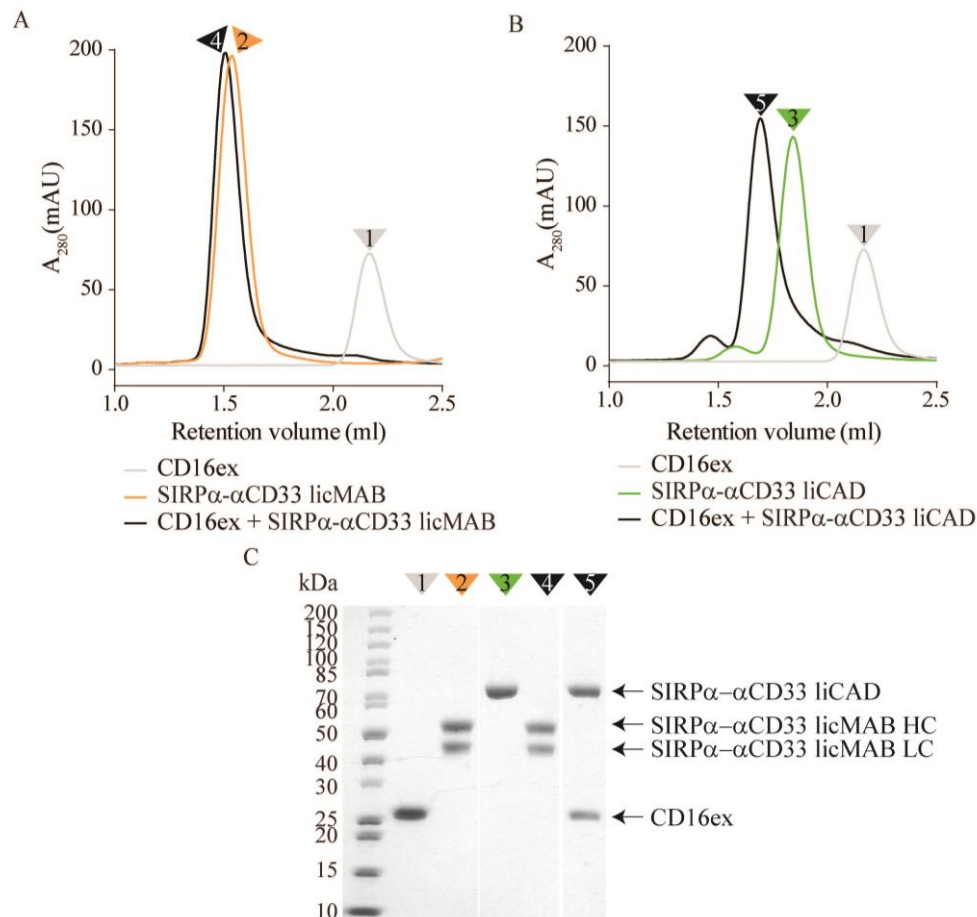


Figure 18. Interaction between liMABs or liCADs and the extracellular domain of CD16 by size exclusion chromatography

Binding studies of (A) liMABs and (B) liCADs with the recombinantly expressed extracellular domain of CD16 (CD16ex) by SEC on an S200 increase 5/150 GL column. (C) SDS-PAGE analysis of SEC peak fractions of single components (1) CD16ex, (2) liMAB and (3) liCAD and the co-incubated proteins (4) liMAB + CD16ex and (5) liCAD + CD16ex.

RESULTS

4.3. Functional characterization of local inhibitory checkpoint molecules

4.3.1. Antibody-dependent cellular cytotoxicity in AML cell lines

Antibody-dependent cellular cytotoxicity (ADCC) is one of the immune effector functions mediated by IgG1 mAbs. Furthermore, several clinically approved mAbs were shown to function throughout this mechanism.^{163, 164} During this process, the Fc domain of mAbs is recognized by CD16A expressed on NK cells and this triggers NK cell activation, which ultimately leads to NK cell degranulation and target cell lysis. Since licMABs and licMABs^{single} were engineered from an IgG1 mAb and liCADs as well recognize CD16, their ability to induce ADCC was investigated. To this end, freshly isolated NK cells were incubated with Calcein-AM-labeled MOLM-13 or SEM cells and local inhibitory checkpoint molecules and cell lysis was correlated with the Calcein-AM released in the supernatant (Figure 19).

Importantly, CD33-targeting licMABs, licMABs^{single} and liCADs efficiently stimulated cytotoxicity of MOLM-13 cells with a maximum specific lysis of around 40% and EC₅₀ values in the low pM range (Figure 19A-C). This rather low maximal specific lysis of MOLM-13 cells is consistent with other studies using this cell line.^{165, 166} In order to study the ADCC effects of local inhibitory checkpoint molecules independent of the tumor antigen targeting, licMABs, licMABs^{single} and liCADs targeting CD19, a B-cell lymphoma antigen not expressed on MOLM-13 cells, were used. The CD19-targeting molecules did not induce significant killing of MOLM-13. This indicates not only that licMABs, licMABs^{single} and liCADs induce specific lysis of cells that express the target antigen but also that the SIRP α domain does not target CD47 by itself. This idea was further supported by the results obtained with the SEM cell line, which expressed the CD19 antigen but not CD33 (Figure 19D). CD19-targeting mAb and licMABs induced specific killing of SEM cells, achieving a maximum specific lysis of 65% at concentrations of 1 nM. On the contrary, CD33-targeting licMABs did not stimulate cytotoxicity of SEM cells. Only the 2xSIRP α - α CD33 licMABs promoted a minor ADCC effect on SEM cells, suggesting that increased SIRP α quantities may function as CD47-targeting agents.

RESULTS

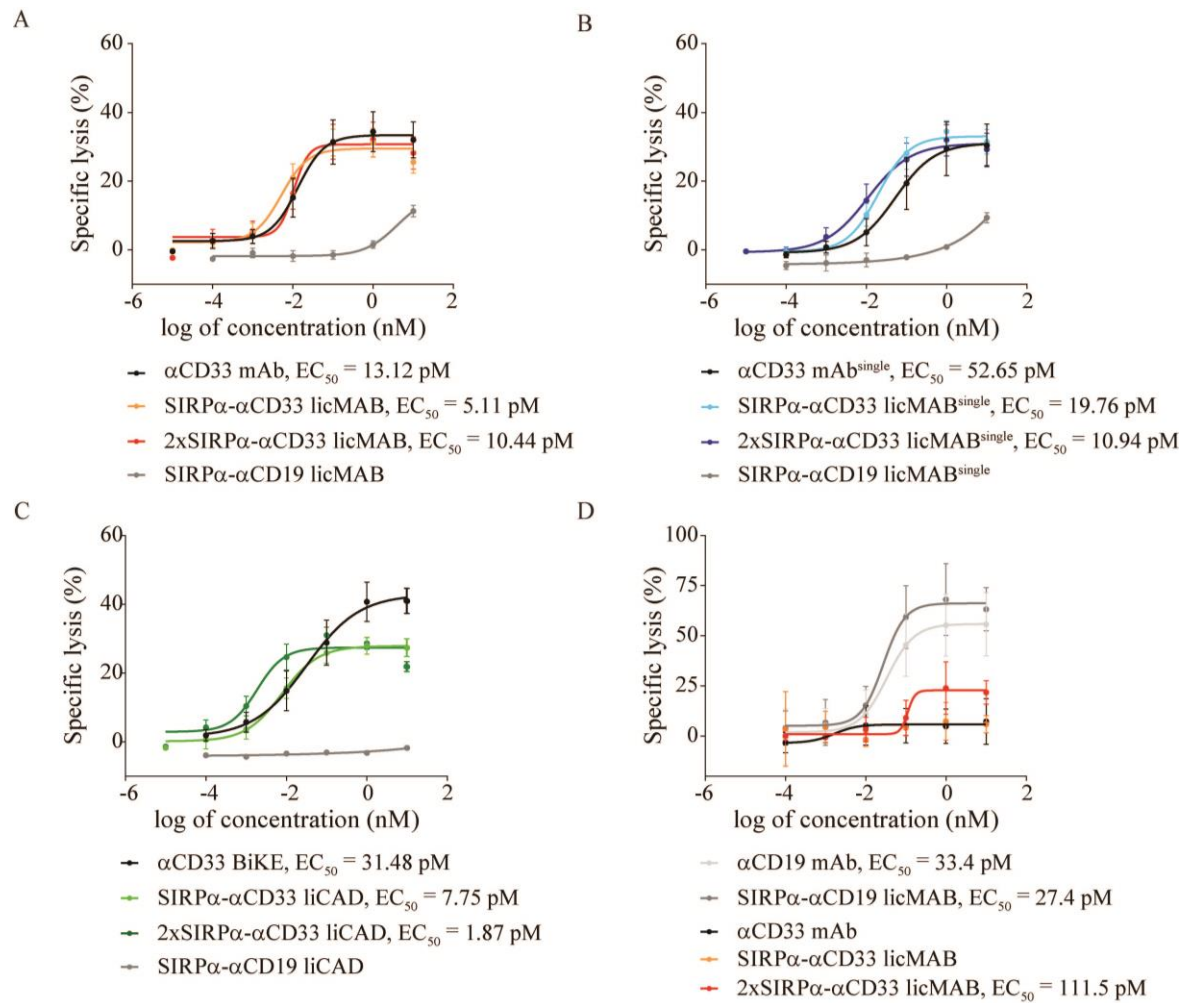


Figure 19. Specific NK cell-mediated tumor lysis induced by local inhibitory checkpoint molecules

CD33- and CD19-targeting licMABs, licMABs^{single} and licADs were incubated with NK cells and (A) MOLM-13 or (B) SEM cells for 4 h and specific target cell lysis was measured. Mean specific lysis of 4 independent experiments and the SEM values (error bars) were plotted as a dose-response curve.

As it was shown, CD33-targeting licMABs induce specific lysis of CD33-expressing AML cells. The surface antigen CD33, however, is also expressed on healthy cells from the myeloid lineage. Therefore, CD33-expressing healthy cells may as well be a potential target for licMABs.¹³⁵ Nevertheless, previous studies demonstrate that CD33 expression is much higher on AML cells than on healthy cells, thus identifying CD33 as a validated AML antigen.¹³⁴ In order to evaluate whether licMABs preferentially bind and induce anti-tumor effects to high CD33-expressing AML cells with respect to low CD33-expressing cells, ADCC assays with a 1:1 mixed population of MOLM-13 and OCI-AML3 cells were performed (Figure 20). OCI-AML3 cells express lower levels of CD33 (MFI ratio = 3.55) than MOLM-13 cells (MFI ratio = 28.71) and therefore exemplify the healthy CD33-expressing cells.

RESULTS

CD33-targeting licMABs and mAb at both 10 nM and EC₅₀ value concentrations favorably induced ADCC of MOLM-13 cells in the presence of OCI-AML3 cells (Figure 20A and B). These results suggest that local inhibitory checkpoint molecules preferentially induce killing of high CD33-expressing cells, such as AML cells.

In conclusion, CD33-targeting licMABs, licMABs^{single} and liCADs activate NK cells upon antigen binding, thus triggering specific lysis of CD33⁺ tumor cells. Furthermore, the activity of local inhibitory checkpoint molecules is directed by the high affinity binding to the tumor antigen and the SIRP α domain does not induce elimination of tumor antigen-negative healthy cells.

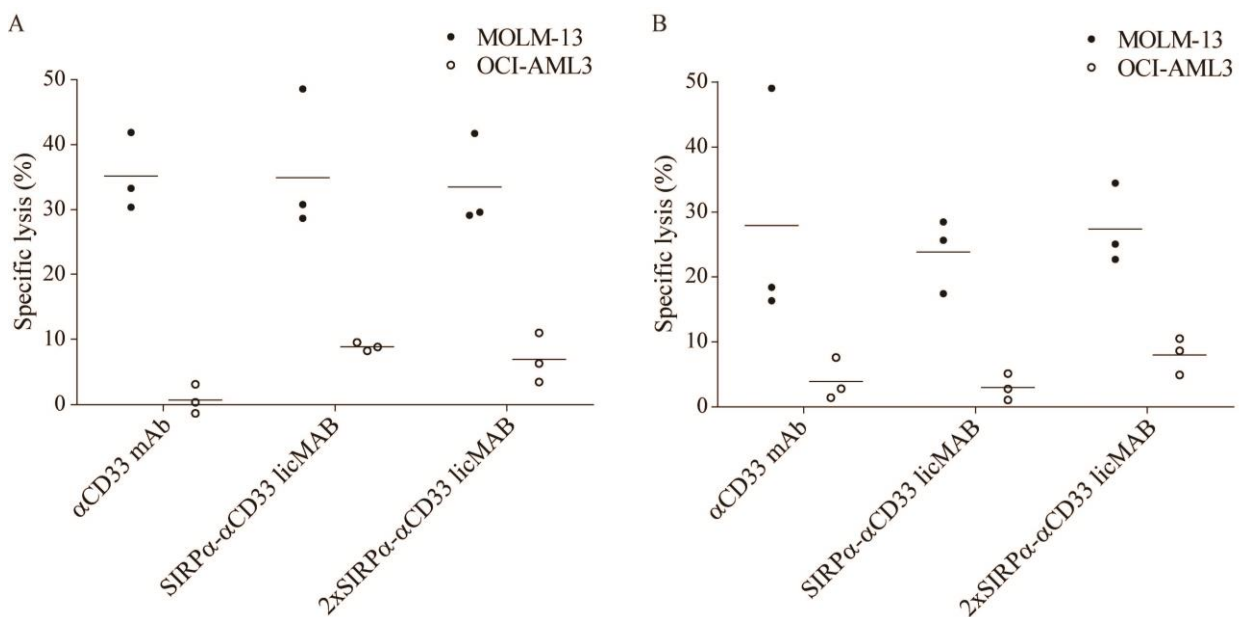


Figure 20. Preferential killing of high CD33-expressing cells by licMABs

Preferential NK cell-mediated lysis of MOLM-13 cells (high CD33 expression) and OCI-AML3 cells (low CD33 expression) in ADCC induced by (A) 10 nM or (B) EC₅₀ concentrations of CD33-targeting mAb and licMABs.

4.3.2. Antibody-dependent cellular cytotoxicity in AML patient samples

After evaluating local inhibitory checkpoint molecules for their capacity to induce NK cell-mediated killing of AML cell lines, the cytotoxicity of these molecules in primary, patient-derived AML cells was analyzed and data was kindly provided by Dr. Christina Krupka from the Subklewe laboratory. Due to the high heterogeneity of AML patients, nine independent assays using AML cells from nine donors were performed. However, the limited available amounts of patient material narrowed the evaluation to licMABs. In order to perform the assay, primary AML cells were incubated with freshly isolated NK

RESULTS

cells and 10 nM licMABs or mAb *ex vivo* in a non-autologous setting. Cytotoxicity was analyzed by flow cytometry (Figure 21).

Elimination of primary, patient-derived AML cells was promoted by α CD33 mAb, SIRP α - α CD33 licMAB and 2xSIRP α - α CD33 licMAB. Even if there was certain variation between the different primary AML cells, which demonstrates the inter-patient heterogeneity, licMABs stimulated significantly higher lysis than the α CD33 mAb. This is presumably due to the avidity binding of the SIRP α domains on licMABs. Notably, five out of nine patients benefited from the single SIRP α domain and seven out of nine benefited from the 2xSIRP α domain.

Taken together, these results demonstrate that licMABs induce higher lysis of primary, patient-derived AML cells than conventional α CD33 mAbs.

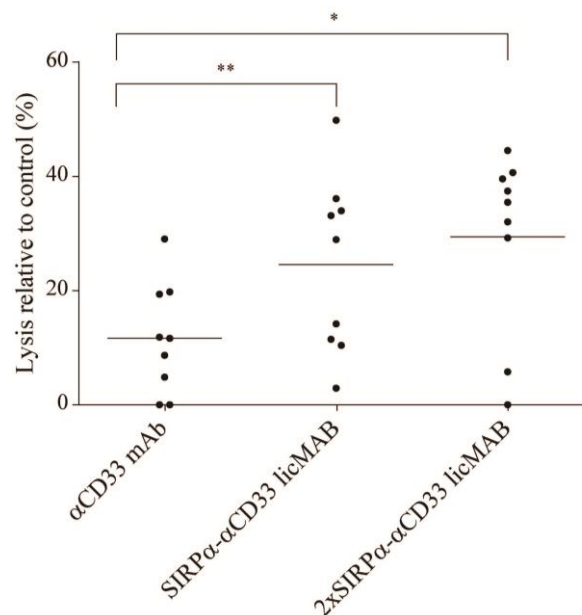


Figure 21. Cytotoxicity of primary, patient-derived AML cells induced by licMABs

Lysis of primary AML cells derived from 9 independent AML patients promoted by 10 nM α CD33 mAb, SIRP α - α CD33 licMAB and 2xSIRP α - α CD33 licMAB. Percentage of CD33- or CD123-expressing cells after licMAB treatment with respect to untreated samples was determined by flow cytometry.

4.3.3. Antibody-dependent cellular phagocytosis in AML cell lines

The main goal of this thesis was to generate novel therapeutic molecules that target AML cells and actively promote their elimination by phagocytosis. Previous work identified two requirements in order to promote active phagocytosis: the induction of a pro-phagocytic signal triggered by Fc γ Rs and the disruption of the CD47-SIRP α anti-phagocytic immune checkpoint.⁹¹ Therefore, all local inhibitory checkpoint molecules

RESULTS

engage FcγRs by either the Fc domain or the αCD16 scFv and prevent the CD47 anti-phagocytic signal by the engrafted endogenous SIRPα domain. Thus, we hypothesized that licMABs, licMABs^{single} and liCADs trigger active phagocytosis of CD33-expressing AML cells.

In order to evaluate the capacity of local inhibitory checkpoint molecules to induce active phagocytosis, an ADCP assay was established in our laboratory. Initially, an imaging flow cytometry-based phagocytosis assay was developed using the αCD33 mAb and licMABs (Figure 22). For that, monocytes were isolated from peripheral blood of healthy donors, stained with PKH67, differentiated to macrophages and co-incubated with PKH26-labelled MOLM-13 cells and increasing concentrations of licMABs and αCD33 mAb. Phagocytic events were defined as single cells positive for PKH67 and PKH26, indicating that macrophages engulfed MOLM-13 cells (Figure 22A). Therefore, the use of an imaging flow cytometer was of high value in order to distinguish real phagocytic events from doublets of macrophages and MOLM-13 cells, which would as well lead to the detection of the two dyes by conventional flow cytometry.

Importantly, SIRPα-αCD33 licMAB and 2xSIRPα-αCD33 licMAB improved phagocytosis of MOLM-13 cells with respect to the αCD33 mAb in all the evaluated concentrations (Figure 22B). SIRPα-αCD33 licMAB promoted the highest phagocytosis rate at concentrations up to 0.1 nM and 2xSIRPα-αCD33 licMAB from 1 to 100 nM. These results suggest that the SIRPα domain of licMABs is able to interact with CD47 on MOLM-13 cells and inhibit the anti-phagocytic signal.

RESULTS

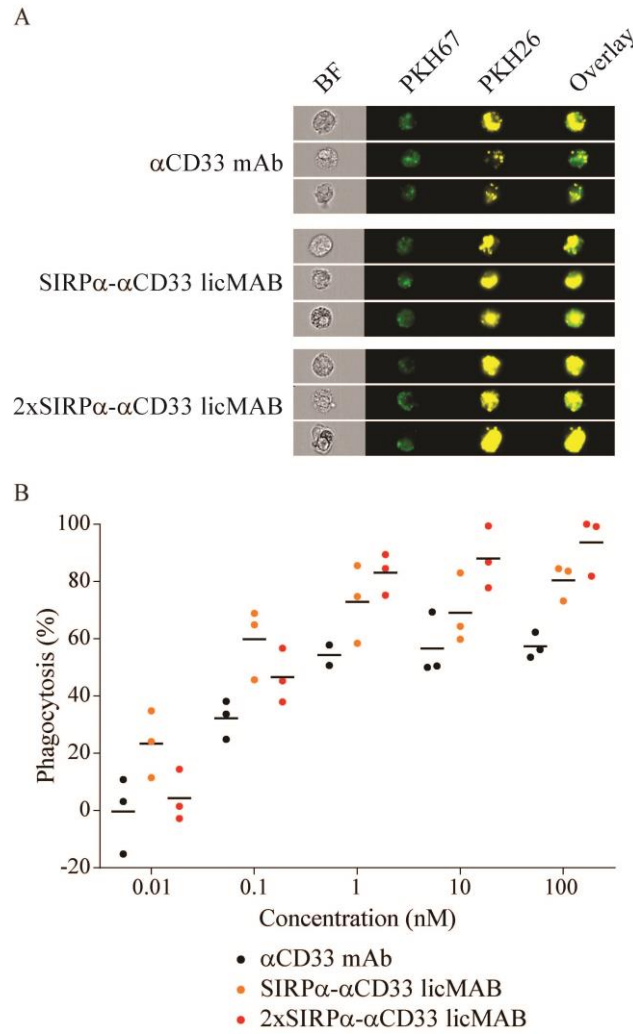


Figure 22. Development of the phagocytosis assay by imaging flow cytometry

(A) Exemplary images of phagocytic events by imaging flow cytometry. (B) Concentration-dependent phagocytosis of MOLM-13 cells induced by α CD33 mAb and licMABs.

Once the ADCP assay was robust, all local inhibitory molecules were subsequently evaluated by conventional flow cytometry for their potential to induce phagocytosis of MOLM-13 at a concentration of 10 nM (Figure 23). Moreover, in order to characterize donor-derived macrophages, the expression of their surface antigens was detected. In general, CD33 and CD16 were poorly expressed, CD47 expression was high and CD32 and CD64 displayed a broad distribution (Figure 23A). Interestingly, donor-derived macrophages could be separated in two different populations according to the expression levels of SIRP α . We defined the SIRP α expression as high (SIRP α^{high}) for MFI values higher than 50 and intermediate (SIRP α^{int}) for MFI values lower than 50. Since high SIRP α -expressing macrophages were recently described to display a suppressed phagocytic activity, the following phagocytosis assays were performed using SIRP α^{int} macrophages.¹⁶⁷

RESULTS

Despite the variation between the single assays, licMABs and licMABs^{single} successfully enhanced ADCP of MOLM-13 cells in comparison to α CD33 mAb and mAb^{single} (Figure 23B). The local inhibitory checkpoint molecule with a higher mean phagocytosis rate was SIRP α - α CD33 licMAB^{single}, followed by 2xSIRP α - α CD33 licMAB^{single} and single and double SIRP α licMABs. LiCADs, however, promoted a rather low phagocytosis of MOLM-13 cells, which is consistent with the low CD16 expression on macrophages.

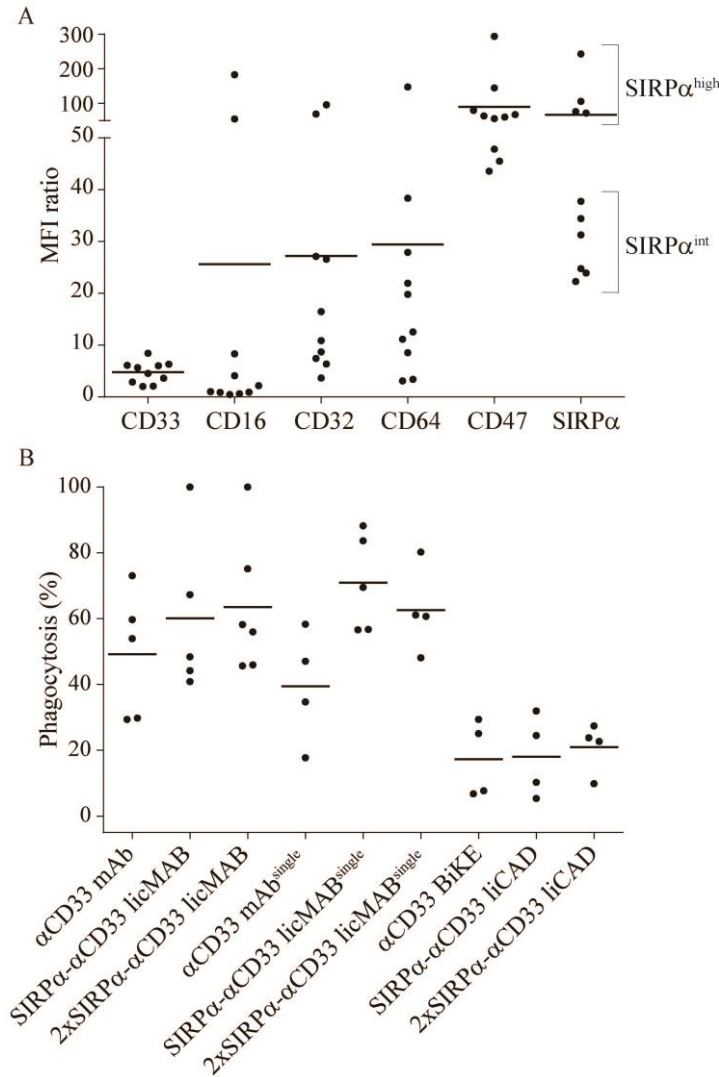


Figure 23. Phagocytosis of MOLM-13 cells mediated by local inhibitory checkpoint molecules

(A) Analysis of surface antigens expressed on donor-derived macrophages. Two distinct populations, high SIRP α (SIRP α^{high} , MFI ratio > 50) and intermediate SIRP α (SIRP α^{int} , MFI ratio < 50) were described. (B) Phagocytosis of MOLM-13 cells by SIRP α^{int} macrophages mediated by 10 nM of local inhibitory checkpoint molecules.

In summary, the ADCP assay was successfully established and demonstrated that by combining the pro-phagocytic Fc-mediated stimulus and the disruption of the CD47-SIRP α immune checkpoint, licMABs and licMABs^{single} are able to enhance active

RESULTS

phagocytosis of MOLM-13 cells with respect to the control molecules by donor-derived SIRP α^{int} macrophages.

4.3.4. Antibody-dependent cellular phagocytosis in AML patient samples

The ability of licMABs and licMABs^{single} to promote active phagocytosis was further investigated using primary, patient-derived AML cells as target cells and results were kindly provided by Dr. Jan-Hendrik Kozik from the Subklewe laboratory (Figure 24). Due to the lack of efficacy of liCADs in stimulating phagocytosis of MOLM-13 cells, these molecules were not tested with primary AML samples.

The response upon application of licMABs and licMABs^{single} was very heterogeneous within the evaluated AML patient samples, inducing active phagocytosis in seven out of thirteen experiments. Based on that, we divided the samples in responsive and resistant, defining “responsive” as these samples with at least one evaluated condition promoting a two-fold increase in relative phagocytosis with respect to the untreated condition (Figure 24A). Concerning the responsive subset, SIRP α - α CD33 and 2xSIRP α - α CD33 licMABs promoted a higher phagocytosis of primary, patient-derived AML cells than the α CD33 mAb and the CD47-blocking mAb (Figure 24B). Specifically, the SIRP α - α CD33 licMAB stimulated the highest mean phagocytosis of all local inhibitory molecules. The phagocytosis induced by licMABs^{single} was higher than the α CD33 mAb^{single}, but lower with respect to licMABs, which may be explained by the avidity effects of licMABs.

The results obtained with primary, patient-derived AML cells further suggest that the SIRP α domain of licMABs inhibits the CD47-SIRP α axis and that the Fc domain engages Fc γ Rs, thus ultimately potentiating phagocytosis of target cells.

RESULTS

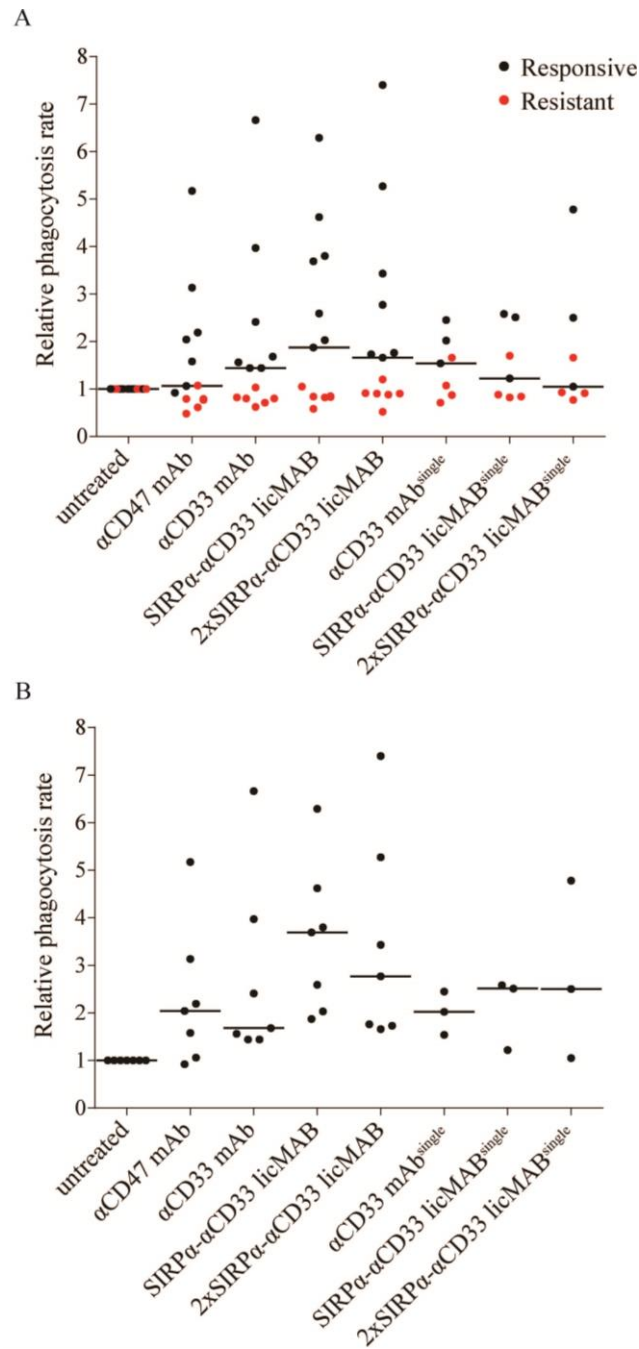


Figure 24. Phagocytosis of primary, patient-derived AML cells induced by licMABs and licMABs^{single}

(A) Relative phagocytosis of primary AML cells derived from thirteen patients. A responsive pair was defined as the assay in which a double-fold increase in phagocytosis was achieved by any of the conditions with respect to the untreated sample. A resistant pair did not achieve a double-fold increase in phagocytosis in any of the evaluated conditions. (B) Relative phagocytosis achieved by the responsive subset.

Next, the expression of surface antigens on primary, patient-derived AML cells and donor-derived macrophages was determined by flow cytometry in order to shed light on the susceptibility of primary AML cells for phagocytosis by licMABs (Figure 25A-B). As

RESULTS

CD33 is an AML antigen, its expression was higher on primary AML cells than on macrophages. In contrast, all FcγRs as well as SIRPα, were expressed on donor-derived macrophages and low expressed, if at all, on AML cells. CD47 was expressed on both cell types but showed a heterogeneous distribution for distinct primary, patient-derived AML samples. Nonetheless, no conclusions could be drawn with respect to the expression of surface antigens and the susceptibility of primary AML cells for licMABs- and liMABs^{single}-mediated phagocytosis.

We therefore proceed to calculate the relative expression of surface antigens on primary, patient-derived AML cells with respect to donor-derived macrophages (Figure 25C). Strikingly, we found that the relative expression of CD47, but no other analyzed marker, significantly influenced the outcome of the ADCP assays. A stronger CD47 expression on primary AML cells with regards to macrophages resulted in an increased phagocytosis of AML cells by licMABs. Accordingly, licMABs were not effective in experiments with higher CD47 expression on macrophages with respect to AML cells. A slight dependence, though not significant, could be observed for CD64 and SIRPα antigens, which may act as decoy receptors for licMABs on AML cells.

Taken together, our results reflect the heterogeneity and complexity of primary, patient-derived AML cells and demonstrate that licMABs and licMABs^{single} successfully mediate active phagocytosis of primary, patient-derived AML cells. Furthermore, CD47 expression on primary AML cells relative to donor-derived macrophages seems to determine the efficacy of licMAB-mediated phagocytosis. Therefore, a screening of CD47 expression levels on AML patients would be required previous to the application of licMABs or licMABs^{single}.

RESULTS

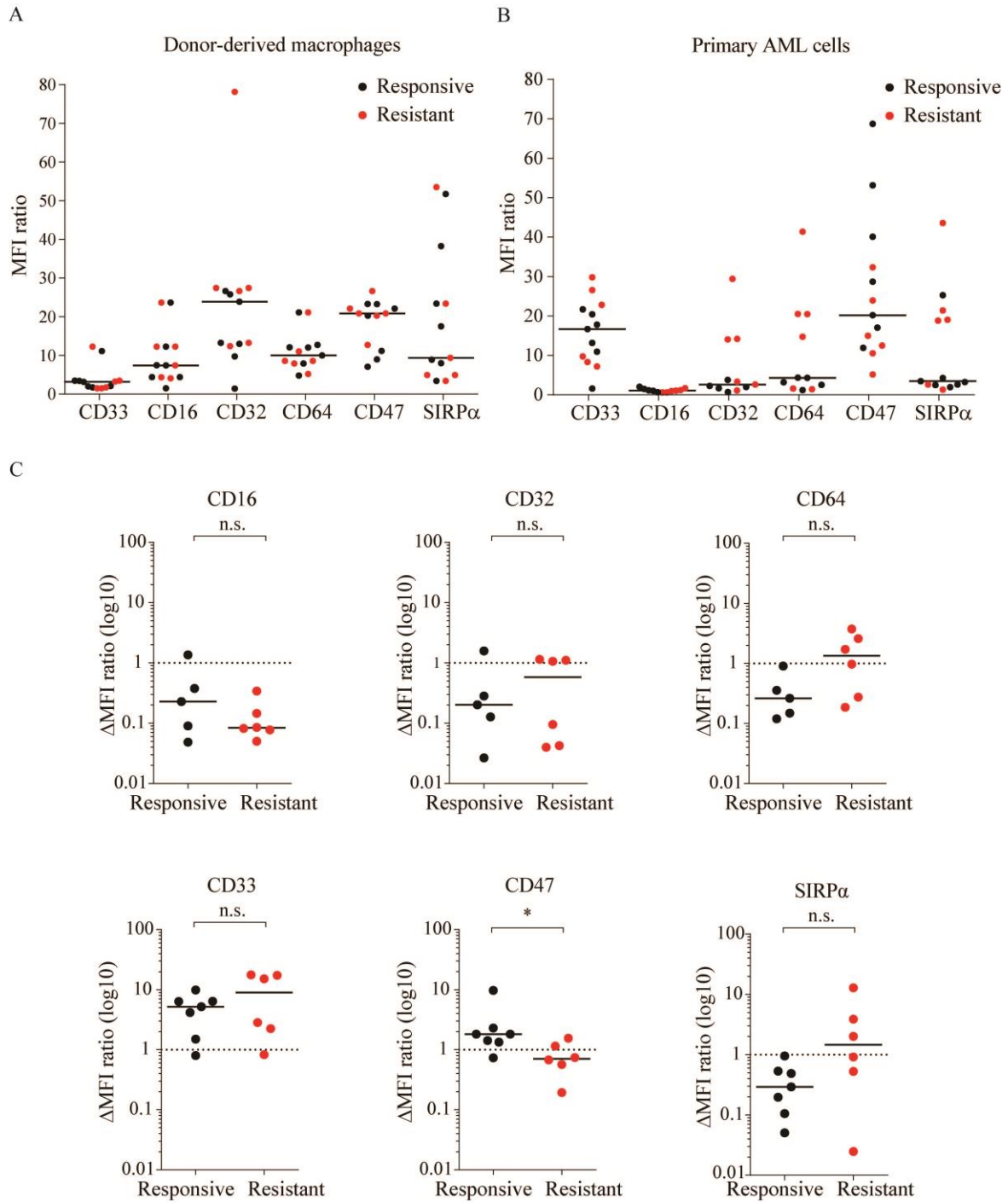


Figure 25. Surface antigen expression on donor-derived macrophages and primary AML cells

Expression levels of CD33, CD16, CD32, CD64, CD47 and SIRPα on (A) donor-derived macrophages and (B) primary AML cells. (C) Relative antigen expression on primary AML cells and macrophages of responsive and resistant subsets for each evaluated antigen. Statistical significance was calculated with the Mann-Whitney test.

5. DISCUSSION

5.1. Local blockade of the CD47-SIRP α innate immune checkpoint

The main goal of this thesis was to develop novel immunotherapeutic molecules that bring the benefits of blocking the CD47-SIRP α myeloid-specific immune checkpoint to AML cells and not endanger healthy cells. CD47 is responsible for ensuring the maintenance of self-tolerance by negatively regulating phagocytosis through binding to its receptor SIRP α .⁷⁶ This mechanism, however, is also utilized by cancer cells to escape the attack of the immune system. Accordingly, the blockade of the CD47-SIRP α immune checkpoint by CD47- or SIRP α -targeting agents induces macrophage-mediated elimination of tumors cells and constitutes a promising strategy for the treatment of AML.^{70, 72, 92, 98, 168}

The blockade of the CD47-SIRP α immune checkpoint, however, also represents a risk for healthy cells as CD47 is ubiquitously expressed on many cells of the body. Despite the results of ongoing clinical trials will clarify the safety of CD47 inhibitors for humans, on-target/off-leukemia toxicities have been observed on pre-clinical evaluations of these agents. Studies that described the CD47-SIRP α interaction on RBCs already reported that the use of a high affinity mAb targeting SIRP α mediated the elimination of wild-type RBCs.⁶² Another work showed that the administration of a high affinity SIRP α CV1 variant fused to a human IgG4 Fc domain resulted in the development of chronic anemia in mice and in a substantial drop in RBC counts in cynomologous monkeys.⁹¹ Furthermore, a dose-dependent anemia due to erythrophagocytosis was observed after the injection of Hu5F9-G4 in cynomologous monkeys.⁹² Overall, these evidences suggest that the systemic blockade of the CD47-SIRP α signaling pathway may cause toxicities to healthy cells, leading to unwanted side effects.

In order to confine the blockade of the CD47-SIRP α immune checkpoint to AML cells, we fused the endogenous low affinity SIRP α domain to a mAb or derivative thereof targeting CD33, a surface antigen highly expressed on AML cells. We showed that licMABs, licMABs^{single} and liCADs, containing one or two SIRP α domains, preferentially bind to CD33-expressing AML cells even in the presence of a 20-fold excess of RBCs. Most importantly, by studying the accessibility of CD47, we demonstrated that the SIRP α domain of local inhibitory checkpoint molecules blocks CD47 on cells that simultaneously express CD33 and not on cells negative for the target antigen.

DISCUSSION

Accordingly, licMABs, licMABs^{single} and liCADs are expected to reduce on-target/off-leukemia toxicities and be advantageous over other high affinity CD47 inhibitors. In addition, by binding through the high affinity CD33-targeting domain, local inhibitory checkpoint molecules also overcome the antigen sink created by CD47 expressed on healthy cells. This would result in a lower therapeutic dose and consequently in a reduction of the production costs.

Different strategies have been investigated in order to restrict the blockade of the CD47-SIRP α immune checkpoint to tumor cells. These include the generation of bispecific antibodies binding to CD47 and a tumor antigen. A dual-variable-domain immunoglobulin (DVD-Ig) was created to bind CD20 and CD47 simultaneously, being the variable domains recognizing CD47 in the middle position and therefore displaying reduced affinity.⁹³ Interestingly, CD20-CD47 DVD-Ig not only recapitulated the anti-tumor effects of the combination of two mAbs targeting CD20 and CD47, but also preferentially bound to CD20-expressing cells with respect to RBCs, thus potentially reducing the unwanted side effects of combination therapies. Based on that, it is expected that licMABs, licMABs^{single} and liCADs are superior to the combination of mAbs targeting CD33 and CD47.

SIRPabodies also confine the blockade of the CD47-SIRP α immune checkpoint to CD20-expressing cancer cells.¹⁶⁹ Similarly to the evaluated licMABs, SIRPabodies are IgG1 mAbs targeting CD20 with the endogenous SIRP α domain engrafted either at the C-terminus or at the N-terminus of the heavy chain. SIRPabodies overpass the antigen sink created by RBCs and, most importantly, do not cause toxicities in cynomolgous monkeys. Studies with these molecules resulted in an extended survival and reduced tumor burden in xenografted mouse models, which further encourages the use of the SIRP α domain as a low affinity CD47-blocking agent. The optimal position of the SIRP α domain in an antibody scaffold, however, needs to be further investigated. An N-terminal fusion retains the native structure of SIRP α but may compromise the CDRs of the parental antibody. Alternatively, a C-terminal fusion of SIRP α may not interfere with the CDRs but can presumably impact the binding to CD47.

Taken together, the engraftment of the endogenous N-terminal SIRP α domain onto an antibody targeting CD33 was demonstrated to be a promising approach to locally restrict the effects of blocking the CD47-SIRP α immune checkpoint to AML cells.

DISCUSSION

5.2. Advantages and limitations of liCADs

As already speculated for CD33-targeting BiKEs, the low molecular weight of liCADs would likely facilitate their infiltration into the bone marrow, which would be beneficial for targeting AML LSC.¹⁵⁰ Thus, the liCAD format is very promising for immunotherapy of AML and specially for eliminating AML cells responsible for relapse.

By targeting CD16 with high affinity, liCADs induced potent NK cell-mediated cytotoxicity of AML cells. This is based on the fact that CD16 is the main FcγR expressed on NK cells and is indispensable for ADCC.^{170, 171} The specificity for CD16 of liCADs, however, made these molecules unable to induce phagocytosis of AML cells. This is due to the low CD16 expression on macrophages, as described in this and previous studies.¹⁷² Consequently, the enhancement of phagocytosis by blocking the CD47-SIRPα immune checkpoint could not be evaluated in the liCAD format.

In order to be able to investigate the potential of liCADs to induce phagocytosis, the specificity of the effector cell-activating domain could be exchanged. CD32A is an activating FcγR expressed on macrophages and described to trigger phagocytosis.¹⁷³⁻¹⁷⁵ Thus, we anticipate that a SIRPα-αCD32A-αCD33 liCAD would promote phagocytosis of AML cells. Importantly, CD32A is also described to be expressed and functional on NK cells of around 45% of the individuals.^{176, 177} This suggests that a SIRPα-αCD32A-αCD33 liCAD could also mediate ADCC by CD32A⁺ NK cells. Hence, in order to obtain an improved anti-tumor immune response, the αCD16 scFv of liCADs could be replaced by high affinity scFv targeting the receptor CD32A. This idea is further supported by fact that mAbs engineered to preferentially bind CD32A were described promote improved ADCC and ADCP effects than conventional mAbs.^{178, 179}

In summary, the engagement of CD16 by liCADs demonstrated successful NK cell-dependent elimination of AML cells but impeded the investigation of liCAD-mediated phagocytosis. Nevertheless, the liCAD format presents some advantages over licMABs and licMABs^{single} and therefore these molecules should be re-evaluated after substituting the CD16 scFv for a CD32A scFv.

5.3. LicMABs and licMABs^{single} enhance phagocytosis of AML cells

LicMABs and licMABs^{single} successfully enhanced the phagocytosis of AML cell lines and primary, patient-derived AML cells. These results are in agreement with studies

DISCUSSION

showing that the combination of a pro-phagocytic stimulus mediated by the Fc domain of an antibody and the blockade of the CD47-SIRP α immune checkpoint stimulates active phagocytosis.^{71, 93, 169}

Interestingly, we reported that the expression levels of CD47 on macrophages and primary AML patient samples dictate the outcome of licMABs-mediated phagocytosis. In other words, patients with a high CD47 expression are more likely to benefit from licMABs. Accordingly, the determination of the expression levels of CD47 on AML patients should be evaluated prior to the administration of licMABs. It is important to note that we and others found CD47 overexpressed on AML cells with respect to normal cells, which suggests that licMABs are effective for a majority of patients.^{70, 152} Despite CD47 expressed on AML cells, CD47 on macrophages also plays an important role in determining licMAB-mediated phagocytosis. Therefore, in order to better understand the anti-tumor effect of licMABs, a phagocytosis assay in an autologous setting should be performed. A limitation for this is that AML cells and macrophages derive from a common myeloid progenitor, which impedes the isolation of both cell types from one patient sample. Thus, an autologous ADCP assay would require healthy macrophages from an AML patient currently cured and previously stored AML cells from the same patient. The limited amount of patient material and the low survival rates of AML patients, however, highly restrict the performance of such assay. A second limitation is that cured AML patients most probably received an allo-SCT.¹¹⁶ In this case, the transplanted immune system develops healthy macrophages that are no longer considered as autologous with respect to the AML cells. Moreover, that AML cells belong to the same hematopoietic lineage as macrophages may also impact the outcome of ADCP due to the expression of myeloid markers on AML cells, such as Fc γ R α and SIRP α .¹⁸⁰ Since these may act as decoy receptors for local inhibitory checkpoint molecules, licMABs may promote stronger anti-tumor effects with tumor types not derived from the myeloid lineage. In summary, the influence of CD47 expression levels on licMAB-mediated phagocytosis needs to be further investigated.

In addition to the stimulation of macrophage-mediated phagocytosis, licMABs and licMABs^{single} are also expected to mediate tumor elimination by adaptive immune responses. One study showed that a mAb targeting SIRP α promoted the activation of macrophages, and neutrophils in mice bearing a human Burkitt's lymphoma, thus limiting the tumor growth and achieving tumor elimination.¹⁰⁹ CD47-blocking mAbs were as well

DISCUSSION

reported to stimulate adaptive immune responses *in vitro* and *in vivo*.¹⁰³ Furthermore, nanobodies targeting CD47 were not able to control melanoma growth, but when combined with a PD-L1-blocking mAb, which restores T cell functions, anti-tumor responses were improved.¹⁸¹ These evidences already suggested that the blockade of the CD47-SIRP α immune checkpoint contributes to the generation of adaptive immune responses, but further clarification was provided by Liu, Xu and co-workers. They described that DCs, and not macrophages, are involved in activating tumor-specific CD8⁺ T cells upon disruption of the CD47-SIRP α axis.^{105, 106} Specifically, the treatment of DCs with a CD47 inhibitor prevented the cytosolic clearance of tumor mitochondrial DNA (mtDNA) that presumably entered through exosomes. Tumor mtDNA was then recognized by cyclic GMP-AMP synthase (cGAS), which activated the cGAS-STING signaling pathway. This stimulated the production of type I interferons and ultimately led to the cross-priming of CD8⁺ T cells.¹⁰⁶ Based on these results, we speculate that the blockade of the CD47-SIRP α immune checkpoint by licMABs and licMABs^{single} also results in the activation of neutrophils, DCs and CD8⁺ T cells.

Taken together, the novel immunotherapeutic molecules licMABs and licMABs^{single} enhance the phagocytosis of primary, patient-derived AML cells by locally disrupting the CD47-SIRP α immune checkpoint and might also induce tumor-specific T cell activation. Consequently, the application of licMABs and licMABs^{single} may lead to the stimulation of a complete anti-tumor immune response that involves both innate and adaptive effector functions.

5.4. Other determinants of macrophage-mediated phagocytosis

Several efforts have been focused on describing novel surface molecules that may play a role in phagocytosis, and the field further speculates on the presence of other phagocytosis-regulating mechanisms not yet described.¹⁸² Thus, despite expression levels of CD47, other factors may influence licMABs and licMABs^{single}-mediated phagocytosis.

The role of calreticulin in macrophage-mediated phagocytosis was discovered after the observation that a CD47-blocking mAb was not inducing phagocytosis of certain healthy cells. Calreticulin was described as a cell surface antigen that interacts with the low density lipoprotein-receptor related protein (LRP). LRP, expressed on phagocytic cells, delivers a pro-phagocytic stimulus upon binding to calreticulin.¹⁸³ Since calreticulin expression occurs after DNA damage, it is absent on healthy cells and this protects them

DISCUSSION

from being phagocytosed when coated with CD47-specific mAbs.^{183, 184} Apoptotic and tumor cells, on the contrary, express calreticulin, which acts as an “eat me” signal and potentiates the elimination of these cells through phagocytosis. It is suggested that the upregulation of CD47 on tumor cells is a mechanism to compensate for calreticulin expression and enable phagocytosis escape. Hence, mAbs targeting CD47 block the “don’t eat me” signal on healthy and tumor cells, but only tumor cells are phagocytosed due to calreticulin expression. In agreement with this, a mAb blocking the binding of calreticulin to LRP completely abrogated the phagocytosis of tumor cells induced by a CD47-blocking mAb. It is also suggested that calreticulin expression substitutes the pro-phagocytic signal triggered by the IgG1 Fc domain and facilitates the stimulation of phagocytosis by IgG4 CD47-blocking mAbs. Calreticulin expression, however, was only observed on non-Hodgkin lymphoma, bladder cancer and neuroblastoma and further evaluations are required to consider it a common tumor antigen. Interestingly, calreticulin was also described to be upregulated on circulating neutrophils, which provides an explanation for the neutropenia seen in *in vivo* studies evaluating CD47 inhibitors.^{69, 185}

An unrelated investigation found that mAbs targeting CD47 induced phagocytosis of hematological cancers but not solid tumors.¹⁸⁶ This was explained by the presence of the hematopoietic receptor SLAMF7, a member of the signaling lymphocytic activation molecule family, on tumor cells susceptible for CD47-mediated phagocytosis. SLAMF7 was initially described as a homotypic receptor involved in regulating natural cytotoxicity of NK cells against cognate cellular and viral ligands.¹⁸⁷ However, downregulation of SLAMF7 on macrophages resulted in defective phagocytosis, which identified SLAMF7 as a pro-phagocytic stimulus.¹⁸⁶ SLAMF7 was shown to interact with Mac-1, also expressed on macrophages, and mediate the signaling cascade through phosphorylation of ITAMs motifs.^{188, 189} Accordingly, mAbs against SLAMF7 inhibited phagocytosis in the presence of α CD47 mAbs.¹⁸⁶ This indicated that SLAMF7 expression on both macrophages and target cells is crucial in order to enhance phagocytosis by blocking the CD47-SIRP α immune checkpoint. Similarly to calreticulin expression, an increased expression of SLAMF7 on tumor cells makes them more sensible to immunotherapies targeting the CD47-SIRP α axis. Interestingly, SLAMF7 expression was lower in AML with respect to chronic lymphocytic leukemia, myelodysplastic syndrome, multiple myeloma and B cell lymphomas, suggesting that AML cells may be less susceptible to CD47 inhibitors than other types of leukemia.

DISCUSSION

Lastly, MHC class I was as well elucidated as a regulator of macrophage-mediated phagocytosis.¹⁹⁰ MHC class I molecules are ubiquitously expressed on most of the cells and are known to play a role in controlling the activation of NK and T cells.^{191, 192} The role of MHC class I on macrophage-mediated phagocytosis was further investigated after the evaluation of the α CD47 mAb Hu5F9-G4.⁹² While Hu5F9-G4 stimulated phagocytosis in most of the tested tumor cell lines, some were resistant to phagocytosis independently of the cancer type and expression levels of CD47. By comparing surface antigens, the authors found MHC class I molecules expressed on cell lines refractory to Hu5F9-G4-mediated phagocytosis and absent on responsive cell lines.¹⁹⁰ MHC class I was described to negatively regulate phagocytosis by interacting with the leukocyte immunoglobulin-like receptor subfamily B member 1 (LILRB1), expressed on a major subset of macrophages.¹⁹³ Hence, mAbs targeting LILRB1 enhanced the phagocytosis of MHC class I-expressing tumor cells *in vitro* and *in vivo* and, most importantly, potentiated the anti-tumor immune responses induced by CD47-blocking mAbs.¹⁹⁰

In summary, besides CD47, MHC class I molecules have been described to negatively regulate phagocytosis and calreticulin and SLAMF7 to be pro-phagocytic signals on tumor cells. The characterization of such antigens on primary, patient-derived AML cells may therefore contribute to the understanding of the anti-tumor effects mediated by licMABs. Moreover, the investigation of surface antigens differentially expressed on responsive/refractory primary AML cells could lead to the discovery of novel surface receptors involved in the regulation of phagocytosis.

5.5. CD33-dependent internalization

The endocytosis of CD33 was initially described to occur upon engagement by conventional mAbs. This mechanism was exploited by ADCs, such as GO, to deliver a toxin inside CD33-expressing tumor cells.¹⁹⁴ Accordingly, we reported that licMABs also induced CD33-dependent internalization. However, as licMABs rely on activating immune cells to mediate anti-tumor effects, the internalization of these molecules may mask their potential as immunotherapies.

The signaling cascade that ultimately triggers CD33 internalization is well described. It involves the phosphorylation of ITIM motifs and the recruitment of several proteins with SH2 domains, such as the ECS E3 ubiquitin ligase complex.¹⁵⁸ Nevertheless, the precise mechanism that initiates this process remains unknown. One study noted that CD33 could

DISCUSSION

be detected on the surface of tumor cells after the incubation with AMG 330, which targets CD33 with one scFv.¹⁴⁹ This suggested that, contrary to conventional mAbs, monovalent targeting does not induce CD33 internalization. Based on that observation, we generated licMABs^{single} and liCADs, which bind to CD33 with either a Fab or a scFv domain and therefore should not mediate CD33-dependent internalization. The evaluation of licMABs^{single} and SIRP α - α CD33 liCAD, however, demonstrated that these molecules internalize to a degree similar to licMABs. This proposed that other factors, besides the binding valency to CD33, influence internalization.

Reports on the internalization of CD19 indicated that the expression of Fc receptors, and specially CD32, may be involved in this mechanism.^{195, 196} It was suggested that mAbs simultaneously bind to CD19 and to CD32 and that this forms a three-component complex that increases the endocytosis of CD19. The isotype of the antibody targeting CD19, in addition, also modulated the amount of internalization. It is therefore possible that licMABs^{single} trigger internalization of CD33 by also binding to CD32 with their Fc domain. However, there is no evidence consistent with the endocytosis of CD33 by SIRP α - α CD33 liCAD, which suggests that further investigations are required to fully understand CD33 internalization mechanisms.

Notwithstanding these limitations, the anti-tumor effects mediated by licMABs, licMABs^{single} and liCADs demonstrate that the internalization of these molecules does not significantly hamper their efficacy.

5.6. Comparative analysis of licMABs, licMABs^{single} and liCADs

All evaluated local inhibitory checkpoint molecules bind to CD33, disrupt the CD47-SIRP α immune checkpoint and activate immune effector cells. However, they differ on the binding valency to CD33 and CD47 and on the nature of the effector cell-activating domain, and these differences determine the potency of the mediated anti-tumor immune responses (Figure 26).

The minimal binding of local inhibitory molecules to RBCs was influenced by the amount of SIRP α domains. The local inhibitory checkpoint molecule containing four SIRP α domains, 2xSIRP α - α CD33 licMAB, showed the highest binding to RBCs. This suggests that 2xSIRP α - α CD33 licMAB potentially presents the highest risk to mediate on-target/off-leukemia effects. Nevertheless, the engagement of RBCs was negligible

DISCUSSION

compared to the high affinity mAb targeting CD47, indicating that unwanted toxicity to healthy cells is still reduced. Furthermore, studies on CD47's accessibility showed that the four SIRP α domains achieved the best blockade of CD47 on MOLM-13 cells. Local inhibitory molecules containing two SIRP α domains, SIRP α - α CD33 licMAB, 2xSIRP α - α CD33 licMAB^{single} and 2xSIRP α - α CD33 liCAD, bound to RBCs marginally and still occupied CD47. Amongst them, 2xSIRP α - α CD33 liCAD showed the smallest binding to RBCs, thus being advantageous over SIRP α - α CD33 licMAB and 2xSIRP α - α CD33 licMAB^{single}. Lastly, local inhibitory checkpoint molecules with one SIRP α domain, such as SIRP α - α CD33 licMAB^{single} and liCAD did not engage RBCs and blocked CD47 on MOLM-13 cells to a lower degree.

Taken together, these results indicate that the blockade of CD47 can be modulated by the amount of SIRP α domains. Moreover, we demonstrate that one SIRP α domain is already able to disrupt the CD47-SIRP α axis and, most importantly, that the preferential binding to CD33-expressing cells is not disturbed by the presence of several SIRP α domains.

The functional evaluation of local inhibitory checkpoint molecules showed that the high affinity of liCADs for CD16 was favorable in inducing ADCC of tumor cells. Thus, liCADs facilitated the most potent NK-cell mediated lysis of AML cell lines. SIRP α - α CD33 licMAB also triggered potent cytotoxicity of tumor cells. However, ADCC effects were slightly reduced by 2xSIRP α - α CD33 licMAB, presumably due to the lower affinity of the double SIRP α molecule. Similarly, licMABs^{single}, which engaged NK cells by the Fc domain and bound CD33 with one Fab fragment, triggered mild NK cell-mediated cytotoxicity to tumor cells.

On the other hand, the high affinity α CD16 scFv of liCADs was disadvantageous in promoting phagocytosis of tumor cells, which is explained by the lack of CD16 expression on macrophages. By engaging all Fc γ R_s through the Fc domain, licMABs and licMABs^{single} successfully mediated comparable levels of phagocytosis of AML cell lines independently of the quantity of SIRP α domains. Phagocytosis of primary, patient-derived AML samples was also effectively induced by licMABs and licMABs^{single}, being SIRP α - α CD33 licMAB the molecule that induced the strongest phagocytosis.

DISCUSSION

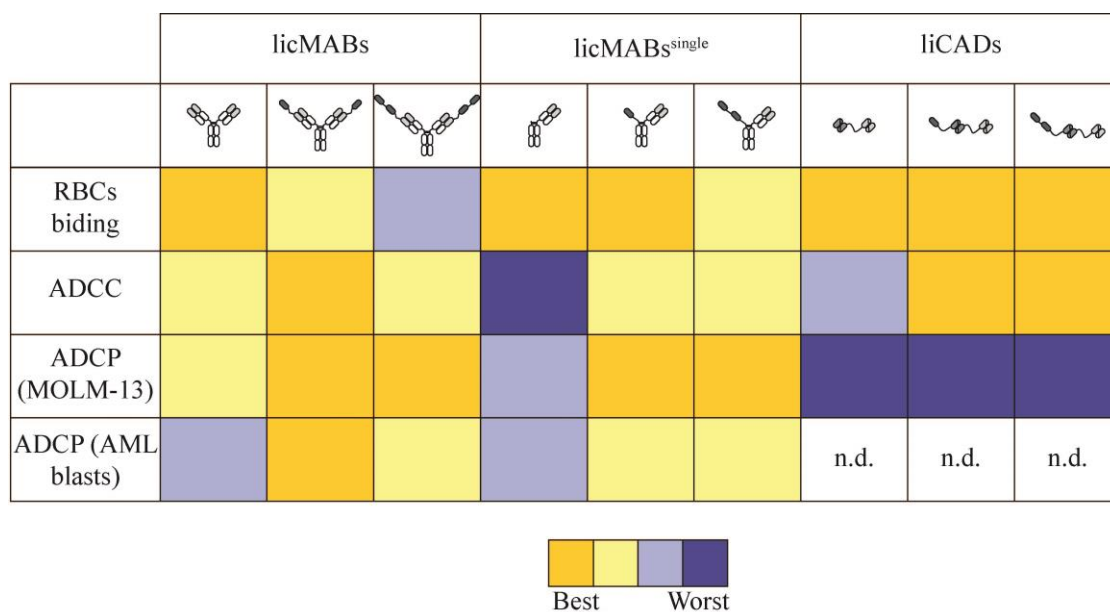


Figure 26. Comparison of anti-tumor effects induced by local inhibitory checkpoint molecules

Evaluation of licMABs, licMABs^{single} and liCADs regarding specific tumor-antigen binding, capacity to induce NK cell-mediated lysis of AML cell lines and ability to mediate phagocytosis of AML cell lines and primary, patient-derived AML cells. n.d., not determined.

Overall, within the evaluated local inhibitory checkpoint molecules, SIRP α - α CD33 licMAB induced the most potent anti-tumor effects based on preferential tumor binding and ability to eliminate tumor cells via ADCC and phagocytosis mechanisms. Hence, licMABs are the molecules of choice to conduct *in vivo* experiments in order to finalize the pre-clinical evaluation and translate this work into a clinical setting.

6. MATERIALS AND METHODS

6.1. Materials

Unless otherwise stated, all chemicals were purchased from Carl Roth, Merck, or Sigma-Aldrich. Restriction enzymes were obtained from Fermentas or New England Biolabs and primers from Metabion.

6.1.1. *E. coli* strain, cell lines and media

The *E. coli* strain XL1 Blue, purchased from Stratagen, was made chemically competent as previously described and used for cloning.¹⁹⁷ XL1 Blue were cultured in lysogeny broth (LB) media (10 g/L tryptone, 5 g/L yeast extract, 5 g/L NaCl, 1.3 ml/L NaOH) and plated in LB agar (LB-Lennox media with 15 g/L agar).

The MOLM-13 cell line was purchased from the Deutsche Sammlung von Mikroorganismen und Zellkulturen (DSMZ) and cultured in RPMI 1640 + GlutaMAX (Gibco, Thermo Fisher Scientific) supplemented with 20% fetal bovine serum (FBS, Gibco, Thermo Fisher Scientific). SEM cells, obtained from American Type Culture Collection (ATCC), and the OCI-AML3 cell line, which was a kind gift from Prof. Marion Subklewe, was cultured in RPMI 1640 + GlutaMAX supplemented with 10% FBS. Schneider 2 cells were purchased from ExpreS²ion Biotechnologies and cultured with Ex-CELL® 420 (Sigma-Aldrich) and Flp-INTM-CHO were obtained from Thermo Fisher Scientific and cultured in Ham's F-12 media (Thermo Fisher Scientific) supplemented with 10% FBS. Flp-INTM-CHO cells were stably transfected with CD33 and CD47 (here designated as CHO_CD33 and CHO_CD47) by Monika Herrmann and Dr. Nadine Magauer, respectively, and were subsequently cultured in Ham's F-12 supplemented with 10% FBS and 500 µg/mL hygromycin B Gold (InvivoGen). Expi293F cells, purchased from Thermo Fisher Scientific, were cultured in Expi293 medium. All cell lines were grown until the recommended cell density and passaged twice a week.

6.1.2. Healthy donors' and AML patients' material

Peripheral blood or bone marrow samples were collected from healthy donors and AML patients after written informed consent in accordance with the Declaration of Helsinki and approval by the Institutional Review Board of Ludwig-Maximilians-University. Peripheral blood from healthy donors was the source of RBCs, peripheral blood

MATERIALS AND METHODS

mononuclear cells (PBMCs), NK cells and monocytes. The characteristics of AML patient material used for ADCC and for ADCP assays are displayed in Table 2 and Table 3, respectively.

Table 2. Characteristics of AML patients' material used for NK cell-mediated ADCC assays

PT	Gender	Disease Phase	Material	<i>NPM1</i> mut.	<i>FLT3-ITD</i>	Karyotype	ELN genetic group	CD33 MFI ratio	CD47 MFI ratio
1	F	ID	BM	+	-	normal	favorable	111.8	47.1
2	F	ID	BM	+	+	normal	intermediate I	110.0	76.3
3	M	ID	PB	-	+	47, xy, +8	intermediate II	73.0	95.2
4	M	Relapse	BM	-	-	complex	adverse	52.3	34.5
5	M	ID	BM	-	-	normal	intermediate I	54.2	58.2
6	M	ID	BM	-	-	normal	intermediate I	12.6	75.9
7	F	Relapse	BM	-	+	46,xx; t(5,11)	intermediate II	90.0	27.1
8	M	ID	PB	-	-	46,xx; der(16)t(1;16)(q12;q21)	intermediate II	37.0	31.7
9	F	ID	BM	+	+	n.a.	n.a.	n.a.	n.a.

Table 3. Characteristics of AML patients' material used for phagocytosis assays

PT	Gender	Disease Phase	Material	<i>NPM1</i> mut.	<i>FLT3-ITD</i>	Karyotype	ELN genetic group	CD33 MFI ratio	CD47 MFI ratio
1	n.a.	ID	BM	+	+	46,XX[20]	intermediate I	16.66	20.19
2	F	ID	PB	n.a.	n.a.	n.a.	n.a.	21.67	11.92
3	F	ID	BM	+	-	46,XX,t(11;19)(q23;p13.3)[14]/46,X X[2]	favorable	8.30	10.51
4	F	ID	BM	+	-	46,XX[20]	favorable	20.42	68.71
5	F	ID	BM	+	-	46,XX[20]	favorable	13.14	53.14
6	F	ID	BM	-	-	46,XX,t(11;19)(q23;p13.3)[14]/46,X X[2]	adverse	7.19	5.16

MATERIALS AND METHODS

7	F	ID	BM	-	+	46,XX[22]	intermediate I	17.79	40.08
8	M	ID	BM	-	+	47,XY,r(8)(? ?),+der(8),del(15)(q22q26)[21]	adverse	9.71	12.49
9	M	ID	PB	+	-	46,XX[24]	favorable	29.79	14.96
10	M	ID	PB	+	-	47,XY,+X[21]	intermediate I	10.95	28.70
11	F	ID	PB	-	+	46,XX[20]	intermediate I	26.54	23.91
12	F	ID	PB	-	-	46,XX;t(6;11)(q27,q23)[14]	adverse	22.82	32.33
13	M	ID	PB	-	-	46,XY,t(1;21)(p36;q22)[24]/46,XY[2]	n.a.	1.58	17.01

6.2. Molecular biology methods

Conventional cloning methods were executed according to standard protocols and commercial kits and enzymes were used following the manufacturer's instructions.¹⁹⁸ Briefly, insert of interest was amplified by polymerase chain reaction (PCR) with the respective restriction sites. PCR products were separated by agarose gel electrophoresis, the desired DNA band was cut out and DNA was extracted from the agarose gel using the NucleoSpin Gel and PCR clean-up kit (Macherey-Nagel). Isolated insert and backbone vector were digested with restriction enzymes, ligated and transformed into *E. coli* XL1-Blue. Next, plasmid DNA of *E. coli* clones was prepared using the NucleoSpin Plasmid Easy Pure kit (Macherey-Nagel) or the NucleoBond® Xtra Maxi kit (Macherey-Nagel). All constructs were verified by DNA sequencing by Eurofins MWG Operon.

6.2.1. Molecular cloning

In order to generate licMABs, the commercial vectors pFUSE2-CLIg-hk and pFUSE-CHIg-hG1 (InvivoGen) were used. The α CD33 V_L and α CD33 V_H domains (clone hP67.6) were engrafted into the respective vectors to create pFUSE-CH-33 and pFUSE2-CL-33. The N-terminal Ig-like domain of SIRP α (residues 1-120) was cloned into the α CD33 LC vector followed by a (G₄S)₄ linker to create the pFUSE2-CL-SIRP-33. Moreover, a preScission protease site was inserted between the SIRP α and the α CD33 V_L

MATERIALS AND METHODS

domains to create a cleavable SIRP α tag (pFUSE2-CL-PreSc-33). An additional SIRP α domain was cloned into the N-terminus of pFUSE2-CL-SIRP-33, thus creating the pFUSE2-CL-2xSIRP-33 vector. LicMABs^{single} were generated from licMABs by exchanging one α CD33 Fab fragment for the endogenous extracellular domain of SIRP α . In order to ensure correct pairing of the two distinct heavy chains, charged mutations were inserted, obtaining a negatively charged HC (with mutations K392D and K409D) and a positively charged HC (E456K and D399K).⁴¹ The plasmids encoding for liCADs, cloned into the pExpreS2-1 vector (ExpreS²ion Biotechnologies), were obtained from Dr. Nadine Magauer and Saskia Schmitt. The amino acid sequences of each domain are specified in Table 4.

Table 4. Amino acid sequences of the SIRP α domain and the antigen-binding sites recognizing CD16 and CD33

Domain	Sequence
SIRP α	EEELQVIQPDKSVLVAAGETATLRCTATSLIPVGPIQWFRGAGP GRELIYNQKEGHFPRVTTVSDLTKRNNMDFSIRIGNITPADAGT YYCVKFRKGGSPDDVEFKSGAGTELSVRAKPS
α CD16 scFv (V _H -(G ₄ S) ₄ -V _L)	VTLKESGPGILQPSQTLSTCSFSGFSLRTSGMGVGVWIRQPSGK GLEWLAHIWWDDDKRYNPALKSRLTISKDTSSNQVFLKIASV DTADTATYYCAQINPAWFAYWGQGTTLTVSAGGGGSGGGGS GGGGSGGGGSGGGGSDTVLTQSPASLAVSLGQRATISCKASQS VDFDGDSEFMNWYQQKPGQPPKLLIYTTSNLESGIPARFSASGS GTDFTLNIHPVEEEDTATYYCQQSNEDPYTFGGGKLEIK
α CD33 scFv (V _L -(G ₄ S) ₄ -V _H)	DIQLTQSPSTLSASVGDRVTITCRASESLDNYGIRFLTWFFQQKP GKAPKLLMYAASNQGSVPSRFSGSGSGTEFTLTISLQPDFA TYYCQQTKEVPWSFGQGTKVEVKGGGGSGGGGSGGGGSGGG GSEVQLVQSGAEVKKPGSSVKVSKASGYTITDSNIHWVRQAP GQSLEWIGYIYPYNGGTDYNQKFKNRATLTVDNPTNTAYMEL SSLRSEDATFYCYVNGNPWLAYWGQGTTLTVSS
α CD33 V _H	EVQLVQSGAEVKKPGSSVKVSKASGYTITDSNIHWVRQAPG QSLEWIGYIYPYNGGTDYNQKFKNRATLTVDNPTNTAYMELS SLRSEDATFYCYVNGNPWLAYWGQGTTLTVSS
α CD33 V _L	DIQLTQSPSTLSASVGDRVTITCRASESLDNYGIRFLTWFFQQKP GKAPKLLMYAASNQGSVPSRFSGSGSGTEFTLTISLQPDFA TYYCQQTKEVPWSFGQGTKVEVK

6.2.2. Transformation of *E. coli*

For transformation, 10 μ l of ligated plasmid was mixed with 100 μ l of chemically competent XL1-Blue and incubated for 15 min on ice. Cells were then heat shocked for

MATERIALS AND METHODS

45 sec at 42°C followed by a second incubation of 2 min on ice. Subsequently, 600 µl of LB were added and cells were incubated at 37°C for 1 h and constant shaking. Cells were plated on a LB agar plate supplemented with 25 µg/ml blasticidine (InvivoGen) or zeocine (Thermo Fisher Scientific) for LC or HC vectors, respectively, and placed in a 37°C incubator over night. Colonies were picked and grown over night in 5 ml LB medium containing the corresponding antibiotic at 37°C and with constant shaking. Plasmid DNA was prepared from grown cultures as previously mentioned.

6.3. Protein biochemistry methods

6.3.1. Expression and purification of licMABs and licMABs^{single}

In order to obtain licMABs and licMABs^{single}, the corresponding vectors were co-transfected into Expi293F cells using the ExpiFectamine™ 293 transfection kit (Thermo Fisher Scientific) following the manufacturer's instructions. For the generation of licMABs, heavy and light chain of licMABs and mAb were transfected in a 1 to 4 ratio. For licMABs^{single}, positively charged HC, negatively charged HC and LC were transfected in a 1 to 1 to 3 ratio.

Five days after transfection, licMABs were purified by protein A affinity chromatography. Cell culture supernatants were collected by centrifugation at 500 RCF for 10 min. 250 µl of nProtein A sepharose 4FF beads (GE Healthcare), previously washed with PBS (8 g/L NaCl, 0.2 g/L KCl, 1.44 g/L Na₂HPO₄·2H₂O, 0.2 g/L KH₂PO₄, pH 7.4) were added and incubated over night at 4°C on a rotating wheel. Beads were collected by centrifugation at 500 RCF for 5 min and loaded into a Bio-Spin® chromatography column (Thermo Fisher Scientific). Washing steps were performed with 4 column volumes of protein A binding buffer (50 mM Tris-HCl pH 7.0) and licMABs were eluted from the beads by 5 to 6 column volumes of protein A elution buffers (0.1 M citrate pH 3.0). Elution fractions were neutralized with protein A neutralization buffer (1 M Tris-HCl pH 9.0). Purified proteins were evaluated by SDS-PAGE and fractions containing licMABs were pooled and dialyzed against PBS.

After dialysis, proteins were concentrated using Amicon spin concentrators (Merck Millipore) and SEC with a Superdex 200 GL increase column (GE Healthcare) was performed. SEC fractions that contained licMABs were pooled and proteins were visualized by SDS-PAGE (Expedeon) and comassie stain (50% (v/v) ethanol, 7% (v/v)

MATERIALS AND METHODS

acetic acid, 0.2% (w/v) Coomassie Brilliant Blue R250). Protein concentration was measured with a spectrophotometer (Nanodrop ND-100, Peqlab Biotechnologies GmbH) and samples were aliquoted, shock frozen in liquid nitrogen and subsequently stored at -80°C.

In addition to the procedures described above, CD33-targeting mAb, mAb^{single} and licMABs^{single} were treated with PreScission Protease in order to cleave the SIRP α tag. Subsequently, a second protein A affinity chromatography was performed to purify the SIRP α -free molecules.

6.3.2. Expression and purification of liCADs

Briefly, pExpreS2-1vectors encoding for liCAD sequences were transfected into Schneider 2 cells using Lipofectamine® 200 (Thermo Fisher Scientific) according to manufacturer's protocol. Next, stable cell lines expressing liCADs were grown in EX-CELL® 420 medium supplemented with 10% FBS and 2 mg/ml zeocin for 26 days. For liCAD expression, cells were cultured in medium without FBS for 4 to 5 days. Cell culture supernatants were harvested and liCADs, containing a histidine-tag, were purified by Ni-NTA affinity chromatography (Qiagen) using wash (20 mM Tris, 10 mM imidazol, 300 mM NaCl, pH 9.0) and elution buffers (20 mM Tris, 200 mM imidazol, 300 mM NaCl, pH 9.0). Next, liCADs were dialyzed into a low salt buffer and an anion-exchange chromatography with a MonoQ 5/50 GL column (GE Healthcare) was performed. After an additional SEC, purified proteins were visualized by SDS-PAGE. SEC fractions were then pooled, measured, aliquoted, shock frozen in liquid nitrogen and stored at -80°C.

6.3.3. Fluorescence thermal shift assay

Fluorescence thermal shift assays were used to determine the stability of licMABs, licMABs^{single} and liCADs. 10 μ g of licMABs, licMABs^{single} or liCADs were diluted in PBS and 1x SYPRO orange (Thermo Fisher Scientific) in a total volume of 25 μ l and analyzed in a real-time PCR machine. The melting curve was measured using a gradient from 5°C to 100°C and one scan per 0.5°C.

6.4. Binding and interaction studies

6.4.1. Binding studies by flow cytometry

Unless otherwise stated, flow cytometry assays were performed using a Guava easyCyte 6HT instrument (Merck Millipore) and data was analyzed and plotted with GuavaSoft software version 3.1.1 (Merck Millipore). Binding analyses were carried out with cell lines expressing the desired antigens. Molecules were used in saturating concentrations of 15 ng/ μ l with an incubation time of 30 min at 4°C in FACS buffer (1% FBS, 1 mM EDTA in PBS). Cells were washed and incubated with the labeled secondary antibody, being FITC- α human IgG Fc (clone ET901, BioLegend) for licMABs and licMABs^{single} and Alexa Fluor 488- α His (polyclonal, Qiagen) for liCADs, for 30 min at 4°C. A second wash was performed before the stained cells were analyzed.

6.4.2. Quantitative determination of cell surface antigens

The QIFIKIT (DAKO) was used, according to the manufacturer's instructions, to describe the number of surface antigens expressed on the cell surface.¹⁹⁹ Briefly, MOLM-13, SEM, CHO_CD33 or CHO_CD47 were incubated with saturating concentrations of unconjugated α human CD33 (clone P67.7, BioLegend) or α human CD47 (clone CC2C6, BioLegend) mAbs for 30 min at 4°C. After washing with FACS buffer, both QIFIKIT calibration beads and cells were incubated with saturating concentrations of the provided secondary antibody and analyzed by flow cytometry. The quantification of surface antigens was obtained by interpolating the MFI values of the samples to the calibration curve.

6.4.3. CD47-blocking assay

CD47-blocking assays were performed in order to study the binding of the SIRP α domain within the local inhibitory checkpoint molecules to CD47. To this end, MOLM-13 cells were incubated with saturating concentrations of licMABs, licMABs^{single}, liCADs or control molecules, such as an α CD47 mAb (clone CC2C6, BioLegend), the extracellular SIRP α domain and the high affinity SIRP α variant (SIRP α CV1), for 30 min on ice. This was followed by a washing step with FACS buffer and a second staining with a FITC-conjugated α CD47 mAb (clone B6H12, BioLegend). Data was displayed as MFI ratio of the conjugated antibody targeting CD47 with respect to the unstained population.

MATERIALS AND METHODS

6.4.4. K_D determination

Equilibrium binding constants (K_D , as an avidity measurement) of licMABs, licMABs^{single} and liCADs on MOLM-13 cells were studied by calibrated flow cytometry.²⁰⁰ MOLM-13 cells were incubated with local inhibitory checkpoint molecules in a concentration range of 0.01 to 5 $\mu\text{g/ml}$, for 30 min and at 4°C. Cells were subsequently stained with the corresponding secondary antibody. For evaluation, the maximum MFI was set to 100% and all data points were normalized accordingly. The data was fitted with a non-linear regression curve using a one-site specific binding model.

6.4.5. Internalization assay by flow cytometry

To study the CD33-dependent internalization of the local inhibitory checkpoint molecules by flow cytometry, 0.1×10^6 MOLM-13 cells were incubated with 15 ng/ μl of protein for 30, 60, and/or 120 min at 37°C. For control conditions, the molecules were incubated for 120 min on ice-cold water. After incubation with local inhibitory checkpoint molecules, MOLM-13 were washed with ice-cold FACS buffer and stained with the corresponding secondary antibodies. Internalization rate was calculated as follows:

$$\text{Internalization (\%)} = \frac{(\text{MFI}_{4^\circ\text{C}} - \text{MFI}_{\text{background}}) - (\text{MFI}_{37^\circ\text{C}} - \text{MFI}_{\text{background}})}{(\text{MFI}_{4^\circ\text{C}} - \text{MFI}_{\text{background}})} \times 100$$

6.4.6. Internalization assay by confocal microscopy

The internalization of licMABs on MOLM-13 cells was confirmed by confocal microscopy. To this end, licMABs were directly labeled with Alexa Fluor 488 using an Antibody Labeling Kit (Thermo Fisher Scientific) and following the manufacturer's instructions. MOLM-13 cells were seeded on a poly-L-lysine (Sigma-Aldrich) coated 96 well plate. 15 ng/ μl of directly labeled licMABs or mAb were added and cells were incubated either at 37°C for 30, 60 and 120 min or on ice-cold water for 120 min. Cells were fixed and permeabilized using a fixation and permeabilization solution (20 mM PIPES pH 6.8, 4% formaldehyde, 0.2% Triton X-100, 10 mM EGTA, 1 mM MgCl_2) at room temperature for 10 min, followed by incubation in blocking solution (3% Milk, 0.05% Tween-20 in PBS). After washing the cells three times with 0.05% Tween-20 in PBS, cells were stored in PBS until examination on a fully automated Zeiss inverted microscope (Leica) equipped with a MS-2000 stage (Applied Scientific Instrumentation), a CSU-X1 spinning disk confocal head (Yokogawa) and a LaserStack Launch with

MATERIALS AND METHODS

selectable laser (Intelligent Imaging Innovations). Images were acquired using a CoolSnap HQ camera (Roper Scientific), a 63 x oil objective and the Slidebook software version 6.0 (Intelligent Imaging Innovations) and processed with Adobe Photoshop CS4 (Adobe Systems).

6.4.7. Size exclusion chromatography analysis

SEC techniques were used in order to study the interaction between CD16 scFv and the extracellular domain of CD16. SIRP α - α CD33 licMAB, SIRP α - α CD33 liCAD and the extracellular domain of CD16 were independently loaded on a Superdex 200 increase 5/150 GL column. Next, SIRP α - α CD33 licMAB or SIRP α - α CD33 liCAD were mixed with equimolar amounts of the extracellular domain of CD16 and the complexes were loaded into the same chromatography column. Complex formation was confirmed by visualization on an SDS-PAGE.

6.5. Functional assays

6.5.1. Red blood cells competition assay

To obtain RBCs, peripheral blood was centrifuged at 1000 RCF and subsequently washed three times with RBC's wash buffer (21 mM Tris, 4.7 mM KCl, 2 mM CaCl, 140.5 mM NaCl, 1.2 mM MgSO₄, 5.5 mM glucose, 0.5% bovine serum albumin, pH 7.4) as previously described.²⁰¹ MOLM-13 cells were stained with the membrane dye PKH26 (Sigma-Aldrich) according to the manufacturer's protocol. PKH26-labeled MOLM-13 cells were then centrifuged, washed with RPMI 1640 + GlutaMAX and mixed with a 5-, 10-, or 20-fold excess of RBCs. Cells were incubated with 15 ng/ μ l of licMABs, licMABs^{single} or liCADs for 30 min at 4°C. Next, FITC- or Alexa Fluor 488-conjugated secondary antibody was added and cells were measured by flow cytometry. For data evaluation, the percentage of MOLM-13 cells (PKH26⁺) or RBCs (PKH26⁻) within the antibody-bound cells was determined.

6.5.2. Antibody-dependent cellular cytotoxicity (ADCC)

NK cells were obtained from PBMCs, which were isolated from peripheral blood of healthy donors by Biocoll density gradient (Biochrom). Briefly, peripheral blood was diluted 50% in PBS and the mixture was carefully pipetted onto the Biocoll solution without disturbing the Biocoll layer. A subsequent centrifugation step was performed at

MATERIALS AND METHODS

500 RCF for 30 min at room temperature and without acceleration and deceleration to allow the separation of PBMCs. After centrifugation, the PBMCs were collected and washed twice with RPMI 1640 + GlutaMAX or PBS. NK cells were subsequently isolated using the human NK cell isolation kit (MACS Miltenyi Biotech) according to manufacturer's instructions.

As target cells, MOLM-13 or SEM cells were labeled with 16.6 µg/ml Calcein-AM (Thermo Fisher Scientific) for 30 min at 37°C according to the manufacturer's protocol. Target and effector cells were mixed in a 1 to 2 ratio in RPMI 1640 + GlutaMAX supplemented with 10% FBS. LicMABs, licMABs^{single} or liCADs were added at final concentrations ranging from 0.1 pM to 10 nM and incubated for 4 h at 37°C.

Background and maximum lysis were included as control conditions. To obtain the maximum specific lysis, Calcein-AM-labeled cells were incubated with 2.5% Triton X-100. Background was determined by co-incubating Calcein-AM-labeled cells and NK cells. After 4 h incubation, cells were centrifuged at 600 RCF for 4 min and supernatant was transferred to a black 96 well plate. Fluorescence intensity of Calcein-AM released on the media was measured with an Infinite M100 plate reader (Tecan) and specific lysis was calculated as follows:

$$\text{Specific lysis (\%)} = \frac{\text{Fluorescence}_{\text{Sample}} - \text{Fluorescence}_{\text{Spontaneous lysis}}}{\text{Fluorescence}_{\text{Maximum lysis}} - \text{Fluorescence}_{\text{Background}}} \times 100$$

Averaged specific lysis of duplicates was plotted according to a dose-response curve and fitted with the integrated four parameter non-linear model.

To assess the preferential killing of licMABs, an ADCC assay was performed with a 1 to 1 mixture of MOLM-13 and OCI-AML3 cells, as target cells, and NK cells as effector cells. Two assays, with either MOLM-13 or OCI-AML3 cells being Calcein-AM-labelled, were executed in parallel. Preferential killing was evaluated using protein concentrations of 10 nM or the previously described EC₅₀ value.

6.5.3. Antibody-dependent cellular cytotoxicity of primary AML cells

Ex vivo expanded primary AML cells of 9 different patients were co-cultured in a long-term culture system with freshly isolated NK cells, at an effector to target cell ratio of 5 to 1, and 10 nM of licMABs at 37°C and for 24 h.^{60, 134} Cells were then harvested, stained

MATERIALS AND METHODS

for CD16 (clone B73.1), CD56 (clone HCD 56), CD33 (clone WM53) and in concrete cases CD123 (clone 6H6, all antibodies from BioLegend) and analyzed by flow cytometry with a BD LSR II (Becton Dickinson). LicMAB-mediated cellular cytotoxicity was determined by the percentage of residual CD33- or CD123-expressing cells in treated cultures with respect to controls.

6.5.4. Antibody-dependent cellular phagocytosis (ADCP)

Monocytes were freshly isolated from PBMCs using the human CD14 MicroBeads Kit (MACS Miltenyi Biotech) and following the manufacturer's instructions. Isolated monocytes were stained with PKH67 dye (Sigma-Aldrich) as described in the manufacturer's protocol and differentiated to macrophages in X-VIVO 15 media (Lonza) supplemented with 10% autologous serum and 20 ng/ml Macrophage Colony-Stimulating Factor (M-CSF, R&D Systems). After 72 h, fresh media containing autologous serum and M-CSF was added to the wells and phagocytosis assay was performed on day 5 or 6.

Macrophages were washed twice with X-VIVO medium and kept in 200 μ l of X-VIVO medium per well. MOLM-13 cells were labeled with PKH26 dye and 100 μ l of X-VIVO media containing PKH26-labeled MOLM-13 cells were added to the macrophage wells. Local inhibitory checkpoint molecules in final concentration from 0.01 to 100 nM were subsequently added to the mixture. As positive control, MOLM-13 cells were substituted by polybead® Carboxylate Red-Dyed Microspheres of 6 μ m (Ploysciences). Cells were incubated at 37°C for 2 h, except for the negative control, which was incubated 2 h at 4°C. After incubation, non-adherent cells were harvested and adherent macrophages were washed with ice-cold PBS and detached using StemPro® Accutase® (Thermo Fisher Scientific) at 37°C for 10 min followed by PBS wash. Cells were centrifuged at 500 RCF for 5 min, resuspended in FACS buffer containing 1% Formaldehyde (Invitrogen) and stored at 4°C until analyzed.

Samples were measured by flow cytometry using either an ImageStream®X Mark II (Merck Millipore) or a SH800 (Sony) instrument and analyzed with IDEAS® and INSPIRE® software (Merck Millipore), SH800 version 2.1.1. (Sony) or Flowing software version 2.5.1 (Perttu Terho, Cell Imaging Core of the Turku Centre for Biotechnology). Single PKH67⁺ and PKH26⁺ cells were considered as phagocytic events, the maximum phagocytosis value was set to 100% and all data points were normalized accordingly.

MATERIALS AND METHODS

6.5.5. Antibody-dependent cellular phagocytosis of primary AML cells

ADCP experiments were performed with primary cells from 13 AML patients. Monocytes were isolated from peripheral blood and differentiated to macrophages over 6 days in RPMI 1640 medium supplemented with 50 ng/ml M-CSF, 10% AB human serum, 1% Penicillin-Streptomycin and 1% HEPES. On the day of the assay, primary, patient-derived AML cells were thawed and stained with pHrodo Red SE dye (Thermo Fisher) according to the manufacturer's protocol. Phagocytosis assay was performed as described above and analyzed with a LSRII flow cytometer (BD). The relative phagocytosis rate was calculated based on double-positive cells (PKH67⁺ and pHrodo Red SE⁺) relative to macrophages (PKH67⁺ and pHrodo Red SE⁻). Unstained macrophages and AML cells were characterized by staining with the following antibodies: APC- α CD16 (clone 3G8), APC- α CD32 (clone 6C4), PE- α CD33 (clone WM58), APC- α CD64 (clone 10.1), APC- α CD47 (clone B6H12), PE- α SIRP α (clone SE5A5, all from BioLegend) and the respective isotype controls.

6.6. Plotting and statistical analysis

Unless otherwise stated, data was analyzed and plotted with GraphPad Prism version 6.00 (GraphPad Software). Error bars indicate the standard error of the mean (SEM). Statistical differences on cytotoxicity studies with primary, patient-derived AML samples were assessed by the Wilcoxon test and on phagocytosis assays with one-way ANOVA with Dunnett's multiple comparisons test. Differences in antigen expression were calculated with the Mann-Whitney U test. Statistical significance was considered for p-value < 0.05 (*), < 0.01 (**), < 0.001 (***) and < 0.0001 (****).

REFERENCES

7. REFERENCES

1. Oiseth SJ, Aziz MS. Cancer immunotherapy: a brief review of the history, possibilities, and challenges ahead. *Journal of cancer metastasis and treatment* 2017; 3:250-61.
2. Coley WB. The treatment of malignant tumors by repeated inoculations of erysipelas: with a report of ten original cases. *The American Journal of Medical Science* 1893; 10:487-511.
3. Coley WB. The Treatment of Inoperable Sarcoma by Bacterial Toxins (the Mixed Toxins of the *Streptococcus erysipelas* and the *Bacillus prodigiosus*). *Proc R Soc Med* 1910; 3:1-48.
4. Isaacs A, Lindenmann J. Virus interference. I. The interferon. *Proc R Soc Lond B Biol Sci* 1957; 147:258-67.
5. Graham JB, Graham RM. The effect of vaccine on cancer patients. *Surg Gynecol Obstet* 1959; 109:131-8.
6. Miller JF, Mitchell GF, Weiss NS. Cellular basis of the immunological defects in thymectomized mice. *Nature* 1967; 214:992-7.
7. Steinman RM, Cohn ZA. Identification of a novel cell type in peripheral lymphoid organs of mice. I. Morphology, quantitation, tissue distribution. *J Exp Med* 1973; 137:1142-62.
8. Zinkernagel RM, Doherty PC. Restriction of in vitro T cell-mediated cytotoxicity in lymphocytic choriomeningitis within a syngeneic or semiallogeneic system. *Nature* 1974; 248:701-2.
9. Kiessling R, Klein E, Wigzell H. "Natural" killer cells in the mouse. I. Cytotoxic cells with specificity for mouse Moloney leukemia cells. Specificity and distribution according to genotype. *Eur J Immunol* 1975; 5:112-7.
10. Kiessling R, Klein E, Pross H, Wigzell H. "Natural" killer cells in the mouse. II. Cytotoxic cells with specificity for mouse Moloney leukemia cells. Characteristics of the killer cell. *Eur J Immunol* 1975; 5:117-21.
11. von Behring E, Kitasato S. Ueber das Zustandekommen der Diphtherie-Immunität und der Tetanus-Immunität bei Thieren. *Dtsch Med Wschr* 1890; 16:1113-4.
12. Winau F, Westphal O, Winau R. Paul Ehrlich--in search of the magic bullet. *Microbes Infect* 2004; 6:786-9.

REFERENCES

13. Klinman NR. Antibody with homogeneous antigen binding produced by splenic foci in organ culture. *Immunochemistry* 1969; 6:757-9.
14. Cotton RG, Milstein C. Letter: Fusion of two immunoglobulin-producing myeloma cells. *Nature* 1973; 244:42-3.
15. Kohler G, Milstein C. Continuous cultures of fused cells secreting antibody of predefined specificity. *Nature* 1975; 256:495-7.
16. Kaplan DH, Shankaran V, Dighe AS, Stockert E, Aguet M, Old LJ, et al. Demonstration of an interferon gamma-dependent tumor surveillance system in immunocompetent mice. *Proceedings of the National Academy of Sciences of the United States of America* 1998; 95:7556-61.
17. Shankaran V, Ikeda H, Bruce AT, White JM, Swanson PE, Old LJ, et al. IFN γ and lymphocytes prevent primary tumour development and shape tumour immunogenicity. *Nature* 2001; 410:1107-11.
18. Hanahan D, Weinberg RA. Hallmarks of cancer: the next generation. *Cell* 2011; 144:646-74.
19. Schumacher TN, Schreiber RD. Neoantigens in cancer immunotherapy. *Science* 2015; 348:69-74.
20. Vinay DS, Ryan EP, Pawelec G, Talib WH, Stagg J, Elkord E, et al. Immune evasion in cancer: Mechanistic basis and therapeutic strategies. *Semin Cancer Biol* 2015; 35 Suppl:S185-S98.
21. Strebhardt K, Ullrich A. Paul Ehrlich's magic bullet concept: 100 years of progress. *Nature reviews Cancer* 2008; 8:473-80.
22. Fagraeus A. Plasma cellular reaction and its relation to the formation of antibodies in vitro. *Nature* 1947; 159:499.
23. Porter RR. The hydrolysis of rabbit γ -globulin and antibodies with crystalline papain. *Biochem J* 1959; 73:119-26.
24. Edelman GM, Cunningham BA, Gall WE, Gottlieb PD, Rutishauser U, Waxdal MJ. The covalent structure of an entire gammaG immunoglobulin molecule. *Proceedings of the National Academy of Sciences of the United States of America* 1969; 63:78-85.
25. Fleischman JB, Porter RR, Press EM. The Arrangement of the Peptide Chains in Gamma-Globulin. *Biochem J* 1963; 88:220-8.
26. Silverton EW, Navia MA, Davies DR. Three-dimensional structure of an intact human immunoglobulin. *Proceedings of the National Academy of Sciences of the United States of America* 1977; 74:5140-4.

REFERENCES

27. Davis MM, Calame K, Early PW, Livant DL, Joho R, Weissman IL, et al. An immunoglobulin heavy-chain gene is formed by at least two recombinational events. *Nature* 1980; 283:733-9.
28. Wu TT, Kabat EA. An analysis of the sequences of the variable regions of Bence Jones proteins and myeloma light chains and their implications for antibody complementarity. *J Exp Med* 1970; 132:211-50.
29. Fridman WH. Fc receptors and immunoglobulin binding factors. *FASEB J* 1991; 5:2684-90.
30. Harris LJ, Larson SB, Hasel KW, McPherson A. Refined structure of an intact IgG2a monoclonal antibody. *Biochemistry* 1997; 36:1581-97.
31. Almagro JC, Fransson J. Humanization of antibodies. *Front Biosci* 2008; 13:1619-33.
32. Hale G, Bright S, Chumbley G, Hoang T, Metcalf D, Munro AJ, et al. Removal of T cells from bone marrow for transplantation: a monoclonal antilymphocyte antibody that fixes human complement. *Blood* 1983; 62:873-82.
33. Wilde MI, Goa KL. Muromonab CD3: a reappraisal of its pharmacology and use as prophylaxis of solid organ transplant rejection. *Drugs* 1996; 51:865-94.
34. Weiner LM, Surana R, Wang S. Monoclonal antibodies: versatile platforms for cancer immunotherapy. *Nature reviews Immunology* 2010; 10:317-27.
35. Cartron G, Dacheux L, Salles G, Solal-Celigny P, Bardos P, Colombat P, et al. Therapeutic activity of humanized anti-CD20 monoclonal antibody and polymorphism in IgG Fc receptor FcγRIIIa gene. *Blood* 2002; 99:754-8.
36. Gagez AL, Tuailon E, Cezar R, Dartigeas C, Mahe B, Letestu R, et al. Response to rituximab in B-CLL patients is adversely impacted by frequency of IL-10 competent B cells and FcγRIIIa polymorphism. A study of FCGCLL/WM and GOELAMS groups. *Blood Cancer J* 2016; 6:e389.
37. Diamantis N, Banerji U. Antibody-drug conjugates--an emerging class of cancer treatment. *Br J Cancer* 2016; 114:362-7.
38. Sau S, Alsaab HO, Kashaw SK, Tatiparti K, Iyer AK. Advances in antibody-drug conjugates: A new era of targeted cancer therapy. *Drug Discov Today* 2017; 22:1547-56.
39. Ridgway JB, Presta LG, Carter P. 'Knobs-into-holes' engineering of antibody CH3 domains for heavy chain heterodimerization. *Protein Eng* 1996; 9:617-21.
40. Davis JH, Aperlo C, Li Y, Kurosawa E, Lan Y, Lo KM, et al. SEEDbodies: fusion proteins based on strand-exchange engineered domain (SEED) CH3 heterodimers in an

REFERENCES

Fc analogue platform for asymmetric binders or immunofusions and bispecific antibodies. *Protein Eng Des Sel* 2010; 23:195-202.

41. Gunasekaran K, Pentony M, Shen M, Garrett L, Forte C, Woodward A, et al. Enhancing antibody Fc heterodimer formation through electrostatic steering effects: applications to bispecific molecules and monovalent IgG. *The Journal of biological chemistry* 2010; 285:19637-46.

42. Schaefer W, Regula JT, Bahner M, Schanzer J, Croasdale R, Durr H, et al. Immunoglobulin domain crossover as a generic approach for the production of bispecific IgG antibodies. *Proceedings of the National Academy of Sciences of the United States of America* 2011; 108:11187-92.

43. Le Gall F, Kipriyanov SM, Moldenhauer G, Little M. Di-, tri- and tetrameric single chain Fv antibody fragments against human CD19: effect of valency on cell binding. *FEBS Lett* 1999; 453:164-8.

44. Schubert I, Kellner C, Stein C, Kugler M, Schwenkert M, Saul D, et al. A single-chain triplebody with specificity for CD19 and CD33 mediates effective lysis of mixed lineage leukemia cells by dual targeting. *MAbs* 2011; 3:21-30.

45. Buie LW, Pecoraro JJ, Horvat TZ, Daley RJ. Blinatumomab: A First-in-Class Bispecific T-Cell Engager for Precursor B-Cell Acute Lymphoblastic Leukemia. *The Annals of pharmacotherapy* 2015; 49:1057-67.

46. Gleason MK, Ross JA, Warlick ED, Lund TC, Verneris MR, Wiernik A, et al. CD16xCD33 bispecific killer cell engager (BiKE) activates NK cells against primary MDS and MDSC CD33+ targets. *Blood* 2014; 123:3016-26.

47. Pardoll DM. The blockade of immune checkpoints in cancer immunotherapy. *Nature reviews Cancer* 2012; 12:252-64.

48. Dadi S, Chhangawala S, Whitlock BM, Franklin RA, Luo CT, Oh SA, et al. Cancer Immunosurveillance by Tissue-Resident Innate Lymphoid Cells and Innate-like T Cells. *Cell* 2016; 164:365-77.

49. Tsai HF, Hsu PN. Cancer immunotherapy by targeting immune checkpoints: mechanism of T cell dysfunction in cancer immunity and new therapeutic targets. *J Biomed Sci* 2017; 24:35.

50. June CH, Vandenbergh P, Thompson CB. The CD28 and CTLA-4 receptor family. *Chem Immunol* 1994; 59:62-90.

51. Takahashi T, Tagami T, Yamazaki S, Uede T, Shimizu J, Sakaguchi N, et al. Immunologic self-tolerance maintained by CD25(+)CD4(+) regulatory T cells

REFERENCES

- constitutively expressing cytotoxic T lymphocyte-associated antigen 4. *J Exp Med* 2000; 192:303-10.
52. Lipson EJ, Drake CG. Ipilimumab: an anti-CTLA-4 antibody for metastatic melanoma. *Clinical cancer research : an official journal of the American Association for Cancer Research* 2011; 17:6958-62.
53. Kim JW, Eder JP. Prospects for targeting PD-1 and PD-L1 in various tumor types. *Oncology (Williston Park)* 2014; 28 Suppl 3:15-28.
54. Herbst RS, Soria JC, Kowanetz M, Fine GD, Hamid O, Gordon MS, et al. Predictive correlates of response to the anti-PD-L1 antibody MPDL3280A in cancer patients. *Nature* 2014; 515:563-7.
55. Straub M, Drecoll E, Pfarr N, Weichert W, Langer R, Hapfelmeier A, et al. CD274/PD-L1 gene amplification and PD-L1 protein expression are common events in squamous cell carcinoma of the oral cavity. *Oncotarget* 2016; 7:12024-34.
56. Iwai Y, Hamanishi J, Chamoto K, Honjo T. Cancer immunotherapies targeting the PD-1 signaling pathway. *J Biomed Sci* 2017; 24:26.
57. Rizvi NA, Hellmann MD, Snyder A, Kvistborg P, Makarov V, Havel JJ, et al. Cancer immunology. Mutational landscape determines sensitivity to PD-1 blockade in non-small cell lung cancer. *Science* 2015; 348:124-8.
58. Van Allen EM, Miao D, Schilling B, Shukla SA, Blank C, Zimmer L, et al. Genomic correlates of response to CTLA-4 blockade in metastatic melanoma. *Science* 2015; 350:207-11.
59. Chen PL, Roh W, Reuben A, Cooper ZA, Spencer CN, Prieto PA, et al. Analysis of Immune Signatures in Longitudinal Tumor Samples Yields Insight into Biomarkers of Response and Mechanisms of Resistance to Immune Checkpoint Blockade. *Cancer Discov* 2016; 6:827-37.
60. Krupka C, Kufer P, Kischel R, Zugmaier G, Lichtenegger FS, Kohnke T, et al. Blockade of the PD-1/PD-L1 axis augments lysis of AML cells by the CD33/CD3 BiTE antibody construct AMG 330: reversing a T-cell-induced immune escape mechanism. *Leukemia* 2016; 30:484-91.
61. Wolchok JD, Chiarion-Sileni V, Gonzalez R, Rutkowski P, Grob JJ, Cowey CL, et al. Overall Survival with Combined Nivolumab and Ipilimumab in Advanced Melanoma. *The New England journal of medicine* 2017; 377:1345-56.
62. Oldenborg PA, Zheleznyak A, Fang YF, Lagenaur CF, Gresham HD, Lindberg FP. Role of CD47 as a marker of self on red blood cells. *Science* 2000; 288:2051-4.

REFERENCES

63. Ishikawa-Sekigami T, Kaneko Y, Okazawa H, Tomizawa T, Okajo J, Saito Y, et al. SHPS-1 promotes the survival of circulating erythrocytes through inhibition of phagocytosis by splenic macrophages. *Blood* 2006; 107:341-8.
64. Ishikawa-Sekigami T, Kaneko Y, Saito Y, Murata Y, Okazawa H, Ohnishi H, et al. Enhanced phagocytosis of CD47-deficient red blood cells by splenic macrophages requires SHPS-1. *Biochem Biophys Res Commun* 2006; 343:1197-200.
65. Yamao T, Noguchi T, Takeuchi O, Nishiyama U, Morita H, Hagiwara T, et al. Negative regulation of platelet clearance and of the macrophage phagocytic response by the transmembrane glycoprotein SHPS-1. *The Journal of biological chemistry* 2002; 277:39833-9.
66. Campbell IG, Freemont PS, Foulkes W, Trowsdale J. An ovarian tumor marker with homology to vaccinia virus contains an IgV-like region and multiple transmembrane domains. *Cancer research* 1992; 52:5416-20.
67. Brown EJ, Frazier WA. Integrin-associated protein (CD47) and its ligands. *Trends Cell Biol* 2001; 11:130-5.
68. Van VQ, Raymond M, Baba N, Rubio M, Wakahara K, Susin SA, et al. CD47(high) expression on CD4 effectors identifies functional long-lived memory T cell progenitors. *Journal of immunology* 2012; 188:4249-55.
69. Jaiswal S, Jamieson CH, Pang WW, Park CY, Chao MP, Majeti R, et al. CD47 is upregulated on circulating hematopoietic stem cells and leukemia cells to avoid phagocytosis. *Cell* 2009; 138:271-85.
70. Majeti R, Chao MP, Alizadeh AA, Pang WW, Jaiswal S, Gibbs KD, Jr., et al. CD47 is an adverse prognostic factor and therapeutic antibody target on human acute myeloid leukemia stem cells. *Cell* 2009; 138:286-99.
71. Chao MP, Alizadeh AA, Tang C, Myklebust JH, Varghese B, Gill S, et al. Anti-CD47 antibody synergizes with rituximab to promote phagocytosis and eradicate non-Hodgkin lymphoma. *Cell* 2010; 142:699-713.
72. Chao MP, Tang C, Pachynski RK, Chin R, Majeti R, Weissman IL. Extranodal dissemination of non-Hodgkin lymphoma requires CD47 and is inhibited by anti-CD47 antibody therapy. *Blood* 2011; 118:4890-901.
73. Zhang H, Lu H, Xiang L, Bullen JW, Zhang C, Samanta D, et al. HIF-1 regulates CD47 expression in breast cancer cells to promote evasion of phagocytosis and maintenance of cancer stem cells. *Proceedings of the National Academy of Sciences of the United States of America* 2015; 112:E6215-23.

REFERENCES

74. Steinert G, Scholch S, Niemietz T, Iwata N, Garcia SA, Behrens B, et al. Immune escape and survival mechanisms in circulating tumor cells of colorectal cancer. *Cancer research* 2014; 74:1694-704.
75. van Beek EM, Cochrane F, Barclay AN, van den Berg TK. Signal regulatory proteins in the immune system. *Journal of immunology* 2005; 175:7781-7.
76. Barclay AN, Van den Berg TK. The interaction between signal regulatory protein alpha (SIRPalpha) and CD47: structure, function, and therapeutic target. *Annual review of immunology* 2014; 32:25-50.
77. van den Berg TK, Yoder JA, Litman GW. On the origins of adaptive immunity: innate immune receptors join the tale. *Trends Immunol* 2004; 25:11-6.
78. Hatherley D, Graham SC, Turner J, Harlos K, Stuart DI, Barclay AN. Paired receptor specificity explained by structures of signal regulatory proteins alone and complexed with CD47. *Molecular cell* 2008; 31:266-77.
79. Brooke G, Holbrook JD, Brown MH, Barclay AN. Human lymphocytes interact directly with CD47 through a novel member of the signal regulatory protein (SIRP) family. *Journal of immunology* 2004; 173:2562-70.
80. Stefanidakis M, Newton G, Lee WY, Parkos CA, Luscinskas FW. Endothelial CD47 interaction with SIRPgamma is required for human T-cell transendothelial migration under shear flow conditions in vitro. *Blood* 2008; 112:1280-9.
81. Takada T, Matozaki T, Takeda H, Fukunaga K, Noguchi T, Fujioka Y, et al. Roles of the complex formation of SHPS-1 with SHP-2 in insulin-stimulated mitogen-activated protein kinase activation. *The Journal of biological chemistry* 1998; 273:9234-42.
82. van Beek EM, Zarate JA, van Bruggen R, Schornagel K, Tool AT, Matozaki T, et al. SIRPalpha controls the activity of the phagocyte NADPH oxidase by restricting the expression of gp91(phox). *Cell Rep* 2012; 2:748-55.
83. Timms JF, Swanson KD, Marie-Cardine A, Raab M, Rudd CE, Schraven B, et al. SHPS-1 is a scaffold for assembling distinct adhesion-regulated multi-protein complexes in macrophages. *Curr Biol* 1999; 9:927-30.
84. Soto-Pantoja DR, Kaur S, Roberts DD. CD47 signaling pathways controlling cellular differentiation and responses to stress. *Crit Rev Biochem Mol Biol* 2015; 50:212-30.
85. Jeanne A, Schneider C, Martiny L, Dedieu S. Original insights on thrombospondin-1-related antireceptor strategies in cancer. *Front Pharmacol* 2015; 6:252.

REFERENCES

86. Csanyi G, Yao M, Rodriguez AI, Al Ghouleh I, Sharifi-Sanjani M, Frazziano G, et al. Thrombospondin-1 regulates blood flow via CD47 receptor-mediated activation of NADPH oxidase 1. *Arterioscler Thromb Vasc Biol* 2012; 32:2966-73.
87. Willingham SB, Volkmer JP, Gentles AJ, Sahoo D, Dalerba P, Mitra SS, et al. The CD47-signal regulatory protein alpha (SIRPa) interaction is a therapeutic target for human solid tumors. *Proceedings of the National Academy of Sciences of the United States of America* 2012; 109:6662-7.
88. Cioffi M, Trabulo S, Hidalgo M, Costello E, Greenhalf W, Erkan M, et al. Inhibition of CD47 Effectively Targets Pancreatic Cancer Stem Cells via Dual Mechanisms. *Clinical cancer research : an official journal of the American Association for Cancer Research* 2015; 21:2325-37.
89. Hussain R, Dawood G, Abrar N, Toossi Z, Minai A, Dojki M, et al. Selective increases in antibody isotypes and immunoglobulin G subclass responses to secreted antigens in tuberculosis patients and healthy household contacts of the patients. *Clin Diagn Lab Immunol* 1995; 2:726-32.
90. Zhao XW, Kuijpers TW, van den Berg TK. Is targeting of CD47-SIRPalpha enough for treating hematopoietic malignancy? *Blood* 2012; 119:4333-4; author reply 4-5.
91. Weiskopf K, Ring AM, Ho CC, Volkmer JP, Levin AM, Volkmer AK, et al. Engineered SIRPalpha variants as immunotherapeutic adjuvants to anticancer antibodies. *Science* 2013; 341:88-91.
92. Liu J, Wang L, Zhao F, Tseng S, Narayanan C, Shura L, et al. Pre-Clinical Development of a Humanized Anti-CD47 Antibody with Anti-Cancer Therapeutic Potential. *PloS one* 2015; 10:e0137345.
93. Piccione EC, Juarez S, Liu J, Tseng S, Ryan CE, Narayanan C, et al. A bispecific antibody targeting CD47 and CD20 selectively binds and eliminates dual antigen expressing lymphoma cells. *MAbs* 2015; 7:946-56.
94. Dheilley E, Moine V, Broyer L, Salgado-Pires S, Johnson Z, Papaioannou A, et al. Selective Blockade of the Ubiquitous Checkpoint Receptor CD47 Is Enabled by Dual-Targeting Bispecific Antibodies. *Mol Ther* 2017; 25:523-33.
95. Kim D, Wang J, Willingham SB, Martin R, Wernig G, Weissman IL. Anti-CD47 antibodies promote phagocytosis and inhibit the growth of human myeloma cells. *Leukemia* 2012; 26:2538-45.

REFERENCES

96. Yoshida K, Tsujimoto H, Matsumura K, Kinoshita M, Takahata R, Matsumoto Y, et al. CD47 is an adverse prognostic factor and a therapeutic target in gastric cancer. *Cancer Med* 2015; 4:1322-33.
97. Xiao Z, Chung H, Banan B, Manning PT, Ott KC, Lin S, et al. Antibody mediated therapy targeting CD47 inhibits tumor progression of hepatocellular carcinoma. *Cancer Lett* 2015; 360:302-9.
98. Edris B, Weiskopf K, Volkmer AK, Volkmer JP, Willingham SB, Contreras-Trujillo H, et al. Antibody therapy targeting the CD47 protein is effective in a model of aggressive metastatic leiomyosarcoma. *Proceedings of the National Academy of Sciences of the United States of America* 2012; 109:6656-61.
99. Kwong LS, Brown MH, Barclay AN, Hatherley D. Signal-regulatory protein alpha from the NOD mouse binds human CD47 with an exceptionally high affinity--implications for engraftment of human cells. *Immunology* 2014; 143:61-7.
100. Iwamoto C, Takenaka K, Urata S, Yamauchi T, Shima T, Kuriyama T, et al. The BALB/c-specific polymorphic SIRPA enhances its affinity for human CD47, inhibiting phagocytosis against human cells to promote xenogeneic engraftment. *Exp Hematol* 2014; 42:163-71 e1.
101. Strowig T, Rongvaux A, Rathinam C, Takizawa H, Borsotti C, Philbrick W, et al. Transgenic expression of human signal regulatory protein alpha in Rag2^{-/-}-gamma(c)^{-/-} mice improves engraftment of human hematopoietic cells in humanized mice. *Proceedings of the National Academy of Sciences of the United States of America* 2011; 108:13218-23.
102. Rongvaux A, Willinger T, Martinek J, Strowig T, Gearty SV, Teichmann LL, et al. Development and function of human innate immune cells in a humanized mouse model. *Nat Biotechnol* 2014; 32:364-72.
103. Tseng D, Volkmer JP, Willingham SB, Contreras-Trujillo H, Fathman JW, Fernhoff NB, et al. Anti-CD47 antibody-mediated phagocytosis of cancer by macrophages primes an effective antitumor T-cell response. *Proceedings of the National Academy of Sciences of the United States of America* 2013; 110:11103-8.
104. Liu X, Pu Y, Cron K, Deng L, Kline J, Frazier WA, et al. CD47 blockade triggers T cell-mediated destruction of immunogenic tumors. *Nature medicine* 2015; 21:1209-15.
105. Liu Q, Wen W, Tang L, Qin CJ, Lin Y, Zhang HL, et al. Inhibition of SIRPalpha in dendritic cells potentiates potent antitumor immunity. *Oncoimmunology* 2016; 5:e1183850.

REFERENCES

106. Xu MM, Pu Y, Han D, Shi Y, Cao X, Liang H, et al. Dendritic Cells but Not Macrophages Sense Tumor Mitochondrial DNA for Cross-priming through Signal Regulatory Protein alpha Signaling. *Immunity* 2017; 47:363-73 e5.
107. Ho CC, Guo N, Sockolosky JT, Ring AM, Weiskopf K, Ozkan E, et al. "Velcro" engineering of high affinity CD47 ectodomain as signal regulatory protein alpha (SIRPalpha) antagonists that enhance antibody-dependent cellular phagocytosis. *The Journal of biological chemistry* 2015; 290:12650-63.
108. Yanagita T, Murata Y, Tanaka D, Motegi SI, Arai E, Daniwijaya EW, et al. Anti-SIRPalpha antibodies as a potential new tool for cancer immunotherapy. *JCI Insight* 2017; 2:e89140.
109. Ring NG, Herndler-Brandstetter D, Weiskopf K, Shan L, Volkmer JP, George BM, et al. Anti-SIRPalpha antibody immunotherapy enhances neutrophil and macrophage antitumor activity. *Proceedings of the National Academy of Sciences of the United States of America* 2017; 114:E10578-E85.
110. Martinez-Torres AC, Quiney C, Attout T, Boullet H, Herbi L, Vela L, et al. CD47 agonist peptides induce programmed cell death in refractory chronic lymphocytic leukemia B cells via PLCgamma1 activation: evidence from mice and humans. *PLoS Med* 2015; 12:e1001796.
111. Mateo V, Lagneaux L, Bron D, Biron G, Armant M, Delespesse G, et al. CD47 ligation induces caspase-independent cell death in chronic lymphocytic leukemia. *Nature medicine* 1999; 5:1277-84.
112. Kaur S, Elkahloun AG, Singh SP, Chen QR, Meerzaman DM, Song T, et al. A function-blocking CD47 antibody suppresses stem cell and EGF signaling in triple-negative breast cancer. *Oncotarget* 2016; 7:10133-52.
113. Irandoust M, Alvarez Zarate J, Hubeek I, van Beek EM, Schornagel K, Broekhuizen AJ, et al. Engagement of SIRPalpha inhibits growth and induces programmed cell death in acute myeloid leukemia cells. *PloS one* 2013; 8:e52143.
114. Lin GHY, Chai V, Lee V, Dodge K, Truong T, Wong M, et al. TTI-621 (SIRPalphaFc), a CD47-blocking cancer immunotherapeutic, triggers phagocytosis of lymphoma cells by multiple polarized macrophage subsets. *PloS one* 2017; 12:e0187262.
115. Ding L, Ley TJ, Larson DE, Miller CA, Koboldt DC, Welch JS, et al. Clonal evolution in relapsed acute myeloid leukaemia revealed by whole-genome sequencing. *Nature* 2012; 481:506-10.

REFERENCES

116. Dohner H, Weisdorf DJ, Bloomfield CD. Acute Myeloid Leukemia. *The New England journal of medicine* 2015; 373:1136-52.
117. Podoltsev NA, Stahl M, Zeidan AM, Gore SD. Selecting initial treatment of acute myeloid leukaemia in older adults. *Blood Rev* 2017; 31:43-62.
118. Alibhai SM, Leach M, Minden MD, Brandwein J. Outcomes and quality of care in acute myeloid leukemia over 40 years. *Cancer* 2009; 115:2903-11.
119. Lindsley RC, Mar BG, Mazzola E, Grauman PV, Shareef S, Allen SL, et al. Acute myeloid leukemia ontogeny is defined by distinct somatic mutations. *Blood* 2015; 125:1367-76.
120. Steensma DP, Bejar R, Jaiswal S, Lindsley RC, Sekeres MA, Hasserjian RP, et al. Clonal hematopoiesis of indeterminate potential and its distinction from myelodysplastic syndromes. *Blood* 2015; 126:9-16.
121. Cancer Genome Atlas Research Network, Ley TJ, Miller C, Ding L, Raphael BJ, Mungall AJ, et al. Genomic and epigenomic landscapes of adult de novo acute myeloid leukemia. *The New England journal of medicine* 2013; 368:2059-74.
122. Marcucci G, Metzeler KH, Schwind S, Becker H, Maharry K, Mrozek K, et al. Age-related prognostic impact of different types of DNMT3A mutations in adults with primary cytogenetically normal acute myeloid leukemia. *Journal of clinical oncology : official journal of the American Society of Clinical Oncology* 2012; 30:742-50.
123. Vardiman JW, Thiele J, Arber DA, Brunning RD, Borowitz MJ, Porwit A, et al. The 2008 revision of the World Health Organization (WHO) classification of myeloid neoplasms and acute leukemia: rationale and important changes. *Blood* 2009; 114:937-51.
124. Cheson BD, Bennett JM, Kopecky KJ, Buchner T, Willman CL, Estey EH, et al. Revised recommendations of the International Working Group for Diagnosis, Standardization of Response Criteria, Treatment Outcomes, and Reporting Standards for Therapeutic Trials in Acute Myeloid Leukemia. *Journal of clinical oncology : official journal of the American Society of Clinical Oncology* 2003; 21:4642-9.
125. Lowenberg B, Ossenkoppele GJ, van Putten W, Schouten HC, Graux C, Ferrant A, et al. High-dose daunorubicin in older patients with acute myeloid leukemia. *The New England journal of medicine* 2009; 361:1235-48.
126. Fernandez HF, Sun Z, Yao X, Litzow MR, Luger SM, Paietta EM, et al. Anthracycline dose intensification in acute myeloid leukemia. *The New England journal of medicine* 2009; 361:1249-59.

REFERENCES

127. Appelbaum FR. The current status of hematopoietic cell transplantation. *Annu Rev Med* 2003; 54:491-512.
128. Breems DA, Van Putten WL, Huijgens PC, Ossenkoppele GJ, Verhoef GE, Verdonck LF, et al. Prognostic index for adult patients with acute myeloid leukemia in first relapse. *Journal of clinical oncology : official journal of the American Society of Clinical Oncology* 2005; 23:1969-78.
129. Thomas DA, O'Brien S, Kantarjian HM. Monoclonal antibody therapy with rituximab for acute lymphoblastic leukemia. *Hematol Oncol Clin North Am* 2009; 23:949-71, v.
130. Topp MS, Stelljes M, Zugmaier G, Barnette P, Heffner LT, Jr., Trippett T, et al. Blinatumomab retreatment after relapse in patients with relapsed/refractory B-precursor acute lymphoblastic leukemia. *Leukemia* 2017.
131. Lichtenegger FS, Krupka C, Haubner S, Kohnke T, Subklewe M. Recent developments in immunotherapy of acute myeloid leukemia. *J Hematol Oncol* 2017; 10:142.
132. Buckley SA, Walter RB. Antigen-specific immunotherapies for acute myeloid leukemia. *Hematology Am Soc Hematol Educ Program* 2015; 2015:584-95.
133. Laszlo GS, Estey EH, Walter RB. The past and future of CD33 as therapeutic target in acute myeloid leukemia. *Blood Rev* 2014; 28:143-53.
134. Krupka C, Kufer P, Kischel R, Zugmaier G, Bogeholz J, Kohnke T, et al. CD33 target validation and sustained depletion of AML blasts in long-term cultures by the bispecific T-cell-engaging antibody AMG 330. *Blood* 2014; 123:356-65.
135. Crocker PR, Varki A. Siglecs, sialic acids and innate immunity. *Trends Immunol* 2001; 22:337-42.
136. Freeman SD, Kelm S, Barber EK, Crocker PR. Characterization of CD33 as a new member of the sialoadhesin family of cellular interaction molecules. *Blood* 1995; 85:2005-12.
137. Paul SP, Taylor LS, Stansbury EK, McVicar DW. Myeloid specific human CD33 is an inhibitory receptor with differential ITIM function in recruiting the phosphatases SHP-1 and SHP-2. *Blood* 2000; 96:483-90.
138. Orr SJ, Morgan NM, Elliott J, Burrows JF, Scott CJ, McVicar DW, et al. CD33 responses are blocked by SOCS3 through accelerated proteasomal-mediated turnover. *Blood* 2007; 109:1061-8.

REFERENCES

139. Cao H, Crocker PR. Evolution of CD33-related siglecs: regulating host immune functions and escaping pathogen exploitation? *Immunology* 2011; 132:18-26.
140. Crocker PR, McMillan SJ, Richards HE. CD33-related siglecs as potential modulators of inflammatory responses. *Ann N Y Acad Sci* 2012; 1253:102-11.
141. Bross PF, Beitz J, Chen G, Chen XH, Duffy E, Kieffer L, et al. Approval summary: gemtuzumab ozogamicin in relapsed acute myeloid leukemia. *Clinical cancer research : an official journal of the American Association for Cancer Research* 2001; 7:1490-6.
142. Petersdorf SH, Kopecky KJ, Slovak M, Willman C, Nevill T, Brandwein J, et al. A phase 3 study of gemtuzumab ozogamicin during induction and postconsolidation therapy in younger patients with acute myeloid leukemia. *Blood* 2013; 121:4854-60.
143. Perl AE. The role of targeted therapy in the management of patients with AML. *Blood Adv* 2017; 1:2281-94.
144. Kung Sutherland MS, Walter RB, Jeffrey SC, Burke PJ, Yu C, Kostner H, et al. SGN-CD33A: a novel CD33-targeting antibody-drug conjugate using a pyrrolobenzodiazepine dimer is active in models of drug-resistant AML. *Blood* 2013; 122:1455-63.
145. Sutherland MK, Yu C, Lewis TS, Miyamoto JB, Morris-Tilden CA, Jonas M, et al. Anti-leukemic activity of lintuzumab (SGN-33) in preclinical models of acute myeloid leukemia. *MAbs* 2009; 1:481-90.
146. Feldman EJ, Brandwein J, Stone R, Kalaycio M, Moore J, O'Connor J, et al. Phase III randomized multicenter study of a humanized anti-CD33 monoclonal antibody, lintuzumab, in combination with chemotherapy, versus chemotherapy alone in patients with refractory or first-relapsed acute myeloid leukemia. *Journal of clinical oncology : official journal of the American Society of Clinical Oncology* 2005; 23:4110-6.
147. Vasu S, He S, Cheney C, Gopalakrishnan B, Mani R, Lozanski G, et al. Decitabine enhances Fc engineered anti-CD33 mAb mediated natural killer antibody dependent cellular cytotoxicity against AML blasts. *Blood* 2016.
148. Eksioglu EA, Chen X, Heider KH, Rueter B, McGraw KL, Basiorka AA, et al. Novel therapeutic approach to improve hematopoiesis in low risk MDS by targeting MDSCs with the Fc-engineered CD33 antibody BI 836858. *Leukemia* 2017; 31:2172-80.
149. Friedrich M, Henn A, Raum T, Bajtus M, Matthes K, Hendrich L, et al. Preclinical characterization of AMG 330, a CD3/CD33-bispecific T-cell-engaging

REFERENCES

antibody with potential for treatment of acute myelogenous leukemia. *Mol Cancer Ther* 2014; 13:1549-57.

150. Wiernik A, Foley B, Zhang B, Verneris MR, Warlick E, Gleason MK, et al. Targeting natural killer cells to acute myeloid leukemia in vitro with a CD16 x 33 bispecific killer cell engager and ADAM17 inhibition. *Clinical cancer research : an official journal of the American Association for Cancer Research* 2013; 19:3844-55.

151. Dutour A, Marin V, Pizzitola I, Valsesia-Wittmann S, Lee D, Yvon E, et al. In Vitro and In Vivo Antitumor Effect of Anti-CD33 Chimeric Receptor-Expressing EBV-CTL against CD33 Acute Myeloid Leukemia. *Adv Hematol* 2012; 2012:683065.

152. Ponce LP, Fenn NC, Moritz N, Krupka C, Kozik JH, Lauber K, et al. SIRPalpha-antibody fusion proteins stimulate phagocytosis and promote elimination of acute myeloid leukemia cells. *Oncotarget* 2017.

153. Galli S, Zlobec I, Schurch C, Perren A, Ochsenbein AF, Banz Y. CD47 protein expression in acute myeloid leukemia: A tissue microarray-based analysis. *Leukemia research* 2015; 39:749-56.

154. Vermeer AW, Norde W. The thermal stability of immunoglobulin: unfolding and aggregation of a multi-domain protein. *Biophys J* 2000; 78:394-404.

155. Roskopf CC, Braciak TA, Fenn NC, Kobold S, Fey GH, Hopfner KP, et al. Dual-targeting triplebody 33-3-19 mediates selective lysis of biphenotypic CD19+ CD33+ leukemia cells. *Oncotarget* 2016; 7:22579-89.

156. Azouzi S, Collec E, Mohandas N, An X, Colin Y, Le Van Kim C. The human Kell blood group binds the erythroid 4.1R protein: new insights into the 4.1R-dependent red cell membrane complex. *British journal of haematology* 2015; 171:862-71.

157. Walter RB, Raden BW, Kamikura DM, Cooper JA, Bernstein ID. Influence of CD33 expression levels and ITIM-dependent internalization on gemtuzumab ozogamicin-induced cytotoxicity. *Blood* 2005; 105:1295-302.

158. Walter RB, Raden BW, Zeng R, Hausermann P, Bernstein ID, Cooper JA. ITIM-dependent endocytosis of CD33-related Siglecs: role of intracellular domain, tyrosine phosphorylation, and the tyrosine phosphatases, Shp1 and Shp2. *J Leukoc Biol* 2008; 83:200-11.

159. Laszlo GS, Gudgeon CJ, Harrington KH, Dell'Aringa J, Newhall KJ, Means GD, et al. Cellular determinants for preclinical activity of a novel CD33/CD3 bispecific T-cell engager (BiTE) antibody, AMG 330, against human AML. *Blood* 2014; 123:554-61.

REFERENCES

160. Maenaka K, van der Merwe PA, Stuart DI, Jones EY, Sondermann P. The human low affinity Fcγ receptors IIa, IIb, and III bind IgG with fast kinetics and distinct thermodynamic properties. *The Journal of biological chemistry* 2001; 276:44898-904.
161. Fleit HB, Wright SD, Unkeless JC. Human neutrophil Fc γ receptor distribution and structure. *Proceedings of the National Academy of Sciences of the United States of America* 1982; 79:3275-9.
162. Mandelboim O, Malik P, Davis DM, Jo CH, Boyson JE, Strominger JL. Human CD16 as a lysis receptor mediating direct natural killer cell cytotoxicity. *Proceedings of the National Academy of Sciences of the United States of America* 1999; 96:5640-4.
163. Wang W, Erbe AK, Hank JA, Morris ZS, Sondel PM. NK Cell-Mediated Antibody-Dependent Cellular Cytotoxicity in Cancer Immunotherapy. *Front Immunol* 2015; 6:368.
164. Bakema JE, van Egmond M. Fc receptor-dependent mechanisms of monoclonal antibody therapy of cancer. *Curr Top Microbiol Immunol* 2014; 382:373-92.
165. Kugler M, Stein C, Kellner C, Mentz K, Saul D, Schwenkert M, et al. A recombinant trisppecific single-chain Fv derivative directed against CD123 and CD33 mediates effective elimination of acute myeloid leukaemia cells by dual targeting. *British journal of haematology* 2010; 150:574-86.
166. Singer H, Kellner C, Lanig H, Aigner M, Stockmeyer B, Oduncu F, et al. Effective elimination of acute myeloid leukemic cells by recombinant bispecific antibody derivatives directed against CD33 and CD16. *J Immunother* 2010; 33:599-608.
167. Alvey CM, Spinler KR, Irianto J, Pfeifer CR, Hayes B, Xia Y, et al. SIRPA-Inhibited, Marrow-Derived Macrophages Engorge, Accumulate, and Differentiate in Antibody-Targeted Regression of Solid Tumors. *Curr Biol* 2017; 27:2065-77 e6.
168. Chao MP, Alizadeh AA, Tang C, Jan M, Weissman-Tsukamoto R, Zhao F, et al. Therapeutic antibody targeting of CD47 eliminates human acute lymphoblastic leukemia. *Cancer research* 2011; 71:1374-84.
169. Piccione EC, Juarez S, Tseng S, Liu J, Stafford M, Narayanan C, et al. SIRPα-Antibody Fusion Proteins Selectively Bind and Eliminate Dual Antigen-Expressing Tumor Cells. *Clinical cancer research : an official journal of the American Association for Cancer Research* 2016.
170. Lanier LL, Ruitenberg JJ, Phillips JH. Functional and biochemical analysis of CD16 antigen on natural killer cells and granulocytes. *Journal of immunology* 1988; 141:3478-85.

REFERENCES

171. Yeap WH, Wong KL, Shimasaki N, Teo EC, Quek JK, Yong HX, et al. CD16 is indispensable for antibody-dependent cellular cytotoxicity by human monocytes. *Sci Rep* 2016; 6:34310.
172. Passlick B, Flieger D, Ziegler-Heitbrock HW. Identification and characterization of a novel monocyte subpopulation in human peripheral blood. *Blood* 1989; 74:2527-34.
173. Petricevic B, Laengle J, Singer J, Sachet M, Fazekas J, Steger G, et al. Trastuzumab mediates antibody-dependent cell-mediated cytotoxicity and phagocytosis to the same extent in both adjuvant and metastatic HER2/neu breast cancer patients. *J Transl Med* 2013; 11:307.
174. Sironi M, Martinez FO, D'Ambrosio D, Gattorno M, Polentarutti N, Locati M, et al. Differential regulation of chemokine production by Fcγ receptor engagement in human monocytes: association of CCL1 with a distinct form of M2 monocyte activation (M2b, Type 2). *J Leukoc Biol* 2006; 80:342-9.
175. Martinez FO, Gordon S. The M1 and M2 paradigm of macrophage activation: time for reassessment. *F1000Prime Rep* 2014; 6:13.
176. Metes D, Ernst LK, Chambers WH, Sulica A, Herberman RB, Morel PA. Expression of functional CD32 molecules on human NK cells is determined by an allelic polymorphism of the FcγRIIC gene. *Blood* 1998; 91:2369-80.
177. Morel PA, Ernst LK, Metes D. Functional CD32 molecules on human NK cells. *Leukemia & lymphoma* 1999; 35:47-56.
178. Veri MC, Gorlatov S, Li H, Burke S, Johnson S, Stavenhagen J, et al. Monoclonal antibodies capable of discriminating the human inhibitory Fcγ-receptor IIB (CD32B) from the activating Fcγ-receptor IIA (CD32A): biochemical, biological and functional characterization. *Immunology* 2007; 121:392-404.
179. Lazar GA, Dang W, Karki S, Vafa O, Peng JS, Hyun L, et al. Engineered antibody Fc variants with enhanced effector function. *Proceedings of the National Academy of Sciences of the United States of America* 2006; 103:4005-10.
180. Ball ED, McDermott J, Griffin JD, Davey FR, Davis R, Bloomfield CD. Expression of the three myeloid cell-associated immunoglobulin G Fc receptors defined by murine monoclonal antibodies on normal bone marrow and acute leukemia cells. *Blood* 1989; 73:1951-6.
181. Sockolosky JT, Dougan M, Ingram JR, Ho CC, Kauke MJ, Almo SC, et al. Durable antitumor responses to CD47 blockade require adaptive immune stimulation.

REFERENCES

- Proceedings of the National Academy of Sciences of the United States of America 2016; 113:E2646-54.
182. Veillette A, Chen J. SIRPalpha-CD47 Immune Checkpoint Blockade in Anticancer Therapy. *Trends Immunol* 2018.
183. Chao MP, Jaiswal S, Weissman-Tsukamoto R, Alizadeh AA, Gentles AJ, Volkmer J, et al. Calreticulin is the dominant pro-phagocytic signal on multiple human cancers and is counterbalanced by CD47. *Sci Transl Med* 2010; 2:63ra94.
184. Gardai SJ, McPhillips KA, Frasch SC, Janssen WJ, Starefeldt A, Murphy-Ullrich JE, et al. Cell-surface calreticulin initiates clearance of viable or apoptotic cells through trans-activation of LRP on the phagocyte. *Cell* 2005; 123:321-34.
185. Ghiran I, Klickstein LB, Nicholson-Weller A. Calreticulin is at the surface of circulating neutrophils and uses CD59 as an adaptor molecule. *The Journal of biological chemistry* 2003; 278:21024-31.
186. Chen J, Zhong MC, Guo H, Davidson D, Mishel S, Lu Y, et al. SLAMF7 is critical for phagocytosis of haematopoietic tumour cells via Mac-1 integrin. *Nature* 2017; 544:493-7.
187. Kumaresan PR, Lai WC, Chuang SS, Bennett M, Mathew PA. CS1, a novel member of the CD2 family, is homophilic and regulates NK cell function. *Mol Immunol* 2002; 39:1-8.
188. ffrench-Constant C, Colognato H. Integrins: versatile integrators of extracellular signals. *Trends Cell Biol* 2004; 14:678-86.
189. Arnaout MA, Mahalingam B, Xiong JP. Integrin structure, allostery, and bidirectional signaling. *Annu Rev Cell Dev Biol* 2005; 21:381-410.
190. Barkal AA, Weiskopf K, Kao KS, Gordon SR, Rosental B, Yiu YY, et al. Engagement of MHC class I by the inhibitory receptor LILRB1 suppresses macrophages and is a target of cancer immunotherapy. *Nat Immunol* 2018; 19:76-84.
191. Klein J, Sato A. The HLA system. First of two parts. *The New England journal of medicine* 2000; 343:702-9.
192. Klein J, Sato A. The HLA system. Second of two parts. *The New England journal of medicine* 2000; 343:782-6.
193. Fanger NA, Cosman D, Peterson L, Braddy SC, Maliszewski CR, Borges L. The MHC class I binding proteins LIR-1 and LIR-2 inhibit Fc receptor-mediated signaling in monocytes. *Eur J Immunol* 1998; 28:3423-34.

REFERENCES

194. Hamann PR, Hinman LM, Hollander I, Beyer CF, Lindh D, Holcomb R, et al. Gemtuzumab ozogamicin, a potent and selective anti-CD33 antibody-calicheamicin conjugate for treatment of acute myeloid leukemia. *Bioconjug Chem* 2002; 13:47-58.
195. Vervoordeldonk SF, Merle PA, van Leeuwen EF, van der Schoot CE, von dem Borne AE, Slaper-Cortenbach IC. Fc gamma receptor II (CD32) on malignant B cells influences modulation induced by anti-CD19 monoclonal antibody. *Blood* 1994; 83:1632-9.
196. van Oosterhout YV, van den Herik-Oudijk IE, Wessels HM, de Witte T, van de Winkel JG, Preijers FW. Effect of isotype on internalization and cytotoxicity of CD19-ricin A immunotoxins. *Cancer research* 1994; 54:3527-32.
197. Hanahan D. Studies on transformation of *Escherichia coli* with plasmids. *J Mol Biol* 1983; 166:557-80.
198. Sambrook J, Russell DW. *Molecular cloning : a laboratory manual*. Cold Spring Harbor, N.Y.: Cold Spring Harbor Laboratory Press, 2001.
199. Olejniczak SH, Stewart CC, Donohue K, Czuczman MS. A quantitative exploration of surface antigen expression in common B-cell malignancies using flow cytometry. *Immunol Invest* 2006; 35:93-114.
200. Benedict CA, MacKrell AJ, Anderson WF. Determination of the binding affinity of an anti-CD34 single-chain antibody using a novel, flow cytometry based assay. *J Immunol Methods* 1997; 201:223-31.
201. Hanson MS, Stephenson AH, Bowles EA, Sridharan M, Adderley S, Sprague RS. Phosphodiesterase 3 is present in rabbit and human erythrocytes and its inhibition potentiates iloprost-induced increases in cAMP. *American journal of physiology Heart and circulatory physiology* 2008; 295:H786-93.

ABBREVIATIONS

8. LIST OF ABBREVIATIONS

Acronym	Definition
ADC	Antibody-drug conjugate
ALL	Acute lymphoblastic leukemia
Allo-SCT	Allogenic hematopoietic stem cell transplantation
AML	Acute myeloid leukemia
ATCC	American Type Culture Collection
BiKE	Bispecific Natural Killer cell engager
BiTE	Bispecific T cell engager
BM	Bone marrow
bsAb	Bispecific antibody
CAR T cell	Chimeric antigen receptor T cells
CD	Cluster of differentiation
CDR	Complementary-determining region
cGAS	Cyclic GMP-AMP synthase
C _H	Constant domains of heavy chain
C _{H1}	Constant 1 domain of heavy chain
C _{H2}	Constant 2 domain of heavy chain
C _{H3}	Constant 3 domain of heavy chain
C _{H4}	Constant 4 domain of heavy chain
C _L	Constant domain of light chain
CR	Complete remission
CTLA-4	Cytotoxic T-lymphocyte-associated antigen 4
DNA	Deoxyribonucleic acid
DSMZ	Deutsche Sammlung von Mikroorganismen und Zellkulturen
ELN	European Leukemia Net
EMA	European Medicines Agency
F	Female
FAB	French-American-British
Fab	Antigen-binding fragment
FBS	Fetal bovine serum
Fc	Fragment crystallizable
Fc α R	Neonatal Fc receptor
FcR	Fc receptor
Fc α R	Fc-alpha receptor
Fc γ R	Fc-gamma receptor
Fc ϵ R	Fc-epsilon receptor
FDA	US Food and Drug Administration
FR	Frameworks
HC	Heavy chain

ABBREVIATIONS

HD	Healthy donor
HSC	Hematopoietic stem cell
IAP	Integrin-associated protein
ID	Initial Diagnosis
Ig	Immunoglobulin
Ig-fold	Immunoglobulin-fold
<i>IgK</i>	IgKappa leader sequence
IgSF	Immunoglobulin superfamily
ITAM	Immunoreceptor tyrosine-based activation motif
ITIM	Immunoreceptor tyrosine-based inhibitory motif
LB	Lysogeny Broth
LC	Light Chain
liCAD	Local inhibitory checkpoint antibody derivative
licMAB	Local inhibitory checkpoint monoclonal antibody
licMAB ^{single}	Single-arm local inhibitory checkpoint monoclonal antibody
LILRB1	Leukocyte immunoglobulin-like receptor subfamily B member 1
LRP	Low density lipoprotein-receptor related protein
LSC	Leukemic stem cells
M	Male
mAb	Monoclonal antibody
mAb ^{single}	Single-arm monoclonal antibody
M-CSF	Macrophage Colony-Stimulating Factor
MFI	Median fluorescence intensity
MHC	Major histocompatibility complex
MRD	Minimal residual disease
mtDNA	Mitochondrial DNA
Mut	Mutation
n.a.	Not available
NK	Natural Killer
Ni-NTA	Nickel-nitrilotriacetic acid
NSG	NOD/SCID/GAMMA mice
PB	Peripheral blood
PBMC	Peripheral blood mononuclear cell
PCR	Polymerase chain reaction
PD-1	Programmed cell death 1
PD-L1	Programmed cell death ligand 1
PT	Patient
RBC	Red blood cell
scFv	Single chain fragment variable
sctb	Single chain triplebody
SDS-PAGE	Sodium dodecyl sulfate polyacrylamide gel electrophoresis

ABBREVIATIONS

SEC	Size exclusion chromatography
SEM	Standard error of the mean
Siglecs	Sialic acid immunoglobulin like lectins
SIRP α	Signal regulatory protein alpha
SLAMF7	Signaling lymphocytic activation molecule 7
SOCS3	Suppressor of cytokine signaling 3
STING	Stimulator of interferon genes
T _m	Melting temperature
TSP-1	Thrombospondin-1
V _H	Variable domain of heavy chain
V _L	Variable domain of light chain
WHO	World Health Organization

ACKNOWLEDGEMENTS

9. ACKNOWLEDGEMENTS

First of all I would like to thank my supervisor Prof. Dr. Karl-Peter Hopfner for the opportunity to join his laboratory and work in the exciting field of cancer immunotherapy. I really appreciate your guidance and the freedom to develop my own ideas.

Special thanks go to Nadja for her infinite scientific and personal support since the very beginning of my PhD. I always enjoy our discussions and I am thankful for your many useful advices. Alongside, I am very grateful to former and current members of the antibody subgroup: Nadine, Moni, Saskia, Siret, Claudia, Anna, Alex and Simon, plus Lisi, for their help and the great atmosphere. I had a lot of fun working with you and sharing chocolate, coffees and lots of smiles. I am also obliged to all the members of the Hopfner lab: you made my time in the lab very enjoyable.

I am thankful to Prof. Dr. Marion Subklewe, Dr. Jan-Hendrik Kozik and Dr. Christina Krupka for our very fruitful collaboration and the time you spent studying the molecules on patient samples. Thanks to my TAC members, Prof. Dr. Veit Hornung and Prof. Dr. Christoph Klein for their time and ideas and to my graduate school “Quantitative Bioscience Munich” for their great support. I am also grateful to Prof. Dr. Veit Hornung and Gunnar Kuut for introducing me to the SH800 flow cytometer; Prof. Dr. Vigo Heissmeyer and Juliane Klein for their support with the imaging flow cytometer; Prof. Dr. Zuzana Storchova and Dr. Verena Passerini for their help with the confocal microscopy; and Prof. Dr. Kirsten Lauber for her advices on the phagocytosis assay. Without them this work would not have been possible.

I would also like to thank my friends from Munich, especially my QBM mates, for sharing good moments out of the lab, and my friends from Barcelona, especially Carmen, for finding time to spend together. I am very happy that I can always count on Chris for anything and everything, and therefore he deserves one of my strongest gracias.

També vull donar les gràcies a la meva família, sobretot al meu pare, la meva germana, les meves tietes i les meves àvies, per recolzar-me des de la distància i fer-se sentir molt a prop. I especialment a la meva estrella, a qui dedico aquesta tesis, per guiar-me i donar-me forces quan em fan falta.

CURRICULUM VITAE

10. CURRICULUM VITAE

Name	Laia Pascual Ponce
Nationality	Spanish
Birth date	June 25 th 1991
Birth place	Vilanova i la Geltrú, Spain
Gender	Female

Education

09.2014 – 04.2018	Doctoral Thesis in Biochemistry Ludwig-Maximilians University, Faculty of Chemistry and Pharmacy, Department of Biochemistry Munich, Germany As part of Quantitative Bioscience Munich (QBM) PhD program
09.2013 – 06.2014	Master of Science, Advanced Immunology University of Barcelona Faculty of Biology
09.2009 – 09.2013	Bachelor of Science, Biotechnology University of Barcelona Faculty of Biology

Work experience

Since 09.2014	Doctoral Thesis in the group of Prof. Dr. Karl-Peter Hopfner Ludwig-Maximilians University, Faculty of Chemistry and Pharmacy, Department of Biochemistry Munich, Germany
09.2013 – 06.2014	Master Thesis in the group of Dr. Thomas Stratmann University of Barcelona Faculty of Biology Department of Immunology, Barcelona, Spain
02.2013-08.2013	Bachelor Thesis in the group of Prof. Dr. med. Dirk Busch Technical University of Munich Faculty of Medicine, Munich, Germany As part of Erasmus exchange program